UNIVERSITY OF VERONA

DEPARTMENT OF MEDICINE

PHD SCHOOL OF LIFE AND HEALTH SCIENCES

PHD IN INFLAMMATION, IMMUNITY AND CANCER

XXXII CYCLE /2016

Unveiling the role of DAB2-expressing macrophages in supporting the metastatic spread

MED/04

Coordinator: Prof./ssa Gabriela Constantin

Signature _____

Tutor: Prof. Vincenzo Bronte

Signature _____

PhD candidate: Francesca Hofer

Unveiling the role of DAB2-expressing macrophages in supporting the metastatic spread

Francesca Hofer

PhD thesis

Verona, 6 May 2020

TABLE OF CONTENTS

ABSTRACT

The dissemination of malignant cells from the primary tumor to distant organs is the main cause of cancer-associated death and consists in a sequential multistep process defined as “metastatic cascade”. Cancer cells undergo genetic and epigenetic aberrations and acquire an invasive phenotype. They detach from the site of origin and, by remodeling basal membranes and the extracellular matrix (ECM), migrate into blood or lymph vessels, extravasate and adapt to an ectopic tissue, creating a secondary tumor mass.

In recent years, researchers have focused their attention on the contribution of tumor-associated immune cells in generating a favorable microenvironment for tumor cell growth. In particular, among leukocyte populations, macrophages are abundantly present in the tumor microenvironment (TME).

Although tumor-associated macrophages (TAMs) have the potential to eliminate neoplastic cells, it has been shown that they exhibit many pro-tumor features. Indeed, they support cancer cells proliferation, ECM remodeling and metastasis formation, and their presence correlates with a poor prognosis. An increasing number of reports supports their pro-tumor and pro-metastatic role, but either the lack of specific markers or molecularly defined mechanisms underlying these processes makes the development of anti-metastatic therapeutic strategies particularly demanding.

To distinguish and target specifically TAMs involved in the pro-tumor and pro-metastatic activities, we decided to investigate the role of TAMs in different tumor settings. Here, we discovered that DAB2 (disabled 2, mitogen-responsive phosphoprotein), an adaptor protein involved in the clathrin-mediated endocytosis (CME), is highly expressed in TAMs and metastasis-associated macrophages (MAMs) and its expression is induced by the TME. In particular, the results obtained with this work allow us to establish DAB2 protein as regulator of TAM-dependent ECM remodeling, a mechanism through which these cells support the cancer spread. Moreover, we identified DAB2 as a promising prognostic marker in several human malignancies, as well as a potential targeting molecule to block or eradicate metastasis formation.

SOMMARIO

La diffusione di cellule maligne dal tumore primario ad organi distali è la principale causa di morte associata al cancro e consiste in un processo a più fasi definito come "cascata metastatica". Le cellule tumorali, a seguito di mutazioni genetiche ed epigenetiche, acquisiscono un fenotipo invasivo. Si staccano dal sito di origine e, rimodellando la membrana basale e la matrice extracellulare (ECM), migrano nei vasi sanguigni o linfatici, extravasano e si adattano ad un tessuto ectopico, generando una massa tumorale secondaria.

Negli ultimi anni, i ricercatori hanno focalizzato la loro attenzione sul contributo delle cellule immunitarie associate al tumore nel generare un microambiente favorevole alla crescita delle cellule tumorali. In particolare, tra le popolazioni leucocitarie, i macrofagi sono abbondantemente presenti nel microambiente tumorale.

Sebbene i macrofagi associati al tumore (TAMs) abbiano il potenziale di eliminare le cellule neoplastiche, è stato dimostrato che essi presentano molte caratteristiche pro-tumorali. Infatti, supportano la proliferazione delle cellule tumorali, il rimodellamento della matrice extracellulare e la formazione di metastasi e la loro presenza è correlata ad una prognosi sfavorevole.

Un numero crescente di pubblicazioni supporta il loro ruolo pro-tumorale e pro-metastatico, ma la mancanza di marcatori specifici o la conoscenza dei meccanismi molecolari alla base di questi processi rende particolarmente impegnativo lo sviluppo di strategie terapeutiche anti-metastatiche.

Per distinguere e raggiungere in modo selettivo i TAMs coinvolti nelle attività pro-tumorali e pro-metastatiche, abbiamo deciso di investigare il ruolo dei TAMs in diversi modelli tumorali. Abbiamo scoperto che DAB2 (disabled 2, mitogen-responsive phosphoprotein), una proteina adattatrice coinvolta nell'endocitosi mediata da clatrina (CME), è altamente espressa nei TAMs e nei macrofagi associati a tumore (MAMs) e la sua espressione è indotta dal microambiente tumorale. In particolare, i risultati ottenuti con questo lavoro ci consentono di affermare che i TAMs $DAB2^{+}$ regolano il rimodellamento della matrice extracellulare e che questo è il meccanismo attraverso il quale i TAMs supportano

la diffusione neoplastica. Infine, abbiamo identificato DAB2 come promettente marcatore prognostico in diverse neoplasie umane, nonché potenziale molecola bersaglio per bloccare o eradicare la progressione metastatica.

INTRODUCTION

Chapter 1: The immune system in cancer

1.1 Hallmarks of cancer

Tumorigenesis is a pathological process in which genetic and epigenetic aberrations lead to a progressive transformation of normal cells into malignant derivatives that proliferate indefinitely inside the host. Despite its heterogeneity, cancer complexity can be summarized in few main features. Indeed, all cancer types share eight common tracts, also referred as "hallmarks" of cancer (*1*) (Figure 1).

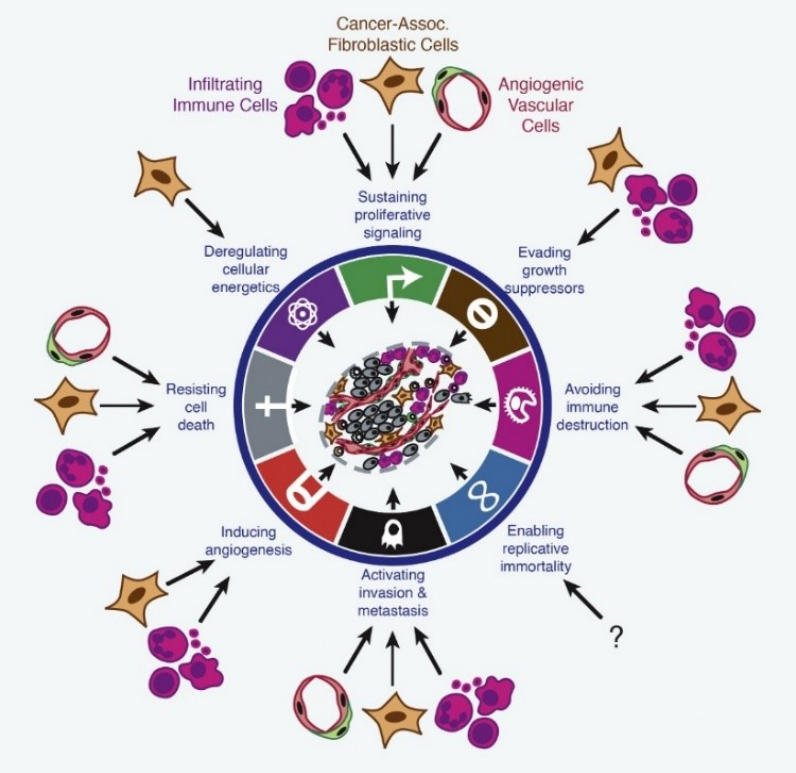

Figure 1. The hallmarks of cancer and the contribution of immune and stromal cells. Among the eight largely accepted hallmarks of cancer, seven of them have been demonstrated to involve infiltrating immune cells and stromal cells from the TME. Each of these cells exert pro- or anti-tumor specific functions. Reproduced from Hanahan and Coussens, 2012 (*2*).

According to this definition, cancer cells are self-sufficient entities, characterized by the ability to stimulate their own growth. They resist to inhibitory signals that

might arrest their proliferation (insensitivity to anti-growth signals), evade programmed cell death (apoptosis) and multiply with a limitless replicative potential. Moreover, since neoplastic cells need to fuel cell growth and division, they restict their energy metabolism largely to glycolysis. This metabolic switch termed "aerobic glycolysis" is thought to sustain high-rate anabolism and proliferation by providing the glycolytic intermediates necessary for amino acid and nucleoside biosynthesis. A sixth hallmark of cancer is angiogenesis, consisting in the formation of new blood vessels in the tumor mass. On one hand, the circulation supplies cells with oxygen and nutrients, thus favoring their aerobic metabolism and further proliferation. On the other hand, angiogenesis ensures cells a way to enter the blood circulation and move elsewhere inside the host or to eliminate the end products released by the rapidly dividing cells. This leads to another key characteristic of cancer: invasion of surrounding tissues and metastatization to distant organs. Finally, the eighth hallmark is the ability of cancer cells to avoid recognition and destruction by the host immune system (*3*). As discussed later, this is achieved by both selection of less immunogenic tumor cell clones and promotion of an immunosuppressive microenvironment able to hamper an efficient immune response against the neoplastic lesions.

Noteworthy, the discovery that a small population of cancer stem cells (CSCs) sustains many types of cancer has extremely important implications for both understanding and treating cancer. CSCs are a rare and chemotherapy-resistant subpopulation of undifferentiated cells defined by the ability to sustain their own self-renewal and, at the same time, to generate more differentiated cells constituting the great bulk of the tumor mass (*4*). CSCs can originate from stem cells that have undergone genetic and epigenetic mutations responsible for the disruption of proliferative and differentiation programs of normal stem cells (*4*), or from differentiated cells that have acquired stem cell properties as consequence of genetic mutations.

1.2 The metastatic spreading

Metastases are responsible for as much as 90% of cancer-associated mortality (*5*), however the metastatic process has a low rate of success. Tumor can release thousands of circulating tumor cells (CTCs) every day, but less than 0.1% of them are able to successfully develop metastasis in the ectopic tissue (*6*) due to many obstacles tumor cells must overcome to produce a secondary tumor (*7*). In solid malignancy, dissemination of cancer cells from the primary tumor to distant organs is a multistep process, defined as "metastatic cascade" (Figure 2). First, cancer cells undergo genetic and epigenetic aberrations and acquire an invasive phenotype. They detach from the origin site and, by remodeling basal membranes and extracellular matrix (ECM), infiltrate into the blood stream or lymph vessels (intravasation), turning into anchorage-independent CTCs. Then, CTCs exit from the circulation (extravasation) and adapt to the new host tissue, generating a secondary tumor mass (*8*).

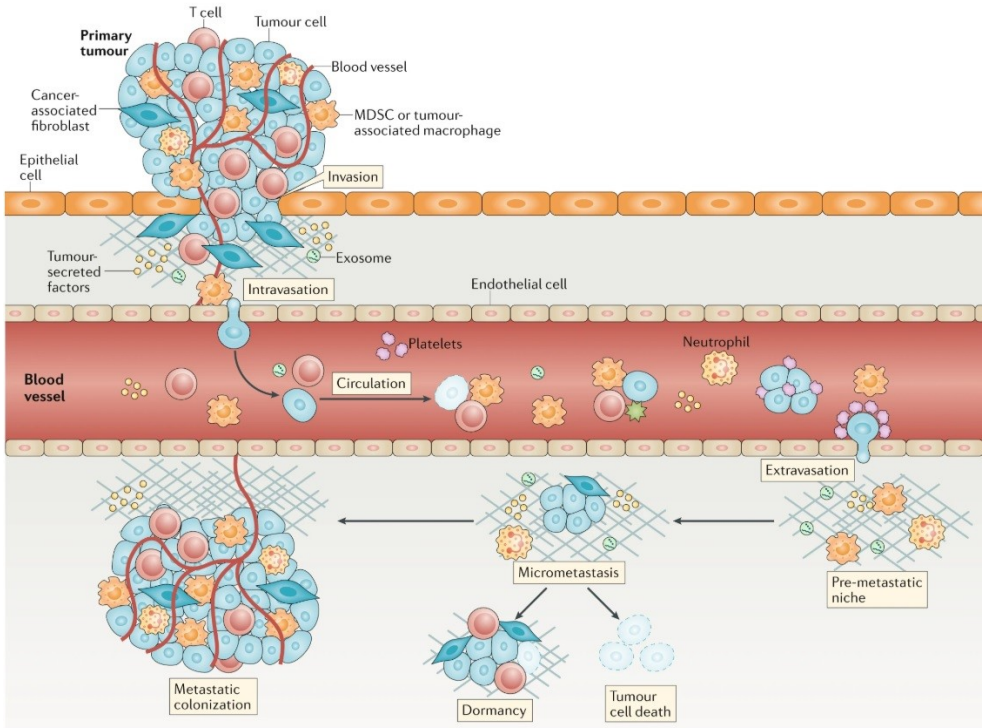

Figure 2. The metastatic process. Several steps characterize metastasis cascade: cancer cells invasion, intravasation, circulation in the blood vessel, homing and extravasation, followed by metastatic colonization. Reproduced from Anderson et al. 2019 (*8*).

The early phase of the metastatic process starts with a profound alteration of the adhesion mechanisms that normally keep the cells bound to the surrounding cells and to the ECM. Indeed, to carry out the invasive program, tumor cells must acquire characteristics of motility and undergo a drastic change of morphology and transcriptional profile that makes the epithelial cells similar to the mesenchymal ones: this process is called epithelial-mesenchymal transition (EMT). EMT is not peculiar to tumor cells but normally occurs under physiological contexts in the adult organism (wound healing) or during embryonic development. EMT is characterized by the activation of transcription factors, such as SNAIL, TWIST and SLUG, which regulate the transcription of many genes, including E-cadherin (*9*). While E-cadherin undergoes a progressive reduction in its expression and epithelial cells lose their characteristic polarity, the expression of several genes of mesenchymal lineage (e.g. vimentin and N-cadherin) increases. In these cells, there is also an augmented deposition of fibronectin (FN) and secretion of metalloproteases, which allow the degradation and remodeling of basement membrane and ECM, respectively. The molecular mechanisms underlying this transition are still not completely understood, but it is certainly a consequence of the activation of a multitude of specific factors. The alterations in the adhesive properties of tumor cells also involve the heterodimeric transmembrane glycoproteins called integrins (ITGs) that connect the cell to the basement membrane and ECM through a dynamic rearrangement of the actin and myosin cytoskeleton. A key role in the metastatic process is played by proteins with GTPase activity included in the Rho-GTPase family, (e.g. Ras homolog family member A (RHOA), Rac GTPase (RAC) and cell division control protein 42 homolog (CDC42)), which contribute to the formation of protruding structures on the cell surface that are essential for migration (*10*). After matrix invasion, cancer cells disseminate through the blood and lymphatic circulation, exit the vessel and colonize another organ. Malignant cells begin to grow, forming micrometastasis, and activate a process called mesenchymal-epithelial transition (MET) which implicates the acquisition of epithelial cell characteristics (*7*). However, much remains to be done to understand the biology of metastasis; in particular, it needs to be further investigated how cancer cells are able to influence

the frequency and the site specificity of metastatic growth. A first hypothesis about metastasis organotropism was formulated by Stephen Paget and colleagues in 1889 (*11*) and named "seed and soil" theory. They proposed that tumor cells (the "seed") grow preferentially in specific organs (the "soil"), highlighting the crucial role of the microenvironment in supporting metastasis formation. However, Paget's proposal was not universally accepted for decades, due to the position of other researchers who claimed that tumor cells follow the circulatory route from the primary tumor to the first organ encountered (*12*). Despite anatomical and mechanical factors definitely influence the site of tumor arrest, some organs, such as brain and bones are poorly supplied by the circulatory volume, but frequently involved as metastatic sites.

In line with Paget's theory, recent publications underline the ability of cancer cells to colonize defined tissues. For example, the major sites of metastasis for breast carcinomas are the bone, the lung and the brain, while liver and lung are the preferential sites for colorectal and pancreatic carcinomas. Moreover, some cancer cells rarely seed in other organs even though they are highly invasive (*13*). All these findings highlight the essential role played by the generation of a supportive and receptive tissue microenvironment at the metastatic site, defined as "pre-metastatic niche" (p-mN) and ready before the arrival of tumor cells. Indeed, p-mN is known to enhance metastatic efficiency and determine metastatic organotropism (*14*). Its development requires that tumor-derived soluble factors (TDSFs), such as cytokines and growth factors, genetically re-program not only resident cells (e.g. fibroblasts) but also non-resident cells such as bone marrow (BM)-derived cells (*15*). Examples of such TDSFs are vascular endothelial growth factor A (VEGFA), tumor necrosis factor (TNF) and transforming growth factor beta (TGF-β), which induce the release of the inflammatory mediators S100A8 and S100A9 in the lungs with subsequent recruitment of myeloid cells (*16*). Lately, it has been demonstrated that also tumor-derived exosomes prime the p-mN and even determine metastatic organotropism, exploiting an ITG-dependent mechanism (*17*).

1.3 Tumor-associated stromal cells as key contributors to the tumor microenvironment

In the recent past, cancer researchers mainly focused their studies on the primary tumor, exploring adhesion, migration and metastasis as intrinsic properties of cancer cells (*1*) and discovering several oncogenic factors, tumor suppressor genes and signaling pathways contributing to the malignant transformation (*2*). However, tumor is a complex entity constituted not only by malignant cells, but by a network in which immune and stromal cells are involved in an intricate mutual relationship with cancer cells (Figure 3). Stromal cells participating in this process belong to two subsets: angiogenic vascular cells and cancer-associated fibroblasts (*2*). The physiological function of these populations is altered in the tumor context, where they can be corrupted by cancer cells to generate a cancer-promoting environment.

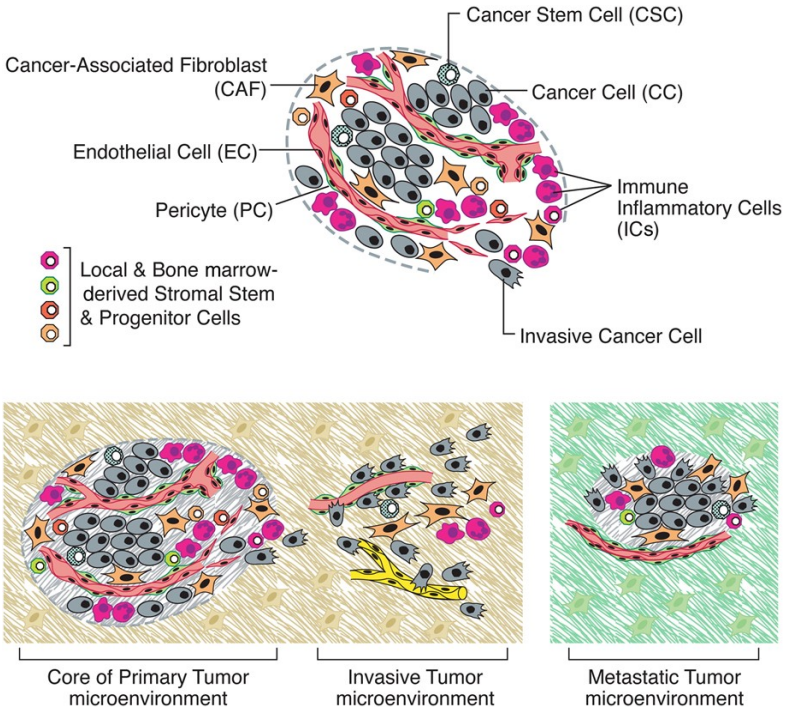

Figure 3. Tumor microenvironment: cell composition. TME includes cancer cells (CCs), cancer stem cells (CSCs), cancer-associated fibroblast (CAFs), endothelial cells (ECs), pericytes (PCs), and immune inflammatory cells (ICs). Reproduced from Hannahan and Weinberg 2011 (*1*).

The angiogenic vascular cells are endothelial cells (ECs) responsible of the tumor-associated vasculature formation. During tumor progression, angiogenesis is essential to supply the tumor with nutrients and oxygen and to allow tissue invasion and metastasis formation. ECs can be activated to construct new blood vessels (angiogenesis) or, in some cases, lymphatic vessels at the periphery of tumors (lymphangiogenesis) (*18*). ECs communicate either by direct contact or by paracrine signal with pericytes (PCs), a type of mesenchymal cells with contractile function. These cells surround the blood vase acquiring a finger-like shape and collaborating with ECs in synthesizing the vascular basement membrane that sustains the hydrostatic pressure within blood vessels (*18*).

Cancer-associated fibroblasts (CAFs), one of the major subset present in the tumor stroma, are able to provide physical and biochemical support to the tumor mass, favoring tumor cell growth, angiogenesis, invasion and metastasis formation. CAFs can orchestrate the remodeling of the stroma, by degrading or synthesizing components of the ECM, and the recruitment of both ECs and PCs by releasing growth factors and chemokines (*19*).

Finally, TME consists in the infiltrating immune cells, leukocytes of both myeloid and lymphoid origins, already present in the tissue or recruited from the circulation, due to the state of chronic inflammation established by the tumor (*20*).

1.4 Tumor-infiltrating immune cells

The ability of the immune system to recognize and eliminate primary developing tumors in the absence of external therapeutic intervention is a concept that has existed for nearly 100 years. Understanding cancer development and how the immune cells impact tumor fate are one of the main challenges in immunology.

Tumors are infiltrated by leukocytes and the degree of these infiltrations is similar to that arising in normal inflamed tissues, suggesting that an inflammatory reaction usually occurs in tumors. Historically, this was interpreted as an attempt of the immune system to eradicate the tumor.

In 1891 William B. Coley documented beneficial effects of infection on bone sarcomas treatment, formulating the idea of immune control of neoplastic disease (*21*). However, such idea was not vigorously pursued until the midpoint of the

twentieth century when the concept of tumor-specific antigen (TSA) was introduced.

The presence of a variety of antigens (Ags) in cancer cells is the result of genetic instability occurring in cancer cells, which leads to the generation of neoantigens exclusive to the transformed cells (TSA) or epitopes from proteins already expressed at low levels in normal tissues (tumor-associated antigen, TAA). T lymphocytes play a pivotal role in recognizing these Ags and aid the immune system in the destruction of the newborns transformed cells long before they become clinically detectable. But the clear evidence of the prominent role of immune system in primary tumors eradications was obtained with the introduction of immunodeficient mice. Studies on mice lacking recombination activating gene 2 (RAG-2) and thus losing the ability to develop T, B, and NKT cells as well as in mice deficient in interferon (IFN)-γ signaling reported increased sarcoma, adenoma and adenocarcinoma incidence compared to the immune-competent hosts (*22*). Moreover, a high infiltration of some lymphoid cell populations in tumor correlates with improved patient's prognosis, along with a reduced recurrence after therapy, indicative of the therapeutic success (*23*).

In order to explain the dynamic interaction between the immune system and the neoplastic cells, Robert Schreiber and collaborators advanced the Cancer Immunoediting theory (*3*), which develops in three different phases: elimination, equilibrium and escape.

In the first phase of "elimination", cancer cells are subjected to the immune surveillance. This phase can be considered concluded only when the immune system eliminates all existing tumor cells. In the case of an incomplete tumor eradication, "equilibrium" phase starts. This second phase is characterized by a balance between the elimination of immunogenic cancer cells and the survival of less-immunogenic ones, due to the acquisition of new mutations (immunoediting). These new tumor variants are able to resist or suppress the antitumor immune response, leading to the "escape" phase. During the "escape" phase, the immune system is no longer able to restrain tumor cells, which evade the host defenses, given rise to malignant progression.

Cancer cells, in the attempt to survive in a hostile tissue, generate a favorable TME through the continuous release of TDSFs, which alter the normal hematopoiesis inducing a blockade in the myeloid differentiation program that leads to the abnormal expansion and accumulation of immature myeloid cells (*3, 15*). These tumor-infiltrating cells are able to suppress actively the immune surveillance as well as to promote tumor growth and invasion in surrounding tissues (*20*). The presence of these reprogrammed immune cells is correlated with poor prognosis in patients and with low efficacy of anti-cancer immunotherapies (*24*). Moreover, immune suppressive cells can also migrate into secondary lymphoid organs and induce immune tolerance to tumor Ags, further impairing the anti-tumor immune response (*25*). Among these cells, the accumulation of $CD11b^+$ myeloid cells and, in particular, of dendritic cells (DCs), tumor-associated neutrophils (TANs), myeloid-derived suppressor cells (MDSCs) and TAMs in a tumor-driven context has been extensively investigated.

- *Dendritic cells*

DCs are myeloid cells that act as antigen presenting cells (APCs) by processing and presenting Ags to T cells. They arise from both myeloid and lymphoid progenitors within BM and comprise two major subsets: conventional DCs and plasmacytoid DCs (*26*).

Conventional DCs are responsible for Ag uptake by phagocytosis and ingestion of a large amount of extracellular fluid by micropinocytosis. They have an immature phenotype that is associated with a low level of major histocompatibility complex class II (MHCII) proteins and B7 co-stimulatory molecules, and thus with the inability to stimulate naïve T cells. Immature DCs are activated by pathogen-associated molecular patterns (PAMPs) or damage-associated molecular patterns (DAMPs), both recognized by the evolutionary conserved toll-like receptors (TLRs) (*27*). The binding of these ligands to TLRs induces differentiation of immature DCs, which can then promote processing of pathogen-derived Ags, the expression of co-stimulatory molecules and T cell-activating cytokines, as well as the up-regulation of chemokine receptors that drive migration of DCs to peripheral lymphoid organs (*27*).

Plasmacytoid DCs recognize viral nucleic acids and self DNA fragments through the TLR pathway and consequently stimulate the production of high amounts of type I interferon, such as IFN-α, to induce innate and adaptive immune responses. Plasmacytoid DCs, as conventional DCs, express low levels of MHCII and co-stimulatory molecules on their surface, but they contribute to the T cell activation acting as helper cells for Ag presentation. Indeed, upon TLR-9 signaling, they promote the production of CD40 ligand (CD40L), a TNF-family transmembrane cytokine, which binds to the CD40 receptor expressed by activated conventional dendritic cells (*26*). This interaction induces the secretion of the pro-inflammatory interleukin 12 (IL-12) by conventional DCs, which, in turn, causes the massive production of IFN-γ by T cells, helping the macrophages to eliminate bacteria. Furthermore, these DCs are known to elicit autoimmunity, if chronically activated, as well as immune tolerance, if they remain resting (*26*).

Tumor-infiltration by mature, activated DCs adequately stimulates immune responses through the recruitment of anti-cancer immune effector cells and guarantees a better outcome for patients (*28*). However, TDSFs including VEGF, macrophage colony-stimulating factor (CSF-1), granulocyte-macrophage colony-stimulating factor (CSF-2), interleukin 6 (IL-6), interleukin 10 (IL-10) as well as hypoxia, can impair terminal DC differentiation. The decreased production of mature DCs causes the expansion of immature DCs, characterized by poor T-cell activating abilities, and the shift of DC precursors towards macrophage differentiation (*29*). These immature, tumor-conditioned DCs may also actively suppress $CD8^+$ T cell responses through the expression of immune suppressive molecules such as arginase 1 (ARG1), IL-10, TGF-β and indoleamine 2,3-dioxygenase (IDO) (*30, 31*). IDO is an enzyme that limits T cell growth by consuming local L-tryptophan and enhances the activity of regulatory T lymphocytes (Tregs), a particular subset of $CD4^+$ T helper (Th) cells that inhibit T cells to sustain peripheral tolerance in tissues (*32*).

Moreover, we recently demonstrated that a particular subset of DCs, the TNF- and inducible nitric oxide synthase (iNOS)-producing DCs (Tip-DCs), is pivotal for increasing the efficacy of adoptive cell therapy (ACT) against the tumor (*33*). Following ACT, Tip-DCs accumulate within the TME where they cross-present

tumor Ags and activate adoptively-transferred and endogenous $CD8^+$ T cells through a pathway requiring CD40-CD40L (*33*).

- *Tumor-associated neutrophils*

Granulocytes, also called polymorphonuclear leukocytes, are leukocytes characterized by cytoplasmic granules and multi-lobed nuclei. They comprise neutrophils, eosinophils and basophils that can be distinguished by the different staining properties of their intracytoplasmic granules. They have short-life and their production is increased during immune responses, when they migrate from the blood circulation to sites of infection or inflammation. Neutrophils, the most abundant granulocyte subtype, are phenotypically defined in mice as $CD11b^+$ $Ly6G^+$. They are highly specialized phagocytic cells that rapidly respond to infections by destroying engulfed pathogens (*34*) using degradative enzymes and other antimicrobial peptides stored in their granules. Because of their short life span and fully differentiated phenotype, their role in cancer-related inflammation has long been considered negligible. However, during tumor progression, two tumor-infiltrating subsets with opposite functions have been identified: N1 neutrophils, with an anti-tumor cytotoxic effect secreting pro-inflammatory cytokines, and N2 neutrophils, expressing ARG1, low levels of pro-inflammatory molecules favoring tumor growth and dampening $CD8^+$ T cytotoxic lymphocyte activation (*35*). Thus, on one hand, neutrophils kill tumor cells by producing reactive oxygen species (ROS) and inhibit the formation of metastasis (*36*). On the other hand, tumor can secrete granulocyte colony-stimulating factor (CSF-3) to induce neutrophil production and attract them to the tumor site; once there, neutrophils favor angiogenesis and secrete matrix metalloproteinase 9 (MMP9), which supports the release of VEGF from the ECM (*37*). Moreover, CSF-3 induces early migration of granulocytes in pre-metastatic lungs of tumor-bearing mice, where they can assist metastasis formation (*38*). An elevated number of neutrophils was also found in the blood of cancer patients and correlated to an increased risk for metastasis (*39*). Finally, recent evidence highlighted the role of neutrophil-derived extracellular trap-associated proteases in ECM degradation and laminin (LN) production which in turn activate Yes-Associated

Protein/transcriptional coactivator with PDZ-binding motif (YAP/TAZ) signaling in cancer cells, awakening dormant metastatic tumor cells in the lungs (*40*).

- *Myeloid-derived suppressor cells*

MDSCs are highly immunosuppressive, immature myeloid cells, whose ontogeny and classification have been under extensive debate (*41*). They share morphological features with conventional monocytes and granulocytes; however they have the ability to inhibit both adaptive and innate immune responses. In 2007 these cells were named myeloid-derived suppressor cells (MDSCs), emphasizing their myeloid origin and their immune-suppressive function on T lymphocytes in a tumor-driven context (*42*). The expansion of these population has been described in different solid and hematologic malignancies occurring in both human patients (*43*) and mouse models (*44*). Moreover, the levels of MDSCs in the blood and at the tumor site correlate with an advanced tumor stage (*45*) and a poor clinical outcome in several human cancers (*46*).

MDSCs were originally described in mice, on the basis of the co-expression of CD11b and Gr-1. However, this classification does not allow the clear identification of these cells. At present, it is widely accepted that, mouse MDSCs can be divided in two main subsets with different phenotypic and biological properties: the polymorphonuclear MDSCs (PMN-MDSCs) and monocytic MDSCs (M-MDSCs) (*47*).

PMN-MDSCs are the most represented MDSC population, defined as $CD11b^{+}$ $Ly6C^{low}$ $Ly6G^{+}$ cells. They can be discriminated from not activated granulocytes for their immunosuppressive activity and for high levels of CD115 and CD244, but low levels of CXC chemokine receptor 1 (CXCR1) and 2 (CXCR2) in mice (*47*). Mouse M-MDSCs are defined as $CD11b^{+}$ $Ly6C^{high}$ $Ly6G^{-}$ cells and express classic monocytic markers as CD115, F4/80 and CC-chemokine receptor 2 (CCR2) (*47*). M-MDSCs are distinct from circulating, inflammatory monocytes because of their immunosuppressive function (higher than the polymorphonuclear counterpart).

In humans, the identification of MDSCs is complex, because of the lack of specific markers. Moreover, there is often no correlation between phenotype and

immune suppressive activity (*46*). Recently, human MDSC population was divided into ten different subsets (*48*), some of which correlated with a poor prognosis in oncological patients (*49*).

The main function of both mouse and human MDSCs is the inhibition of T cell recruitment, activation and proliferation with both direct and indirect mechanisms (*20*). MDSCs are able to produce nitric oxide (NO), ROS and reactive nitrogen species (RNS), which impair $CD8^+$ T cell responsiveness (by downregulating the CD3ζ chain in the T-cell receptor - TCR), proliferation (by interfering with IL-2 receptor signaling) and ability to migrate within TME and kill cancer cells (by nitrating CCL2) (*50*). MDSCs contribute to the deprivation of essential amino acids, necessary for T cell metabolism, such as L-arginine and L-tryptophan through the activity of ARG1 and IDO-1 enzymes, respectively (*46*). Further the functions of these immature myeloid cells are the induction of T cell tolerance through the expression of programmed death ligand-1 (PD-L1) and the cytotoxic T-lymphocyte antigen 4 (CTLA-4) receptors, as well as the expansion of regulatory cells like $CD4^+$ Tregs and M2-polarized macrophages by TGF-β and IL-10 release, respectively (*20, 51, 52*). Like Tregs, MDSCs may represent a control system to avoid excessive and dangerous immune responses. In support of this theory, it seems that the some immunosuppressive activity of MDSCs requires IFN-γ to be unleashed and IFN-γ mainly derives from activated $CD8^+$ CTLs and Th1 cells (*20*). All these immunosuppressive mechanisms are correlated with the induction of specific transcriptional factors such as the nuclear factor kappa-light-chain-enhancer of activated B cells (NF-κB) (*53*) and the CCAAT-enhancer-binding proteins (c/EBP)-β (*54*). Recently, the role of signal transducer and activator of transcription (STAT) 3 in the monocyte reprogramming has emerged (*49*). In addition, MDSCs can also exert non-immunosuppressive actions promoting tumor progression, invasion and metastatization. They are able to release metalloproteinases for ECM degradation (e.g. MMP2 and MMP9), differentiate into endothelial-like cells, promote angiogenesis and prepare the p-mN for tumor cell arrival. They also induce EMT-associated signaling pathways such as those dependent on TGF-β, epidermal growth factor (EGF) or hepatocyte growth factor (HGF) (*55*).

- *Tumor-associated macrophages*

Macrophages are terminally differentiated and highly heterogeneous myeloid cells that act as specialized phagocytes. In adults, TAMs originate from circulating inflammatory monocytes recruited to the tumor site through tumor- or stroma-derived chemotactic factor, such as CCL2, or from self-renewal of tissue-resident macrophages (*56, 57*). Resident macrophages are found in almost all peripheral tissues of the body and are not derived from BM-derived progenitors, as previously thought, but from yolk sac or fetal liver (*57, 58*). Indeed, macrophages can originate from at least three different embryonic sources (from erythro-myeloid progenitor (EMP) in the yolk sac and fetal liver, and from macrophage/dendritic cell progenitor cells (MDPs) in the bone marrow) and differentiate in tissue-specific macrophages according to their origin (*59*). Some tissue-specific macrophages in adults are almost exclusively derived from one source, while in other tissues different proportions of macrophages derive from different precursors (*58*).

Phenotypically, macrophages mainly express F4/80, CD115 (also known as CSF1R, colony-stimulating factor 1 receptor) and MHCII markers in mice and CD68, CD163, CD115, human leukocyte antigen (HLA)-DR markers in humans (*20*). According to a historical and simplistic definition, macrophages can polarize into two opposite phenotypes, depending on their high ability to integrate distinct signals from the microenvironment (*60*). The 'M1' or 'classically activated' macrophages are induced by microbial components (e.g. Lipopolysaccharide, LPS) and Th1 cytokines (e.g. IFN-γ). They promote Th1 response and, through the upregulation of inflammatory cytokines (e.g. IL-1β, TNF, IL-6), iNOS and ROS-generating enzymes, they efficiently support anti-microbial and anti-tumor actions (*60*). Contrary to DCs, macrophages are not specialized APCs, but when they are polarized toward the M1 phenotype, they become efficient APCs. They upregulate the MHCII, the co-stimulatory molecule CD86 and the pro-inflammatory cytokine IL-12. Therefore, M1 macrophages can present Ags to $CD4^+$ Th cells and drive a Th1-oriented adaptive response (*61*). The 'M2' or 'alternatively activated' phenotype is induced on macrophages by IL-4 and IL-13 cytokines (*62*), produced by Th2 cells during helminth infection and allergy. M2

macrophages display a poor antigen presenting capacity, produce low levels of IL-12 and high levels of the anti-inflammatory cytokine IL-10, thus inhibiting the induction of Th1 cells (*60*). In constrast, they produce Th2-, Treg- and basophils-attracting chemokines (e.g. CCL17, CCL22 and CCL24) (*61, 63*). Moreover, M2 macrophages upregulate ARG1 and consequently produce polyamines and L-proline, which support either the production of ECM components or nutrients for active replicating cells, and deplete local L-arginine, suppressing $CD8^+$ T cell responses (*61*).

Thus, according to this simplistic definition, M1 macrophages represent the pro-inflammatory subset, while the M2 macrophages the anti-inflammatory one. The M1/M2 classification constitutes only a simplification to distinguish between the many functions that macrophages can potentially exploit within tissues (*63*). Therefore, M1 and M2 phenotypes should be considered as extreme conditions of a full spectrum of polarizations with several overlapping functions that macrophages can assume *in vivo* (*64*). Thus, it becomes difficult to identify rare myeloid subpopulations due to the presence of complex tissue-derived signals, which generate intermediate phenotypes, and to the lack of specific markers (*56*). In mouse tumors, a further level of complexity is given by the fact that TAMs may also express MHCII and CD11c, which are typical DC markers. Remarkably, a gene signature comprising 37 genes from TAMs correlated with highest expression of CSF-1 response signature and with a shorter disease-specific survival (DSS), indicating sialic acid binding Ig like lectin 1 (SIGLEC1/CD169) as discriminating TAM marker. High levels of this gene were found in TAMs in invasive breast cancer tissue specimens and, to a much lower extent, in circulating monocytes (*65*).

To capture the full heterogeneity of tumor-infiltrating macrophages, single-cell RNA sequencing (scRNA-seq) can offer the opportunity to investigate the whole transcriptome of individual cells, without the limit of prior knowledge of specific markers. As highlighted from a single-cell analysis performed on myeloid cells in non-small lung cancer (NSCLC) as well as in a mouse model of this disease, several distinct populations of macrophages can be identified and clustered by their gene expression (*66*).

1.5 Tumor promoting functions of TAMs

Macrophages display a plethora of different functions according to the surrounding microenvironment, which influences their polarization. They have a role in primary tumor, where they stimulate neovascularization, intravasation and tumor cell invasion; and in the metastatic site, promoting tumor cell extravasation, survival and permanent growth (Figure 4). Macrophages are also involved in immunosuppression, either protecting cancer cells from natural killer (NK) and T cells during tumor progression and after chemo- or immunotherapy treatment (*6*). For this reason, the presence of TAMs in tumor infiltrates of patients correlates with a poor prognosis (*67*).

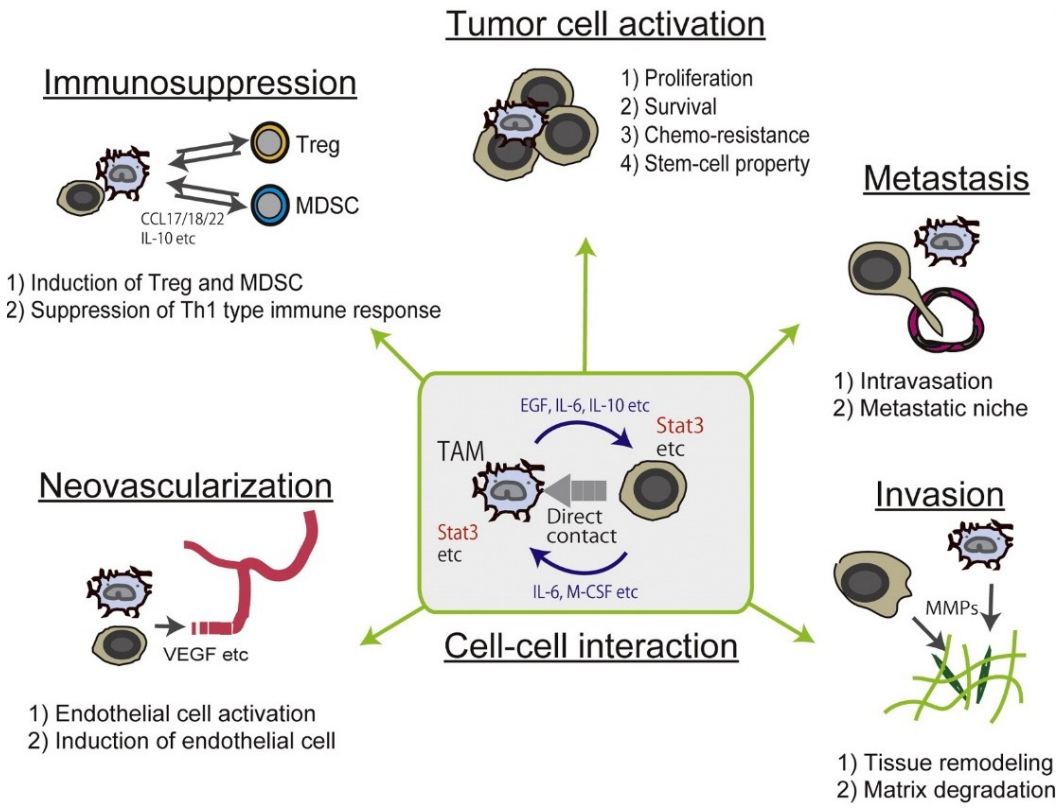

Figure 4. The pro-tumor functions of TAMs. Macrophages in the TME can sustain cancer progression by inducing tumor cell activation and invasion, neovascularization, immunosuppression and metastasis. Reproduced from Komohara et al. 2016 (*68*).

- *TAMs favor tumor activation*

TAMs can induce both *in vitro* and *in vivo* tumor cell activation and proliferation. In particular, TAM-derived heparin-binding EGF-like growth factor (HB-EGF)

and oncostatin M, IL-6 or IL-10 stimulate EGF receptor (EGFR) and STAT3 in cancer cells, respectively. The activation of STAT3 signaling pathway also enhances stem cells features in tumor cells that can survive and resist to anti-cancer therapies (*69*). Notably, an M2-like population of peri-vascular TAMs induced by the CXCL12 (also known as stromal cell-derived factor 1, SDF1) chemokine was recently retained responsible for re-vascularization and relapse after chemotherapy (*70*).

Through the release of TNF-α or other cytokines, TAMs are able to induce NF-κB, a transcription factor involved in the activation of stemness and therapeutic resistance in neoplastic cells (*71*). The same pro-tumor effects seem to be obtained also following physical interaction between macrophages and tumor cells, with involvement of membrane CSF-1, intracellular adhesion molecule-1 (ICAM-1) and ephrin (*72*).

- *TAMs favor angiogenesis and lymphangiogenesis inside the tumor*

Tumors, in order to grow beyond a certain size and spread into distal organs, require the activation of a process defined as "angiogenic switch". VEGF, TGF-β and platelet-derived growth factor (PDGF) released by TAMs are directly responsible of the regulation of this switch (*73*). TAMs can also induce angiogenesis in an indirect way, synthetizing the WNT family ligand WNT7B or the MMP-9, which in turn stimulates VEGF release from matrix (*74, 75*). Moreover, Tie2-expressing macrophages (TEMs), a subpopulation of TAMs, are able to differentiate in perivascular macrophages and, since they express the receptor for angiopoietin 2 (ANG2), interact with $ANG2^{+}$ ECs to induce the angiogenic process (*76*). The targeting of ANG2 or Tie2 is associated with an impaired neoangiogenesis in different mouse tumor models (*76*). Unlike normal blood vessels, tumor blood vessels form a leaky but denser vascular network. The angiogenic potential of TAMs has been proven further by depletion studies, which demonstrated a correlation between TAMs and blood vessel density, mirroring the interaction between these two components of the TME (*77*). Furthermore, TAMs are also responsible of lymphangiogenesis, an important route for malignant cells spreading to regional lymph nodes and distant metastasis, in a VEGF-C/VEGFR-3

axis-dependent manner. This interaction favors lymphangiogenesis by either directly affecting the lymphatic endothelial cells (LECs) activity or indirectly promoting cathepsin secretion (*78*). Treatment with VEGF-C/VEGFR-3 targeting antibody or genetic ablation of heparanase in mouse models significantly altered the lymphatic vessel phenotype, leading to an impaired primary tumor growth and metastasis (*79*).

- *TAMs favor tumor invasion*

In the early stages of metastasis, tumor cells lose cell-cell adhesion and their apical-basal polarity, acquiring a mesenchymal phenotype and the ability to invade the basement membrane. It has been reported that TAMs are involved in the regulation of this process, defined as EMT transition (*80*), via secreting various soluble factors, such as IL- 1β, IL-8, TNF-α, and TGF-β (*81*). The co-culture of TAMs with different cancer cell lines reduced the expression of E-cadherin and enhanced the expression of N-cadherin and SNAIL (*81*). TAMs can also directly stimulate the directional tumor cell migration and invasion by secreting EGF paracrine factor. EGF-activated tumor cells can in turn release CSF-1 to promote the motility of TAMs (*82*). Furthermore, perivascular TAMs promote the synthesis of fibrillar collagen type-I (COL I), speeding up tumor cells migration along stroma fibers toward blood vessels, where TAMs support their intravasation (*83*). To enhance this process, TAMs secrete CCL18 and osteonectin (also known as SPARC - secreted protein acidic and rich in cysteine), which modulates the ECM adhesive properties of cancer cells (*84, 85*). According to recent studies, SPARC supports FN and vitronectin (VN) interaction with cancer cells via ITGs activation, creating a traction force that trails tumor cells within stroma and toward blood vessels (*85*). The degradation and the remodeling of the ECM are likewise essential to permit tumor cell escape beyond basal membrane, facilitating both invasion of surrounding healthy tissues and formation of metastasis in distant organs.

TAMs support the proteolytic disruption of cell-cell and cell-ECM interactions, expressing high levels of several membrane-anchored and secreted proteases, such as cysteine cathepsins (e.g. cathepsin B and S), serine proteases (e.g. plasminogen

activator) and matrix metalloproteinases (e.g. MMP2 and MMP9). These enzymes target cell-adhesion molecules (such as E-cadherin) or stromal proteins (such as collagens) (*83, 86*).

- *TAMs favor the generation of an immunosuppressive tumor microenvironment*

TAMs exert also an immunosuppressive activity, through the expression of a wide range of molecules, including cell surface receptors, cytokines, chemokines and enzymes. Under hypoxic conditions, they express the ligand for PD-1 and CTLA-4 that, upon activation, suppress cytotoxic functions of T and NK cells (*33, 87*). While upregulation of death receptors FAS and TRAIL by TAMs promotes the apoptosis of target cells, the expression of non-classical HLA-G can inhibit NK and T cell function. TAMs are not efficient APCs and, when isolated from tumors and stimulated *in vitro* with microbial products, release high levels of IL-10 and low/null levels of IL-12 (*88*). Consequently, TAMs are not able to activate NK and Th1 cells and induce an anti-tumor response; by contrast, they lead to the development of Th2 cells, which in turn maintain an M2-like phenotype of TAMs by secreting IL-4 (*89*).

Moreover, IL-10 and TGF-β secreted by TAMs induce $CD4^+$ T cell differentiation in Tregs, and TAMs also release chemokines CCL5, CCL20, CCL22 that attract Treg cells in the tumor mass (*90*). In turn, Tregs, together with Th2 cells, promote macrophage M2 polarization. This is achieved through the release of IL-4, IL-10 and IL-13, which increase the expression of the mannose receptor CD206 and the scavenger receptor CD163 on macrophages and inhibit macrophage responsiveness to the M1-polarizing bacterial stimuli (*91*). Also tumor cells induce the M2 phenotype by secreting TNF-α, which is able to upregulate both type I and II scavenger receptors on macrophages . Thus, TAMs favor the generation of an immunosuppressive microenvironment inside the tumor mass by recruiting and activating regulatory cell populations; in turn, these cells sustain TAM accumulation and immune-modulatory properties in a positive loop.

TAMs secrete the enzyme ARG1 that, depleting L-arginine, inhibit TCR ζ chain re-expression on plasma membrane after the endocytosis in activated T cells (*92*).

- *TAMs favor tumor metastasis*

Myeloid cells and, in particular, MAMs are known to provide a road map for the homing of CTCs into the p-mN and to support their adaptation and survival in the new hostile tissue (*6*).

During metastasis formation, the accumulation of pro-tumor myeloid cells such as BM-derived classical inflammatory monocytes ($F4/80^{low}CD11b^{+}Ly6C^{+}$ in mice and $CD14^{high}CD16^{-}$ in humans) occurs through CCL2-CCR2 dependent mechanism (*93*). After extravasation, these monocytes turn into metastasis-associated macrophages precursor cells - MAMPCs ($F4/80^{high}CD11b^{high}Ly6C^{high}$), which are induced by CSF-1 to differentiate into a distinct population of macrophages defined MAMs ($F4/80^{low}CD11b^{high}Ly6C^{low}$) (*15, 94*). *Ex vivo* imaging of the metastatic lung revealed that macrophages directly take contact with extravasating cancer cells, and genetic ablation or blockade of MAMs reduced the number of cancer cells that migrate from the blood vessels into the surrounding tissues (*94*). Even after metastases are established, their loss inhibits further metastatic growth, suggesting that MAMs are necessary for cancer cell survival and proliferation (*93, 94*). These macrophages are also known to increase further vascular permeability by secreting VEGF or mediating protease-dependent release of matrix-bound VEGF (*95*), and to inhibit cytotoxic T cells (*93, 94*), maintaining an immunosuppressive environment, which in turn favors metastasis formation (*96*).

Moreover, MAMs increase the survival of disseminated human breast cancer cells through engagement of VCAM1 on tumor cells, which results in signaling for cell survival through the activation of protein kinase B (*97*). Acting on several steps of the malignant progression, MAMs are considered metastasis promoters and, therefore, they represent compelling therapeutic targets to enhance immunotherapy efficiency.

1.6 Macrophages as therapeutic targets

Considering the complexity of TAMs and MAMs population, it is essential to understand the cellular and molecular mechanisms underlying their regulation and

identify possible therapeutic targets, either reducing or blocking their pro-tumor and pro-metastatic features. Several strategies have been investigated, including TAM depletion, inhibition of their recruitment and reprogramming.

Considering that CSF-1 growth factor is involved in the differentiation of monocytes and macrophages, it represents an attractive therapeutic target to deplete these cells. Different antibodies and small molecules are now under pre-clinical and clinical evaluation (*98*). Among them, an anti-CSF1R blocking antibody recently used to treat synovial giant-cell tumors overexpressing CSF-1 elicited some anti-tumor responses (*99*). In other works, treatment with an anti-CSF-1 neutralizing antibody or an inhibitor of the CSF1R signaling cascade enhanced the efficacy of chemotherapy, mice survival and $CD8^+$ T cell response, but also reduced tumor-initiating cells, tumor growth, metastasis and angiogenesis (*100*). Moreover, our group recently demonstrated that blocking CSF1R signaling before ACT reduced the accumulation of TAMs and their suppressive activity without altering Tip-DC generation from precursors and increasing their presence at the tumor site; this resulted in an increased efficacy of the ACT therapy (*33*). Despite some promising results, the overall depletion of monocytes and macrophages by the inhibition of CSF1R is not specific for TAMs and it is reported to be toxic over a long period of time (*101*). Alternatively, transient ablation of TAMs requires a deep knowledge of immune reactions occurring in each phase of tumor progression. Indeed, the treatment can be effective only if the period between one drug administration and the subsequent is sufficient to guarantee monocyte recruitment at the site of inflammation and their differentiation in anti-tumor TAMs.

Interestingly, another therapeutic strategy for TAM-targeting consists in blocking their accumulation at the primary tumor or metastatic site. In particular, tumor cells, through the secretion of CCL2, are able to recruit classical monocytes that express CCR2. High levels of CCL2 in serum and in tumors are correlated with poor prognosis in different type of tumors (*102*). Unfortunately, clinical trials using CCL2-neutralizing antibodies reported no therapeutic advance (*103*).

Instead of targeting all macrophages or blocking their recruitment, a more efficient approach is to reprogram only macrophages with pro-tumor action,

restoring their anti-tumor activity. In this way, long-term toxicity due to the ablation of all macrophages can be overcome. Among the treatments tested to date in pre-clinical and clinical trials there are anti-CD47 antibodies, toll like receptor agonists, anti-CD40 antibodies, MARCO-neutralizing antibodies and histone deacetylase (HDAC), phosphatidylinositol 3-kinase (PI3K), miRNA inhibitors (*104*). Furthermore, TAMs express high levels of PD-L1 and PD-L2, as well as PD-1. TAM-specific PD-1 inhibition reduced tumor growth, whereas CSF1R inhibition enhances the therapeutic efficacy of PD-1 blockade in melanoma models (*104*).

Chapter 2: Disabled Homolog 2; structure and functions

2.1 DAB2 molecular structure

DAB2 (disabled 2, mitogen-responsive phosphoprotein) is an adaptor protein involved in the CME of specific transmembrane receptors, in signal transduction pathways (*105*), cell adhesion, hematopoietic cell differentiation and angiogenesis. The human transcript of DAB2 (originally named as DOC2) was discovered by Liang and Pardee (*106*), while the mouse orthologous protein was identified by Xu and colleagues in the BAC1.2F5 macrophage cell line (*107*). The name of the protein derives from its homology with the Disabled (Dab) gene previously identified in Drosophila melanogaster and known to interact with the Abl tyrosine kinase during neuronal development (*108*).

The DAB2 gene is located in chromosomes 5 and 15 (*109*) in human and mouse genome respectively. Transcripts derived from these two species present approximately 83% identity (*109*).

DAB2 is alternatively spliced to generate two isoforms, named p96 and p67 for their molecular weight of 96 and 67 kDa, respectively. Over the past years, the majority of works describing the role of DAB2 in endocytosis were conducted on the p96 isoform and, for this reason, little is known about the functions of the p67 isoform. The p96 is reported to be phosphorylated in BAC1.2F5 macrophages upon CSF-1 stimulation, a cytokine required *in vivo* and *in vitro* for the differentiation, proliferation and survival of hematopoietic precursor cells of the mononuclear phagocyte lineage, which comprises macrophages and monocytes (*107*).

DAB2 possesses a highly conserved N-terminal PTB (phosphotyrosine-binding) domain with a NPXY motif for the membrane proteins binding, a central clathrin- and adaptor protein-binding domain highly similar to the Drosophila protein, and a proline/serine-rich C-terminal (PRD) domain with binding sites for SH3-domains and myosin VI (Figure 5) (*107, 110*).

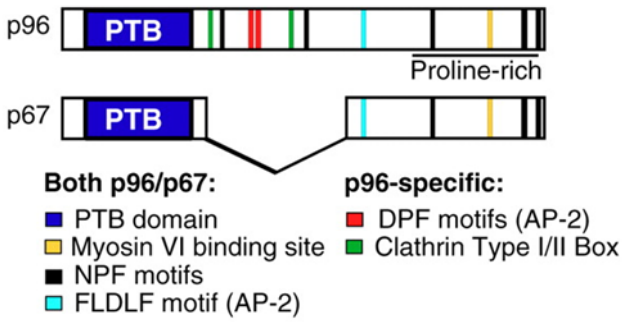

Figure 5. Schematic representation of the two isoforms of DAB2, p96 and p67. Reproduced from Maurer et al., 2005 (*111*).

DAB2 recognizes and binds, through its PTB domain, the NPXY amino acidic sequence present in the intracellular domains of several membrane receptors, like the low-density lipoprotein receptors (LDLRs), megalin, ITGs and E-cadherin (*105, 112, 113*). After binding with receptors which have to be internalized, DAB2 is engaged underneath the plasma membrane, where promotes the formation of clathrin assemblies. The interaction between p96 isoform and clathrin is mediated by an amino acidic sequence in the central region of DAB2 (Figure 5) (*111*). This sequence is missing in p67 isoform, but in the long form it is suitable to bind other endocytic proteins like adaptor protein (AP) 2 (*112*). Intracellular transport of clathrin-coated vesicles requires myosin VI, whose cargo-binding domain interacts with the C-terminus of DAB2 (*114*). Therefore, DAB2 acts as a linker between myosin VI and clathrin, allowing the transfer of clathrin-coated vesicles from the plasma membrane into the cell along actin filaments (*115*). Besides the clathrin-coated vesicles, the DAB2-mediated endocytosis of membrane receptors requires the anchoring of DAB2 to phospholipids through a poly-lysine sequence, close to the PTB domain and able to recognize phosphoinositides with a negative charge. DAB2 binding to phospholipids can be positively or negatively regulated through the phosphorylation of the Ser24 residue, near the poly-lysine sequence (*111*).

2.2 The physiological functions of DAB2

DAB2 is an endocytic adaptor protein widely distributed among body tissues, highly expressed in many epithelial cell types and entailed in several physiological processes as well as in embryonic development (*116*).

Endocytosis is the conserved mechanism used by eukaryotic cells to internalize plasma membrane proteins lipids, extracellular fluids, molecules, exosomes and pathogens. Through this process, cells are able to uptake nutrients, receive and transmit signals from microenvironment, recycle membrane components, present Ags, carry out neurotransmission at synapses, and migrate (*115*).

Endocytic pathway can be divided in: CME (also referred as receptor-mediated endocytosis), phagocytosis, pinocytosis and caveolae-dependent.

CME is the most studied endocytic route, although it is not the most frequent one. It is involved in the internalization of a great variety of transmembrane receptors and associated ligands, forming 50-100 nm membrane vesicles (*117*). CME consists of five steps: nucleation, cargo selection, coat assembly, scission and uncoating (Figure 6). The first phase starts with an alteration of the plasma membrane curvature in the region to be internalized. In particular, many AP complex intervene in the CME process either acting directly, by promoting the bending of the membrane and acting as scaffold molecules, or indirectly by recruiting auxiliary proteins (such as AP180, epsins and auxilin) (*117*). In mammals, different AP complexes have been identified, including AP-2, which is recruited to the nucleation module and connects at the same time the membrane, the target receptor, cargo-specific accessory proteins and clathrin. Examples of cargo-specific adaptor and accessory proteins are β-arrestins and Dishevelled for G protein-coupled receptors (GPCRs), low density lipoprotein receptor adapter protein 1 (ARH) for LDLRs, Numb for Notch receptors, Arf-GAP domain and FG repeats-containing protein (AGFG1) for SNARE proteins, stonin for synaptotagmin and DAB2 for LDLRs, megalin, ITGs and E-cadherin (*105, 118*).

Once cargo is selected, recruited soluble clathrin polimerizes beneath the inner face of the cell membrane (*117*). This coating structure promotes the deformation of the membrane to form clathrin-coated pits (CCPs) and stabilizes its curvature. Clathrin and adaptor proteins force a further bending of the CCP until the upper

edges are close enough to allow the binding of the scission protein dynamin, a GTPase that causes the scission of the clathrin-coated vesicle (CCV) and its release into the cytoplasm (*119*). After this phase, CCVs lose their clathrin coating aided by the ATPase heat shock cognate 70 (HSC70) and other proteins (*117*).

Actin polymerization might enhance membrane bending in the case of large cargoes (i.e bacteria), when the membrane is particularly rigid, as in yeast, or submitted to high tension, such as in adherent cells (*120*). Moreover, actin filaments are required for CCV trafficking inside the cell. Myosins are actin-bound motor proteins that associate with the newly formed CCVs favoring their directional movement from the membrane towards the destination compartment. An example is myosin VI, a minus-end-directed motor protein that can be recruited by DAB2 (*114*).

Finally, the CCVs fuse with early/sorting endosomes to deliver their cargoes. Internalized receptors can be recycled back to the surface membrane for a continuous ligand binding and transduction of the signal, or targeted to more mature compartments known as late endosomes or multivesicular bodies (MVBs), which can fuse with lysosomes for degradation of the internalized material (*121*), for normal protein turnover or termination of the signaling. Alternatively, receptor-bound ligands inside endosomes can begin a signal amplification pathway inside the cell (*117*).

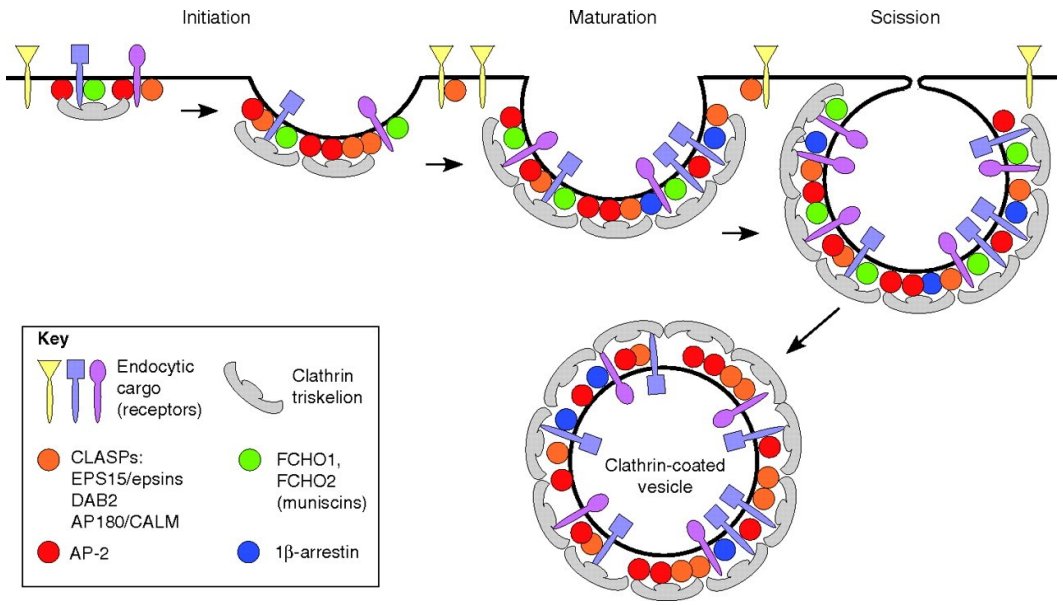

Figure 6. Schematic representation of clathrin-mediated endocytosis. The process begins when adaptor and clathrin complexes associate with the selected cargo, initiating the formation of a coated pit. As the pit matures, additional adaptor and scaffold proteins (CLASPs) bind the inner face of the cell membrane, promoting its bending. Upon dynamin intervention, the forming vesicle is released from the original site to the cytoplasm (scission). Finally, the clathrin-coated vesicle loses its coating and the cargo can be trafficked to the endosomal compartment of destination. Examples of different cargos are reported in different colors. Blue and violet cargos contain motifs able to recognize and bind clathrin-associated adaptors. These type of cargos can therefore be engulfed into the forming CCP. Conversely, yellow cargos are internalized through a clathrin-independent pathway. Reproduced from Reider and Wendland, 2011 (*122*).

The ability of DAB2 to internalize and mediate the recycling of surface receptors like ITGs and E-cadherin is associated to the modulation of the spatial organization and polarization of the cells (*105*). DAB2 downregulation determines a disorganized and basement membrane-independent growth of cells, as it occurs in ovarian and breast carcinomas (*123*). Furthermore, DAB2 is important for a normal embryonal development, mediating the internalization of megalin, cubilin, cholesterol and E-cadherin in the visceral endoderm of mice embryos (*111*). Before the formation of placenta, transport across the visceral endoderm is the only way the developing embryo can assimilate maternal proteins and lipids. As consequence, the genetic ablation of *Dab2* in mice results lethal due to developmental defects, caused by loss of nutrients and endodermal cell organization (*114*).

DAB2 was shown to have a role also in kidney functioning. Conditionally mutant *Dab2* KO mice showed defects in the formation of CCP in kidney proximal tubule cells and in the transport of the megalin lipoprotein receptor. Consequently, KO mice had excessive levels of plasma proteins in the urine (*114*).

DAB2 is also expressed in platelets and has been implicated in homeostasis and in the positive control of blood clotting by interacting with G protein-mediated thrombin signaling (*124*).

2.3 DAB2 can act either as tumor suppressor or promoting factor

DAB2 is considered to be a tumor suppressor and has long been described as a predictor of poor prognosis and metastasis (*125*). DAB2 depletion or downregulation has been observed in tumors of the ovary, colon, breast, prostate, oesophagus, bladder, head and neck, nasopharynx, and in some of these cases in

the associated metastases (*125-127*). Forced re-expression of *Dab2* restrained cell growth and tumorigenicity of cancer cell lines (*123*). However, DAB2 negatively regulates cell growth and survival not only in cancer. For example, during pregnancy and lactation in mice, mammary epithelial cells proliferate and their DAB2 level is low; in contrast, during mammary gland evolution, mammary epithelial cells are partially eliminated and DAB2 level is high.

The tumor suppressor and growth inhibitory role of DAB2 derives from its intervention in the modulation of several cancer-related pathways including Ras/mitogen-activated protein kinase (Ras/MAPK) (*110*), TGF-β (*128*), and Wnt (*129*) signaling.

The Ras/MAPK pathway is activated by mitogens like EGF and leads to the transcriptional regulation of several genes, a prominent fraction of which is involved in cell cycle entry and proliferation (*130*). Under physiological conditions, DAB2 inhibits this pathway by blocking extracellular signal-related kinase (ERK) and c-Fos activation (*130*), whereas under a pathological context, DAB2 is downregulated, often by the oncogene *Ras* itself, and cells can proliferate without control (*130*).

DAB2 was also shown to participate in the signal transduction from the TGF-β receptors to the transcriptional activators belonging to the small mothers against decapentaplegic homolog (SMAD) family (*125*). In normal epithelial cells, TGF-β acts as tumor suppressor by inhibiting cell proliferation and stimulating apoptosis. DAB2 depletion in cancer cells is associated with the loss of the TGF-β tumor suppressor function and a promotion of TGF-β–aided cell motility, EMT and tumor growth (*125*).

In the late phases of tumor progression, TGF-β assumes a pro-metastatic role that might be due to its ability to stimulate EMT (*131*). Autocrine TGF-β signaling loop, stimulated by the tumor-associated activation of Ras/MAPK signaling, can stabilize further EMT phenotype and tumor cell invasive properties *in vitro* and *in vivo* (*132*). Moreover, DAB2 loss caused a reduction in TGF-β receptor internalization via CME and the consequent accumulation of TGF-β in extracellular space resulted into conversion of naïve $CD4^+$ T cells to pro-tumor Tregs (*133*).

Finally, the Wnt pathway plays a pivotal role in modulating cellular proliferation and differentiation, as well as tissue organization and embryonic development. It initially requires caveolin-dependent internalization of low-density lipoprotein receptor-related protein 6 (LRP6). DAB2 acts as a negative regulator of the Wnt signaling in several ways, but in particular by engaging LRP6 in CME so that it is not available for caveolin-mediated endocytosis (*134*). Cancer cells can suppress this DAB2-mediated inhibitory activity and can divide in an uncontrolled manner (*134*).

In addition to the literature showing a role for DAB2 as a tumor suppressor, other evidence suggests a DAB2 pro-tumor role. Recently, a signature of genes including *DAB2* (e.g. *DOCK10, DAB2, ITGA11, PDGFRA, VASN, PPAP2B*, and *LPAR1* genes) was described to be expressed by an epigenetically distinct subpopulations of breast tumor cells. These cells are named "trailblazer" cells due to their enhanced capacity to initiate collective invasion and guide migration of passenger cancer cells. This seven-gene signature correlated with poor outcome in human triple negative breast cancer (TNBC) patients (*135*). Moreover, DAB2 is required for migration and invasion of prostate cancer cells (*136*). In another work, DAB2-expressing cancer cells were showed to release TGF-β, which in turn induced ECs migration and angiogenesis (*137*).

2.4 DAB2 in myeloid cell populations

Despite studies on tumor cells and fibroblasts, the role of DAB2 in myeloid cells has not been completely elucidated yet. One of the few works about the localization and the function of DAB2 in these cells was published by Rosenbauer and colleagues. They demonstrated that DAB2 is expressed in BM-derived macrophages and is essential for both cellular adhesion and spreading on the ECM components LN and collagen type IV (COL IV) (*138*).

DAB2 was reported to be expressed in M2 macrophages and down-regulated in M1 macrophages isolated from both humans and mice. Interestingly, mice lacking *Dab2* in myeloid lineage and treated with LPS or fed with high-fat food showed an increased M1 macrophage polarization along with a pro-inflammatory gene

signature compared to control mice. DAB2 directs phenotypic polarization interacting with TNF receptor-associated factor 6 (TRAF6) and reducing the activation of the pro-inflammatory transcription factor NF-κB p65 (*139*).

A role for DAB2 was also proposed in both human and mouse DCs, where DAB2 was significantly induced during the CSF-2–driven differentiation and required the activation of STAT5 and heterogeneous nuclear ribonucleoprotein (hnRNPE) 1 as well as the expression of forkhead box P3 (FOXP3). Remarkably, DAB2 was associated with a reduced IL-12 and IL-6 expression, Ag uptake, migration, T cell stimulation and therapeutic efficacy when DCs were used as vaccines. In contrast, *Dab2*-depleted DCs displayed an increase in all these functions (*140*). These studies indicate that DAB2 has an anti-inflammatory role, but further work is necessary to elucidate its function and regulation in the myeloid compartment.

Chapter 3: Integrins and extracellular matrix in mechanotransduction

3.1 Extracellular matrix: composition

ECM is one of the major components of the cellular microenvironment. It provides physical scaffolding for cellular constituents and participates in several key processes such as cellular growth, differentiation, survival, adhesion and migration. ECM is a complex three-dimensional macromolecular network, composed of a variety of fibrillary molecules, such as COL and FN, and non-fibrillar molecules like proteoglycans and glycosaminoglycans. These components interact with each other and with resident cells (fibroblasts, immune cells, endothelial cells, epithelial cells and pericytes) through cell surface receptors (ITGs, discoidin domain receptors – DDRs, HA receptors etc.), with the aim of regulating the biochemical and biomechanical properties of each tissue. Notably, ECM is highly heterogeneous and dynamic; indeed, ECM undergoes a constant remodeling, either enzymatical or non-enzymatical, and its components are subject to a large number of post-translational modifications. Considering that ECM is continuously remodeled either during normal and pathological conditions, a fine-tuning of ECM composition and structure is necessary for tissue wholeness and functionality.

- ***Collagen***

Collagens are the most abundant fibrous components in the ECM and connective tissue, representing approximately 25% of the total dry weight of mammals. They provide extensive tensile strength, regulate cell adhesion, support chemotaxis and direct tissue development (*141*). They also participate in cell organization through the binding with other matrix proteins and cellular receptors. In particular, COL interact with four different ITGs (α1β1, α2β1, α10β1 and α11β1). Considering that the family comprises 28 different collagen types, classified in fibrillary and non-fibrillar collagens, tissues are characterized by a heterogeneous network of fibers with a triple helical conformation or packed side-by-side to form a stronger reticulum.

Extensive COL deposition is one of the main pathological characteristic of some cancers and results in poor survival outcome in patients (*142*). Under hypoxic conditions, the upregulation of lysyl-hydroxylase (LOX) mediates the cross-linking of COL I microfibrils and the promotion of invasive properties of human cancer cells through focal adhesion kinase (FAK) activity and cell-matrix adhesion (*143*). LOX has recently been implicated in hypoxia-induced metastasis and it might be required to create a permissive niche for metastatic growth (*144*).

During cancer progression, mutations to oncogenes also alter the COL conditions within the tumor matrix. Mutated p53 in cancer cells, along with the activation of STAT3, influence COL production (*145*). Similarly, deletion or silencing of PTEN result in the increased recruitment of CAFs, which promote COL deposition (*146*). An increased COL synthesis is also promoted by NF-κB and STATs transcription factors (*147*), as well as by the crosstalk between TGF-β and RAS/MAK pathway (*148*). High-density COL significantly impairs tumor-infiltrating $CD8^+$ T cell proliferation in mammary tumors compared to low-density matrix (*149*).

Fibrillar COL I, COL III, and COL V are mainly produced by fibroblasts, whereas COL IV is predominantly expressed by epithelial and endothelial cells. Notably, cancer cells and TAMs also produce COL under some circumstances (*150*). COL interacts with cells mainly by directly binding with DDRs. COL-DDRs interaction promotes EMT transition and MMPs secretion (*151*). TAMs orchestrate the deposition, crosslinking, and linearization of COL fibers at areas of tumor invasiveness. Additionally, degraded COL acts as a strong chemoattractant for macrophages that mediate cancer promotion (*152*). Although macrophages do not exhibit efficient COL internalization of mesenchymal origin, those originating from circulating CCR2 monocytes internalize COL in an MMP-dependent manner (*153*).

Considering that the increased expression and the dense organization of COL are indicative of cancer progression (*154*) and poor clinical outcome (*155*), these molecules can be viewed as predictor of prognosis. In esophageal cancer, increased COL content was associated with chemotherapy resistance via the MAPK and PI3K/AKT signaling pathways (*156*). In the same way, COL

crosslinking at the metastatic site correlated with increased tissue stiffness and reduced treatment efficacy (*157*). Therefore, the combination of COL inhibitors and standard therapeutics could represent a promising anticancer strategy.

- ***Fibronectin***

FN is a fibril-forming glycoprotein, which dimerizes starting from two identical proteins of 250 kDa, covalently attached via disulfide bonds at their C-terminal. FN can be found in soluble form in the plasma or self-assembled in interconnected fibers. FN is highly resilient to mechanical stress and its force-dependent unfolding causes the exposure of ITG-binding sites, among which the α5β1 ITG binding site. Considering its activity in this process, FN could be considered a mechano-regulator.

Under homeostatic conditions, FN is involved in cell growth, differentiation, migration, wound healing and blood coagulation (*158*). However, it has been demonstrated that this protein has also a role in cancer progression and cancer cell exposure to cellular FN is sufficient to activate the EMT transition via STAT3 signaling pathway (*159*). In cancer, the upregulation of FN by CAFs is linked to a decreased survival and a limited tumor cell responsiveness to therapy (*160*). Besides increasing production, CAFs align FN fibers in a highly organized structure that allows the tumor cells to move according to a mechanism called haptotaxis. The aligned fibers in fact provides tensile support for cancer cells to pull itself outside the primary tumor (*161*). When CAFs are removed, ECM assumes a disorganized structure at the tumor interface, which translates into slower tumor invasion.

From a molecular point of view, the interaction between FN and α5β1 heterodimers rapidly activates FAK, which in turn trigger a downstream invasion cascade. Notably, FAK inhibition is sufficient to abrogate the ability of FN to drive invasiveness in lung cancer (*162*).

Considering its pro-tumor role, FN has emerged as possible therapeutic target. Nowadays, human trials are still preliminary but promising (*163*). Other therapeutic approaches rely on interrupting the interactions between FN and its

ITG partners. At the present time, a growing preclinical literature supports the anti-tumor effect of α5β1-directed antibody (*164*).

- ***Laminin***

LN is an important component of basement membranes consisting of large cross-shaped heterodimers of α, β and γ-chains, encoded by five LAMA, three LAMB and three LAMC genes, respectively. Although numerous possible heterodimers could exist, only 16 LN combinations have been found *in vivo*. These proteins are known to form a self-assembled network, which interacts with COL IV and epithelial cells through cell surface receptors. Four ITGs recognize laminins as their extracellular ligands: α3β1, α6β1, α7β1 and α6β4 (*165*).

Over the last decades evidence for a LN role in cancer has emerged (*166*). LN -332, -511 and -111 appear to be particularly important in tumor cell growth and migration. α3β1, α6β1, and α6β4 are entailed in cancer development and progression, but there is little evidence for such role of α7β1 in tumorigenesis (*167*). Among these ITGs, α6β1 heterodimer has been described as tumor promoter, contributing to the tumor cell spreading as well as mediating dissemination and the formation of metastasis in areas rich in LN (*168*). Recently, LNs were defined as regulators of CSCs, suggesting their role in long-term cancer maintenance, metastasis development and therapeutic resistance. The accumulating evidence in this emerging research area indicates that LNs represent potential therapeutic targets for anti-cancer treatments against CSCs and that they may be used as predictive and prognostic markers (*169*).

- ***Other proteins***

Matricellular proteins are nonstructural matrix glycoproteins whose function is dependent on the interaction with ECM components, cell-surface receptors (ITGs, TLRs, growth factor receptors), cytokines and proteases that, in turn, interact with the cell surface (*170*). They are present in the ECM, but they can be also found in the body fluids. Among these proteins thrombospondins, tenascins, ospeopontin, periostin and VN can be listed. VN is defined as matricellular protein due to its substantial presence in plasma and its function as organizer of the extracellular

microenvironment. The activity of VN is determined by interactions with ligands, which induce conformational change and multimeric complexes formation. The VN interaction with αvβ1, αvβ3, αvβ5, αvβ6, and αvβ8 ITGs (*171*) stimulates phosphorylation of intracellular targets and ITG clustering on the cell surface, linking ECM components to outside-in signaling cascades. Through interactions with cancer cell-surface ITGs and urokinase-type plasminogen activator receptor (uPAR), VN modulates cancer metastasis, acting as a scaffold for tumor and ECs migration during invasion and angiogenesis, respectively (*172*). *In vitro*, migration of highly metastatic breast cancer cell lines is affected when αvβ3 and αvβ5 receptors are blocked with antagonists (*173*). These ITGs are also critical for angiogenesis. Indeed, in the absence of VN, the structural components of coagulation (e.g. FN, fibrinogen, COL and serine protease zymogens) are not able to self-assemble and regulate 'outside-in' and 'inside-out' signaling events (*174*). VN is also known to be up-regulated in the extravascular space of tissues experiencing stress, e.g. pro-inflammatory response (*175*). It also accumulates in the interstitial space around tumor islands (carcinomas and sarcomas) and in immune complexes associated with chronic inflammatory diseases (e.g. rheumatoid arthritis) and chronic fibrotic diseases (e.g. lung, liver and kidney fibrosis) (*175*).

3.2 Contribution in cancer cell invasion: ECM stiffness and degradation

The TME is the cellular environment in which tumor cells co-exist along with tumor-infiltrating immune cells (e.g. lymphocytes, DCs, MDSCs and TAMs) and non-hematopoietic stromal cells such as CAFs and ECs. The TME also consists in ECM and cytokines secreted by those cells (*2*) and the interaction between the stromal compartment and immune cells within TME promote tumor growth, metastasis and chemoresistance (*176*). During tumor progression, ECM undergoes extensive changes, among which rearrangement, cross-linking, deposition and degradation of specific proteins can be listed.

Deposition of new matrices is a typical process occurring in neoplastic tissues, considerably stiffer compared to their normal counterpart (*177*). This ECM

protein accumulation provides tumor support, drug resistance and causes the disruption of tissue morphogenesis by increasing cell tension. In clinic, the ratio of stiff tissue (proteins and connective tissue) and soft tissue (adipocites) correlates positively with the risk of developing breast cancer (*178*). ECM stiffness can also be predictive of an increased number of metastases and a poor clinical outcome (*179*).

The other main modification that occurs during tumor progression is the matrix proteolysis, which involves the release of growth factors, cytokines and MMPs. VEGF and TGFβ promote neo-angiogenesis facilitating tumor cell intravasation, while MMPs, a family of highly conserved zinc-dependent endopeptidases, are responsible for ECM degradation, which in turn favors cancer cell escape from the primary tumor and neoplastic cells dissemination to distant organs. These enzymes are released in an inactive form and, in healthy tissues, their activity is under strict control of endogenous tissue inhibitors (TIMPs), which guarantee a balance between enzyme activation and inhibition. Under pathological conditions (i.e. tumors), the ratio MMP/TIMP is destroyed and MMPs are activated by oxidation or proteolytic cleavage. Notably, cancer cells are known to contribute in the MMP activation process releasing reactive oxygen species (*180*).

3.3 Signals related to ECM-cells contact

Interactions between cells and ECM are bi-directional. On one hand, cells actively modify ECM through remodeling, degradation and deposition of new matrix. On the other hand, the composition and the mechanical properties of the ECM modulate key processes in cells (*177*). Cells sense the surrounding environment through mechanical linkers such as ITGs (*181*). As previously mentioned, ITGs are 24 different heterodimers yielded by the combination of 18 α and 8 β subunits, each specific for one or more ligands (*182*). ITGs regulate a large number of cellular biological functions, acting as bidirectional signal transducers. These receptors take contact with specific ECM proteins through their extracellular domains, whereas their cytoplasmic domains indirectly interact with actin cytoskeleton.

When ITG receptors undergoes activation, other ITGs, APs (e.g. talin and vinculin) and kinases (e.g. FAK) accumulate in proximity of the activated site, inducing downstream pathways in a process called mechanotransduction (*181*).

ITG activation could be triggered by an inside-out or an outside-in signal. Inside out activation requires the interaction between the cytoplasmic tail of ITG β-subunit and the intracellular protein talin, which provokes a conformational change in the ITG structure. Talin promotes the separation of α and β cytoplasmic domains, causing the intracellular interaction with vinculin and then, in turn, with actin cytoskeleton. The subsequent extension of extracellular domains is associated with an increased ligand affinity (*113*).

Alternatively, ITGs can activate a cascade of outside-in signaling. ITG bound to ECM proteins are able to sense the tissue rigidity by an increased tension on the actin cytoskeleton, which results in focal adhesion complexes (FAs) formation (*183*) and cell migration. FAK are one of the major component of the FA and, in fibroblasts, their recruitment has been suggested to precede talin recruitment (*184*), while their activation occurs by an auto phosphorylation at tyrosine 397 (Y397) after ITG clustering (*185*). This post-translational modification generates a high affinity site for binding with Src proteins to form a FAK-Src complex (*186*). However, Src may also bind FAK in a process independent from Y397 phosphorylation (*187*). Upon binding, Src trans-phosphorylates FAK at multiple sites (Y576 and Y577), and exposes binding sites for scaffold/adaptor proteins like paxillin and CAS30. This process leads to downstream activation of Rho-family of GTPases: Rac, Ras and Rho (*188*). Rac induces actin polymerization (*189*) and activation of MMPs. Ras promotes the ERK/MAPK pathway, which stimulates mitogenesis, proliferations and MMP secretion (*185*). Rho is a regulator of adhesion and cytoskeleton dynamics, proliferation, migration and MMP secretion (*190*). Moreover, Rho inhibits myosin light chain 6 phosphatase (MLCP) and activates myosin light chain kinase (MLCK) via Rho-associated kinase (ROCK) activity, increasing actomyosin contractility (26). Similarly to ROCK, ERK prompts actomyosin contractility through MLCK activation (*188*). Furthermore, the FAK-Src complex can activate PI3K, which phosphorylates PIP2 (phosphatidylinositol 4,5-bisphosphate) to form PIP3 (phosphatidlyinositol-

3,4,5-trisphosphate). PIP3 activates the serine/threonine-specific protein kinase AKT (*185*), a key factor involved in regulation of proliferation and survival (*191*). ECM-unbound (i.e. inactive) ITGs, freely diffusing in the phospholipidic bilayer or localized in focal adhesions that are no more useful for the cell, are internalized by DAB2 adaptor protein (*192*). In this way, DAB2 maintains an internal pool of ITGs that can be either degraded for normal ITG turnover or recycled back to the plasma membrane in order to assemble new focal adhesions for either anchorage or migration (*193, 194*). The position of these new contact sites with the ECM depends on the cell type and on the biological context: for example, in some cases cell motility requires assembly of focal adhesions at the front of the cell (leading edge-driven movement), while in others at the cell rear (rear-steering movement) (*192*). Thus, the CME-dependent vesicular trafficking that occurs inside the cell has the important function to arrange ITGs in specific regions of the plasma membrane where they can carry out their functions. The resultant 'molecular polarization' of the cell confers to DAB2 a key role in many processes, such as epithelial cell spatial organization, cellular adhesion to the ECM, cell migration and spreading. Up to date, DAB2 involvement in ITG endocytosis has been studied almost exclusively in fibroblasts and tumor cell lines (*194, 195*).

3.4 Role of YAP/TAZ in cell-matrix adhesion-mediated signaling and mechanotransduction

Cells sense the surrounding environment not only through soluble signals, but also through physical and mechanical cues, such as ECM stiffness or cell-cell contact. By mechanotransduction, cells translate these stimuli into biochemical signals, inducing the activation of specific downstream pathways, including the regulation of cell growth, cell differentiation, tumor progression and ECM reorganization. Among transcriptional factors regulated by ECM, YAP and TAZ are related to cancer progress, well-studied in tumor cells and fibroblast, and recently emerged as sensors of ECM mechanical properties (Figure 7). Indeed, soft matrices induce their cytoplasmic retention, whereas rigid matrices cause their nuclear transfer and activation (*196*). Once in the nucleus, YAP and TAZ interact with other

transcription factors, in particular the transcriptional enhancer factor TEF (TEAD) family members, and activate the expression of growth- and differentiation-related genes (*196, 197*). Once bound to DNA, they promote enhancer acetylation and transcription elongation (*198*).

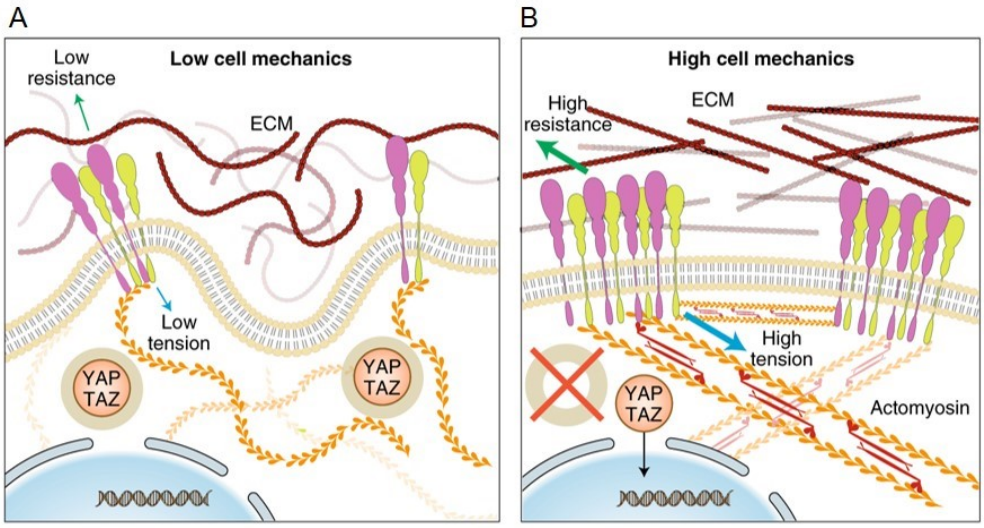

Figure 7. YAP and TAZ as sensors and mediators of mechanical inputs from the extracellular matrix. (A) In soft matrices, YAP and TAZ are inactivated and localized into the cytoplasm. Reduced YAP and TAZ activity determines apoptosis and growth arrest. (B) In stiff condition, YAP and TAZ accumulate in the nucleus, activating pathway related to cellular proliferation and inhibition of apoptotic signals. Adapted from Totaro et al. 2018 (*199*).

It has to be mentioned that, YAP/TAZ activation is not only depended on the physical shape of the microenvironment, but it is the result of the integration of several signals. YAP and TAZ are negatively regulated by the kinases of Hippo pathway and they respond to growth factors and soluble signals through crosstalk with many signaling pathways, including WNT, TGFβ and EGFR signaling. The YAP/TAZ activity is also mediated by the G-protein-coupled receptors activation and by cellular metabolic state, intended as nutrient availability (glucose, amino acids and lipids) (*200*). Under physiological conditions, YAP/TAZ participate in tissue repair process, provoking the regrowth of the missing or damaged tissue. This mechanism is potentiated during tumorigenesis, where changes in ECM composition and rigidity are common. Considering that neoplastic tissues are stiffer in comparison to healthy tissues, it is not surprising that YAP/TAZ

transcriptional factors are highly expressed in human and mouse malignancies and that their activation seems to sustain stiffness-dependent tumor initiation and progression (*198*). In transformed cells, they foster excessive proliferation (even when contact inhibition of proliferation should block it), survival and motility in response to mechanical inputs from the ECM (*197*). The genes they activate are involved in DNA duplication and repair, S-phase entry and mitosis. Moreover, YAP/TAZ could turn on c-Myc (*201*) and other proto-oncogenic transcription factors, such as AP-1 family (JUN and FOS-like factors) (*202*).

YAP/TAZ in cancer cells have also been associated with increased resistance to anoikis and apoptosis, preventing both the intrinsic and the extrinsic pathways (*203*), as well as increased autophagy rate aimed at rescuing cells from senescence (*204*). Interestingly, these transcription regulators are expressed in CSC subpopulations and promote CSC characteristics, such as the abilities to generate undifferentiated precursors, initiate tumor growth, survive chemotherapy and form metastases (*205*). Furthermore, YAP and TAZ promote the cytoskeletal remodeling necessary for the metastatic process, by the regulation of F-actin dynamics through the promotion of the transcription of genes encoding Rho-GTPase activating proteins (*183*). The communication between the YAP/TAZ-expressing tumor cells and the neighbors stromal cells is bi-lateral. On one hand, YAP/TAZ in tumor cells coordinate the responses of stromal cells. On the other hand, CAFs have been demonstrated to express YAP/TAZ in a pathway that foster the deposition of ECM by CAFs themselves in order to increase ECM stiffness and sustain expression of YAP/TAZ in a self-reinforcing loop (*206*). Another pro-tumor mechanism of action carried out by YAP/TAZ in cancer cells consists in their capacity to reprogram the TME: for example, they induce epithelial cells to release angiogenic factors like amphiregulin (AREG) or recruit myeloid suppressor populations (*197, 207*).

In conclusion, all these findings on YAP and TAZ activities can explain why their expression in human and mouse cancers correlates with malignant clinico-pathological features, such as high histological grade, cancer stemness, metastasis, chemoresistance, relapse and general poor outcome (*198*).

AIM OF THE STUDY

Metastases represent the end product of a multi-step biological process that involves the spreading of malignant cells to anatomically distant organ sites and their subsequent adaptation to a favorable microenvironment. Despite high frequency and mortality associated to the metastasis development, the knowledge of cellular and molecular mechanisms that underlies this pathological process remain limited.

During tumor progression, cancer cells have the capacity to arrange intricate interactions within TME and to reprogram stromal cells, receiving their support in ECM synthesis or degradation, neoangiogenesis and tumor cell growth. Transformed cells are also able to affect normal hematopoiesis, recruiting myeloid cells with pro-tumor functions. Among these cells, TAMs are one of the most abundant leukocyte population in the tumor context, responsible of ECM remodeling and metastatic promotion.

Considering the recent exciting literature regarding the importance to overcome TAM functions for the therapy of established cancers, we aimed at identifying new molecular pathways involved in tumor dissemination. Here, we propose DAB2, a clathrin adaptor protein upregulated in tumor-infiltrating myeloid cells, as a novel target to control the metastatic process.

The aim of this project was to dissect the role of DAB2 in regulating the myeloid-assisted tumor cell spreading and metastasis formation. For this purpose, we exploited conditional *Dab2* deficient mice, missing the gene in the hematopoietic lineage. The first step of our work was to identify in which myeloid subset DAB2 was expressed and where $DAB2^+$ cells were localized within the TME. We then evaluated the mechanism through which $DAB2^+$ macrophages were able to guide cancer cell invasion and, in particular, we explored the ITG-mediated ECM remodeling process with both *in vitro* and *in vivo* experiments. To confirm further the role of DAB2-expressing macrophages in tumor promotion, we used the genome editing CRISPR/Cas9 technology, which allowed us to fully prevent the expression of DAB2 and DAB2-interacting ITGs in a mouse macrophage cell line

and demonstrate how ECM composition was essential for the tumor invasive ability promoted by DAB2.

Successively, we identified which stimuli were responsible for DAB2 expression and whether this protein was involved in other steps of the metastatic cascade (e.g. extravasation, cell seeding and proliferation).

Finally, considering the functions exerted by DAB2-expressing macrophages in mouse tumor models, we moved to the clinic in order to disclose the presence of these $DAB2^{+}$ cells in human patients and, overall, to confirm DAB-expressing macrophages as a potential biomarker for cancer patient stratification and outcome.

MATERIALS AND METHODS

Animal studies

Eight-week-old C57BL/6 WT mice were purchased from Charles River Laboratories Inc. (Calco, Italy). *Tie2-Cre* and *Dab2*$^{flox/flox}$ mice were originally provided to P.J. Murray (then at St. Jude Children's Research Hospital) from J.A. Cooper (Fred Hutchinson Cancer Center) and were crossbred in order to generate *Dab2* KO mice. *LySM-Cre* mice were a gift from P. Scapini (University of Verona, Italy). MMTV-PyMT mice on the C57BL/6 background were kindly provided by M.P. Colombo (Fondazione IRCCS Istituto Nazionale dei Tumori, Milan, Italy). MMTV-PyMT, *Dab2*$^{flox/flox}$, *Tie2-Cre*$^{+}$ mice were generated in house by crossing three strains and maintained by intercross. *Yap/Taz* KO mice were kindly provided by S. Piccolo (University of Padua, Italy). OT-1 TCR-transgenic mice (C57BL/6-Tg(TcraTcrb)1100Mjb/J) and CD45.1^{+} congenic mice (B6.SJL-PtrcaPepcb/BoyJ) were purchased from Jackson Laboratories (Bar Harbor, ME, USA). All mice were maintained under specific pathogen-free conditions in the animal facility of the University of Verona. Animal experiments were performed according to national (protocol number 12722 approved by the Ministerial Decree Number 14/2012-B of January 18, 2012 and protocol number BR15/08 approved by the Ministerial Decree Number 925/2015-PR of August 28, 2015) and Europeans laws and regulations. All animal experiments were approved by Verona University Ethical Committee and conducted according to the guidelines of Federation of European Laboratory Animal Science Association (FELASA). All animal experiments were in accordance with the Amsterdam Protocol on animal protection and welfare: mice were monitored daily and euthanized when displaying excessive discomfort.

Breast cancer patients

In order to explore the prognosis (in terms of disease-free survival, DFS) according to DAB2 expression, tumor samples with clinical annotations from a

series of 32 patients affected by pure invasive lobular carcinoma (ILC) (Table 1), surgically treated at the University Hospital of Verona, were collected. A database for individual data and information was appropriately fulfilled. The study was approved by the local Ethics Committee (Prot. CESC n° 24163, May 20th, 2014)

Clinical-pathological characteristics	Subcategories	Number of Patients (%)
Menopausal status	Premenopausal	10 (31.2)
	Postmenopausal	22 (68.8)
Performance status (ECOG)	0	28 (87.5)
	1	3 (9.4)
	2	1 (3.1)
Ki67	≤4%	9 (28.1)
	>4%	21 (65.6)
	Unknown	2 (6.3)
Grading	1	4 (12.5)
	2	7 (21.8)
	3	6 (18.8)
	Unknown	15 (46.9)
Oestrogen Receptor status	Positive	27 (84.3)
	Negative	2 (6.3)
	Unknown	3 (9.4)
Progesterone Receptor status	Positive	22 (68.8)
	Negative	3 (9.4)
	Unknown	7 (21.8)
HER2 status	Positive	3 (9.4)
	Negative	15 (46.9)
	Unknown	14 (43.7)
T category according to TNM	1	11 (34.4)
	2	18 (56.3)
[7° Edition]	3	2 (6.3)
	4	1 (3.1)
Lymph-nodal Status	Positive	13 (40.6)
	Negative	19 (59.4)
Vascular Invasion	Present	9 (28.1)
	Absent	11 (34.4)
	Unknown	12 (37.5)
Multifocality	Present	6 (18.8)
	Absent	26 (81.2)
Type of Surgery	Conservative	16 (50.0)
	Mastectomy	16 (50.0)
Lymph-node Dissection	Yes	26 (81.2)
	No	6 (18.8)

Table 1. Clinico-pathological characteristics of invasive lobular breast cancer patients.

Gastric cancer patient

The potential prognostic role of DAB2 in gastric cancer was evaluated in terms of cancer-specific survival (CSS) and overall survival (OS). Data and samples from 59 patients affected by gastric cancer undergone surgery at the University

Hospital of Verona were collected (Table 2). Tumor samples were available in tissue microarrays with tumor cores of each considered case and obtained from the inner part of the tumors. The study was approved by the local Ethics Committee (Prot. CESC n° 19147 November 28th, 2011).

Clinical-pathological characteristics	Subcategories	Number of Patients (%)
Gender	Male	18 (30.5)
	Female	41 (69.5)
Grading	1	9 (15.3)
	2	24 (40.7)
	3	21 (35.5)
	Unknown	5 (8.5)
T category according to TNM [7° Edition]	2	9 (15.3)
	3	18 (30.5)
	4a	28 (47.5)
	4b	4 (6.7)
Node status according to TNM [7° Edition]	0	18 (30.5)
	1	11 (18.6)
	2	15 (25.4)
	3a	9 (15.3)
	3b	6 (10.2)
Site	Antrum	22 (37.3)
	Body	15 (25.4)
	Fundus	20 (33.9)
	Gastric stump	2 (3.4)
Type of Surgery	Partial gastrectomy	15 (25.4)
	Total gastrectomy	39 (66.1)
	Gastroesophagectomy	5 (8.5)

Table 2. Clinico-pathological characteristics of gastric cancer patients.

Cell culture

Mouse E0771 breast cancer cells derived from C57BL/6J mice (*CH3 BioSystems*) were cultured in RPMI 1640 supplemented with 2mM L-glutamine, 10mM HEPES, 1mM sodium pyruvate, 150U/mL streptomycin, 200U/mL penicillin/streptomycin (all from Euroclone, Milan, Italy) and 10% heat-inactivated fetal bovine serum (FBS; Superior, Merck, Darmstadt, Germany). Mouse MN-MCA1 fibrosarcoma cell line (gift from Prof. A. Sica, Istituto Humanitas, Milan, Italy), RAW264.7 macrophages cell line (ATCC®), SVEC4-10 endothelial cell line (gift from Prof. A. Viola, Istituto di Ricerca Pediatrica, Padua, Italy), EL4 lymphoblast cell line (ATCC®), MCA203 3-

methylcholanthrene-induced fibrosarcoma cell line (ATCC®) and MCA205 weakly immunogenic fibrosarcoma cell line (gift from Prof. L. Zitvogel, Institut Gustave Roussy, Vilejuif, France) were cultured in Dulbecco's modified Eagle's medium (Euroclone, Milan, Italy) supplemented with 10% heat-inactivated FBS (Superior, Merck, Darmstadt, Germany), 2mM L-glutamine, 10mM HEPES, 150U/mL streptomycin, 200U/mL penicillin/streptomycin (all from Euroclone, Milan, Italy) and 20μM β-Mercaptoethanol (Sigma-Aldrich, Saint Louis, MO, USA). The cultures were maintained at 37°C in 5% CO_2-humidified atmosphere.

In vitro BMDMs generation

Tibias and femurs were removed in sterility from C57BL/6J and *Dab2* KO mice, and BM cells were flushed. Red blood cells were lysed with a hypotonic solution containing 8.3% NH_4Cl, 1% $KHCO_3$ and 0.5M EDTA. To obtain differentiated macrophages, BM-cells were cultured in RPMI 1640 (Euroclone, Milan, Italy) supplemented with 100ng/mL CSF-1 (Miltenyi Biotec, Bologna, Italy), 10% heat-inactivated FBS (Superior, Merck, Darmstadt, Germany), 2mM L-glutamine, 10mM HEPES, 1mM sodium pyruvate, 150U/mL streptomycin, 200U/mL penicillin/streptomycin (all from Euroclone, Milan, Italy). Cultures were maintained at 37°C in 5% CO_2-humidified atmosphere for 7 days. On day 4 of culture, fresh cytokine-supplemented complete medium was added. To evaluate the number of macrophages during *in vitro* CSF-1–induced differentiation of BM precursors, every two days cells were harvested and counted. Final values were obtained multiplying the number of counted cells for the percentage of macrophages, as assessed by flow cytometry.

Spontaneous and experimental metastases assays

For spontaneous metastasis formation, breast cancer (E0771) and fibrosarcoma (MN-MCA1) cell lines were orthotopically injected into the mammary fat-pad ($5x10^5$ cells/mouse) and into the left quadriceps of mice (10^5 cells/mouse) respectively. Tumor growth was monitored every 2 days using a digital caliper.

The greatest longitudinal diameter (length) and the greatest transverse diameter (width) were determined and tumor volume calculated by the modified ellipsoidal formula: tumor volume = 1/2 (length × width^2). In the case of E0771-injected mice, tumors were resected at 800mm^3 of volume, to favor distal dissemination. For experimental metastasis formation, eight-week-old WT or *Dab2* KO females were injected with 4x10^5 E0771 cells into the tail vein. Mice were euthanized 20 days after tumor cell injection and lungs were analysed for metastasis formation. 10^6 E0771-mCherry/Luc cells were intravenously injected in WT or *Dab2* KO mice to follow metastasis seeding and growth at the metastatic site using *in vivo* bioluminescence imaging every week (Imager Ottico (OI) IVIS Spectrum). For spontaneous tumorigenesis and metastasis studies, MMTV-PyMT female mice carrying the specific oncogenes were examined weekly for mammary tumors to define tumor incidence. 13 weeks after the appearance of the first tumor, mice were euthanized and lungs were analysed for metastasis formation.

Lung metastasis detection and quantification

In already euthanized mice, lungs were flushed from blood by injecting PBS solution into the right ventricle. Organs were then harvested and fixed in 10% formaldehyde (PFA). To optimize the detection of microscopic metastases and ensure systematic uniform and random sampling, lungs were cut transversally into 2 mm-thick parallel slabs with a random position of the first cut in the first 2 mm of the lung, resulting in 5-8 slabs per lung. The slabs were then embedded and sections stained with hematoxylin and eosin (Bio-Optica, Milan, Italy). The number of lung micrometastases was blindly evaluated by two pathologists with a Leica DMRD optical microscope.

Anti-PD-1 immunotherapy

The effect of anti-PD-1 immunotherapy was investigated in C57BL/6J mice, WT or *Dab2* KO, after a subcutaneous challenge with 8×10^5 MCA205 cells. Tumor-bearing mice with established tumor masses were treated using 4 iterative

intraperitoneal administrations of anti-PD-1 mAb (clone RMP1-14; InVivoMAb, West Lebanon, NH) or isotype Ab (clone 2A3;) every 2 days. The complete treatment consists in 1 mg of Ab. Tumors were measured using digital calipers. Mice were euthanized when tumor area reached 1680 mm^3.

CRISPR-Cas9 gene editing

For each DNA target coding sequence (*Dab2, Itgβ1, Itgα5, Itgα6*), three sgRNAs (small guide RNAs) with the highest scores on target and lowest numbers of off-targets were chosen using the MIT CRISPR design tool (http://crispr.mit.edu/) and cloned in pSpCas9(BB)-2A-GFP (PX458) vector (Addgene, Massachusetts, USA), coding also for a reporter gene (green fluorescent protein, GFP) and Cas9 protein. Control digestion and Sanger sequencing were performed to evaluate the success of cloning. Plasmid transfection in RAW264.7 cells was performed with K2® reagent (Biontex, München, Germany). After two days, cells were collected, enriched for GFP using FACS Aria II flow-cytometer-cell-sorter (BD biosciences, San Jose, CA, USA) and cultured as single cell-derived clones. Clones were screened by protein (flow cytometry and WB) and genetic analysis (Sanger sequencing) (Table 3).

	Forward sequence	**Reverse sequence**	**Function**
Dab2 KO_1	Deletion 1bp at 63bp	Deletion 1bp at 61bp	Stop at 144 bp (48aa)
Dab2 KO_2	Insertion 1bp at 61bp	Insertion 1bp at 61bp	Stop at 96bp (32aa)
Dab2 KO_3	Deletion 2bp at 73bp	Deletion 2bp at 73bp	Stop at 96 bp (32aa)
Itgβ1 KO_1	Deletion 2bp at 99bp (frameshift)	Deletion 2bp at 99bp (frameshift)	Stop at 192bp (63aa)
Itgβ1 KO_2	Deletion 2bp at 98bp (frameshift)	Deletion2bp at 98bp (frameshift)	Stop at 192bp (63aa)
Itgβ1 KO_3	Deletion 2bp at 99bp	Deletion 2bp at 99bp	Stop at 192bp (63aa)
Itgα5 KO_1	Deletion 8bp at 142bp	Deletion 8bp at 142bp	Stop at 258bp (86aa)
Itgα5 KO_2	Deletion 2bp at 145bp	Deletion 2bp at 145bp	Stop at 258bp (86aa)
Itgα5 KO_3	Deletion 2bp at 145bp	Deletion 2bp at 145bp	Stop at 258bp (86aa)
Itgα6 KO_1	Deletion 2bp at 272bp	Deletion 2bp at 272bp	Stop at 294bp (98aa)
Itgα6 KO_2	Insertion 2bp at 273bp	Insertion 2bp at 273bp	Stop at 387bp (129aa)
Itgα6 KO_3	Deletion 1bp at 107bp	Deletion 1bp at 107bp	Stop at 387bp (129aa)

Table 3. CRISPR-Cas9 single-cell derived clones screened by genetic analysis (Sanger sequencing).

Endocytosis assays

In vitro uptake experiments were performed on differentiated WT or *Dab2* KO BMDMs to evaluate the endocytosis of ECM proteins. FN (ThermoFisher Scientific, Waltham, MA, USA), COL I (Corning Inc., New York, USA), COL IV (BD Biosciences, San Jose, CA, USA) and LN (ThermoFisher Scientific, Waltham, MA, USA) were labelled by using the FluoReporter FITC Protein Labeling Kit (ThermoFisher Scientific, Waltham, MA, USA) in accordance with the manufacturer's instructions. At day 7 of culture, macrophages were starved at 4°C for 30 minutes in complete medium without FBS to synchronize cell cycle and increase the endocytic ability. Labelled proteins were diluted in serum-free media, supplemented with CSF-1 (100 ng/ml), and added on cells for 2 hours at 4°C to permit binding to cell membranes. Macrophages were incubated at 37°C for 5, 18 or 22 hours. Not treated macrophages were used as basal background control; in addition, cells treated with proteins but not incubated (0-hour control) were used to assess the signal of non-internalized, surface-bound proteins. At the end of culture, cells were resuspended in 0.04% Trypan Blue (Sigma-Aldrich, Saint Louis, MO, USA) to quench the FITC fluorophore on non-endocytosed proteins and fixed in 4% PFA (Sigma-Aldrich, Waltham, MA, USA). Finally, samples were analysed with LSR II flow cytometer (BD Biosciences, San Jose, CA, USA) and uptake of ECM proteins was expressed as percentage of $FITC^+$ cells normalized on the 0-hour control.

Invasion assays

In vitro invasion assays were performed using matrigel (Corning Inc., New York, USA), a fibrosarcoma-derived matrix, and 8µm pores-transwells (Corning Inc, New York, USA). BMDMs or RAW264.7 cells were resuspendend in 2% FBS growth medium and seeded on the top of the polymerized matrigel, whereas 20% FBS growth medium was added in the well as cell chemoattractant. For BMDMs, CSF-1 (100 ng/ml) was added both in the underneath well and on top of the matrigel. After 4 days, matrigel was removed, invading cells were fixed, stained with crystal violet and eluted with a solution containing 50% ethanol and 0.1%

acetic acid. Absorbance was measured at 595nm using a microplate reader (VersaMax™, Molecular Devices, San Jose, USA). In the invasion assay with tumor cells, BMDMs were left in culture for 3 days to remodel the matrix and finally killed with puromycin (5 µg/ml) for 48h. After several washes, E0771 breast cancer cells were seeded on top of the matrigel in 2% FBS culture medium, while 20% FBS medium was added in the underneath well. Breast cancer cells invasion ability was evaluated after 24h by crystal violet elution and absorbance measurement. To study the correlation between DAB2, ITGs and EMC components in the metastatic process, Puramatrix synthetic matrix (Corning Inc., New York, USA) was mixed with different amounts of FN and LN (ThermoFisher Scientific, Waltham, MA, USA); COL I and VN (Corning Inc., New York, USA); COL IV (BD Biosciences, San Jose, CA, USA), coated on 8µm pores-transwells. Invading ability was assessed by crystal violet elution after 72h.

Inverted invasion assay

Macrophage ability to remodel the ECM and to guide invasion of cancer cells was tested by *in vitro* inverted invasion assays. Breast cancer cells (E0771) and TAMs or RAW264.7 cells were labelled with CellVue™ (ThermoFisher Scientific, Waltham, MA, USA) and PKH dyes (Sigma-Aldrich, Saint Louis, MO, USA) respectively and mixed with matrigel (Corning Inc., New York, USA) on chambered cell culture slides (ThermoFisher Scientific, Waltham, MA, USA). After the polymerization, a layer of matrigel mixed with 5% COL I−FITC conjugate was added on the top. Once polymerized, matrigel was covered with complete medium, creating a chemotactic gradient. After 72h, 6 random field for each condition were imaged at fixed intervals (10µm) starting at the fluorescent layer and in a direction towards the chemotactic gradient using z-stack setting of Leica TCS SP5 confocal microscope. To evaluate tumor cell invasion ability, distance travelled and invaded areas were quantified using ImageJ software.

xCELLigence

Invasion ability of monocytes to cross an endothelial cell monolayer was monitored using the xCELLigence Real Time Cell Analysis (RTCA) technology (Acea Bioscience, San Diego, CA, USA). The impedance-based detection of cell invasion was assessed by using gold microelectrodes attached to the well bottom. Briefly, mouse SVEC4-10 endothelial cell line were seeded in E-16-well plates and allowed to grow until they form a confluent monolayer, evidenced by a flattening of cell index. Then, E0771 and monocytes sorted from spleen of tumor-bearing mice, were seeded as mono- or co-culture on the top of the endothelial monolayer. The drop in electrical resistance, due to the retraction of endothelial junctions and penetration by invading cells through SVEC4-10 cells layer, was monitored in real-time for at least 12h. Results were normalized to the time of addition of monocytes. The level of cell invasion was assessed by slope analysis of the generated curves.

Chemotaxis assay

In vitro chemotaxis assays were performed using 8µm pores-transwells (Corning Inc, New York, USA). Serum-deprived RAW264.7 and BMDM cells, WT or *Dab2* KO, were added on top of the filter membrane and let migrate towards the lower chamber containing serum-free media supplemented with 100ng/ml of different cytokines (CXCL12, CCL2 or CCL3; R&D Systems, Minneapolis, USA) or 20% FBS growth media. After 24h, transwell membranes were fixed and stained with crystal violet. The directional movement towards chemokine gradient was assessed using an elution solution containing 50% ethanol and 0.1% acetic acid. Absorbance was measured at 595nm using a microplate reader (VersaMax™, Molecular Devices, San Jose, USA).

Organ cryoconservation and tissue sectioning

Tumors and lungs were explanted and immediately fixed in 4% PFA for 3h at 4°C. After fixation, organs were progressively dehydrated in 20% sucrose for 48h

and, subsequently, in 30% sucrose for other 48h. Then, organs were included in cryostat embedding medium (Killik, Bio-Optica, Milan, Italy), frozen on liquid nitrogen vapours and stored at -80°C. Frozen organs were cut with a Leica CM 1950 cryostat in 7µm-thick slices, which were stored at -20°C until staining for immunofluorescence or immunohistochemistry.

Immunofluorescence (IF)

For IF on cell lines or tissue sections, respectively coverslips and slides were rehydrated, fixed in 4% PFA and washed once in PBS and twice in PBS + 0.1% Tween20 (Sigma-Aldrich, Saint Louis, MO, USA). Cells were permeabilized with PBS + 0.1% Triton X-100 (Sigma-Aldrich, Saint Louis, MO, USA) and then washed. Unspecific binding sites were blocked with either PBS + 10% FBS or PBS + 15% FBS + 3% BSA + 0.25% gelatin for more intense backgrounds to be reduced. Primary antibodies were incubated over-night at 4°C in PBS + 10% FBS. After washes, conjugated secondary antibodies were added and kept for 2h at RT, while nuclei were stained with DAPI (ThermoFisher Scientific, Waltham, MA, USA) for 10 minutes at RT. To visualize YAP on tissue sections, some variations were introduced (adapted from (*208*)). Permeabilization was done in PBS + 0.3% Triton X-100; blocking antibody and wash solutions were supplemented with a 0.1% of Triton X-100 to enhance intra-cellular staining. Coverslips and slides were mounted by using Fluorescent Mounting Medium (DAKO) and analysed with a Leica TCS SP5 confocal microscope. Images were acquired and processed with the Leica LAS AF software. The following primary antibodies were used for IF: rabbit anti-DAB2 H-110, mouse anti-YAP 63.7, rabbit anti-YAP H-125 (all from Santa Cruz Biotechnology), rabbit anti-YAP1 (Proteintech Europe, Manchester, UK), rat anti-F4/80, Cl:A3-1 (Bio-Rad laboratories, Hercules, CA, USA), mouse anti-CD68, KP1 (Abcam, Cambridge, UK). The secondary conjugated antibodies were purchased from Jackson ImmunoResearch: anti-rabbit RRX, anti-rat Alexa Fluor 647, anti-mouse Alexa Fluor 488.

Immunohistochemistry (IHC)

For IHC on tissue sections from mouse organs, slices were fixed as in IF and endogenous peroxidases were inactivated with PBS supplemented with 0.3% FBS and 0.3% H_2O_2. Permeabilization, blocking and incubation with primary antibodies were performed as in IF. The subsequent steps were performed following Elite ABC Kit (Vectastain) protocol. Briefly, slices were incubated with the provided anti-rabbit biotinylated secondary antibody, washed, incubated with the avidin-HRP (horse radish peroxidase) reagent, washed and stained with the DAB chromogen (Sigma-Aldrich, Saint Louis, MO, USA) until colour developed. Nuclei were stained with Mayer's hematoxylin (Sigma-Aldrich, Saint Louis, MO, USA) and dehydrated in increasing concentrations of ethanol. Finally, slices were mounted with the Eukitt mounting medium (Bio-Optica) and observed with a Leica DMIL LED inverted optical microscope equipped with a Leica EC3 CCD camera.

For histological evaluations on tissue sections from patients, paraffin was removed from slices with xylene and decreasing concentrations of ethanol. Ags were unmasked by heating slices at sub-boiling temperature in 10mM citrate buffer (pH 6). The profiling for DAB2 was automatically performed on a Bond TM Polymer Refine Detection System (Leica). Then, sections were lightly counter stained with hematoxylin.

For prognosis and survival correlation analyses in patients, an average number of $DAB2^+$ cells into the peritumoral and intratumoral infiltrates was obtained by analyzing 10 HPFs (40x). Positive endothelial and neoplastic cells were not retained for scoring.

The IHC staining for DAB2 in gastric cancers was scored in the TMA scores and the number of positive cells with a macrophage-like morphology were counted in three separate 40x HPFs. Tumors were dichotomized as DAB2 low if the number of $DAB2^+$ cells was <20 and DAB2 high when ≥ 20.

Second harmonic generation (SHG) imaging

In order to evaluate possible differences in ECM organization within tumors derived from WT or *Dab2* KO mice, we took advantage from second harmonic generation imaging (SHG) to image fibrillar, crosslinked COL in tissues. SHG signal was acquired through an 80-µm z-stack in fixed tumor samples, using a 25x NA 1.05 water-immersion objective (Olympus XLPLN25XWMP2) on a custom-build microscope, described in details elsewhere (*209*). A 800nm laser wavelength/ 395nm ± 25nm emission wavelength was used to collect SHG signal from COL I fibres. Images were then analysed for signal intensity of each single z-step (8µm steps) or maximum projection intensity of z-stack, using ImageJ software.

Preparation of cell suspensions from organs

Spleens, lungs and tumors were collected from sacrificed mice and processed as previously described (*210*). Spleens were mechanically disaggregated and filtered (Corning Inc, New York, USA). Tumors and lungs were cut in small pieces with scissors, enzymatically digested at 37°C for 1h with a solution containing collagenase IV (1mg/ml), hyaluronidase (0.1mg/ml) and DNase (4.5mg/ml) (Sigma-Aldrich, Saint Louis, MO, USA). Cells were then collected, filtered and red blood cells were lysed. Cell suspensions were used for immunomagnetic sorting, FACS or Western blot analysis.

Flow cytometry

0.5-2x10^6 cells were washed in PBS and incubated with FcReceptor Blocking reagent CD16/32 (Biolegend, San Diego, CA, USA) to saturate FcR. The following mAbs were then used for cell labelling: anti-mouse CD11b (M1/70), Ly6C (HK1.4), Ly6G (1A8), B220 (RA3-6B2), CD3 (145-2C11), CD45 (A20), CD45.2 (104), I-A/I- E (M5/114.15.2), F4/80 (Cl:A3-1), CD11c (N418), CD8 (53-6.7), NK1.1 (PK136), Aqua LIVE/DEAD dye. For ITG surface expression analysis, cells were detached with PBS-2mM EDTA, kept on ice, stained with

Aqua LIVE/DEAD dye (ThermoFisher Scientific, Waltham, MA, USA) and fixed in 4% PFA. The ITG staining was performed using anti-mouse CD29 (ITGβ1; clone HMb1-1), CD49a (ITGα1; clone Ha31/8), CD49e (ITGα5, clone 5H10-27) and CD49f (ITGα6; clone GoH3) antibodies. All the antibodies were purchased from the following companies: BD Bioscience (San Jose, CA, USA), eBiosciences (ThermoFisher Scientific, Waltham, MA, USA), Bio-rad Laboratories (Hercules, CA, USA) and Biolegend (San Diego, CA, USA). The MFI (mean fluorescence intensity) of ITGs was used to calculate the fold change relative to WT BMDMs or RAW264.7 cells. Samples were acquired with FACS Canto II (BD, Franklin Lakes, NJ, USA) and analyzed with FlowJo software (Tree Star, Inc., Ashland, OR, USA).

Immunomagnetic sorting

Mouse $CD11b^+$ cells were isolated by immunomagnetic sorting (using CD11b Microbeads, Miltenyi Biotec, Bologna, Italy) according to manufacturer's instructions and their purity was evaluated by flow cytometry. For all separations, the positive fraction was obtained with a purity of ≥ 95%.

***Ex vivo* T cell suppression assays**

The immunosuppressive activity of $CD11b^+$ cells immunomagnetically sorted from MN-MCA1, E0771 and PyMT tumors growth in WT or *Dab2* KO mice was evaluated. $CD11b^+$ cells were plated in 96-wells plate at decreasing percentages of total cells (24%, 12%, 6%, 3%) in culture in presence of splenocytes from OT-I transgenic mice, labelled with 1μM CellTrace (Thermo Fisher Scientific, Waltham, MA, USA) and diluted 1:10 with $CD45.1^+$ splenocytes, in the presence of SIINFEKL peptide (1μg/ml final concentration; JPT Innovative Peptide Solutions, Berlin, DE). After 3 days of co-culture, cells were stained with anti-CD45.2 (clone 104, eBioscience, Thermo Fisher Scientific, Waltham, MA, USA) and anti-CD8 (clone 53-6.7, eBioscience, Thermo Fisher Scientific, Waltham, MA, USA). CellTrace signal of gated lymphocytes was used to analyze cell

proliferation. Samples were acquired with FACS-Canto II (BD, Franklin Lakes, NJ, USA) and analyzed by FlowJo software (Tree Star, Inc., Ashland, OR, USA). The percentage of suppression exerted by tumor-infiltrating $CD11b^+$ cells was calculated with the formula [1-(% divided cells in sample/% divided cells in activated control)]x100, as previously described (*211*).

In vitro Dab2 induction

In order to understand if *Dab2* expression is modulated by adhesion, $CD11b^+$ cells were isolated from tumor-free mice and cultured for 6h in adhesion on a plastic surface or in suspension. In both conditions, CSF-1 or E0771 supernatant were added to the serum-free growth media. Samples were harvested for RNA isolation. *Dab2* expression was analysed by real-time PCR and normalized on unstimulated cells.

Real-time PCR

Total RNA from BM precursors ($CD11b^+$) was isolated by TRIzol reagent (Thermo Fisher Scientific, Waltham, MA, USA). The amount and purity of isolated RNA was analyzed by the ND-1000 Spectrophotometer (NanoDrop Technologies). cDNA was prepared using the SuperScript® VILO cDNA Synthesis Kit (Thermo Fisher Scientific, Waltham, MA, USA) according to the manufacturer's instruction. Real Time PCR was run using 2x SYBR Green master mix (ThermoFisher Scientific, Waltham, MA, USA). All samples were normalized using GAPDH endogenous control primers. Post-qRT-PCR analysis to quantify relative gene expression was performed by the comparative Ct method ($2^{-\Delta\Delta Ct}$).

Western blot (WB)

Cell lysates were prepared in Laemmli Buffer (for DAB2 detection) or in a lysis buffer (for YAP detection) (*212*), sonicated and denatured at 100°C. Insoluble

materials was removed by centrifugation. Samples were subjected to SDS-polyacrylamide 10% Tris-Glycine or Bis-Tris gel electrophoresis and blotted onto PVDF-membrane (Immobilon P membranes, Millipore, Billerica, MA, USA). Tris-buffered saline plus 0.05% Tween-20 and 5% non-fat dry milk were used to block unspecific sites. Membranes were incubated with rabbit anti-DAB2 primary antibody (H-110 clone, Santa Cruz Biotechnology Inc., Dallas, USA) or rabbit anti-YAP primary antibody (Proteintech Europe, Manchester, UK) and with donkey anti-rabbit HRP-conjugated secondary antibody (GE Healthcare, Chicago, Illinois, USA). HRP-conjugated anti-β actin (Cell Signaling Technologies, Danvers, MA, USA) and HRP-conjugated anti-GAPDH (Cell Signaling Technologies, Danvers, MA, USA) were used as reference. Proteins were revealed by GE ImageQuant LAS400 with Femto substrate (ThermoFisher Scientific, Waltham, MA, USA).

Analysis of gene expression data

Gene expression data of mouse invasive TAMs, general TAMs, and splenic macrophages are publicly available at GSE18295 and GSE18404. The annotated gene-centered expression matrix comprising 15,242 unique gene symbols for a total of 18 samples has been obtained from the authors of the original publications (*213, 214*). Data have been normalized, background-corrected and log2 scaled using a robust multi-array procedure (RMA) as implemented in NimbleScan software.

For functional enrichment, the expression profile of *Dab2* in TAMs and normal splenic macrophages has been used as input in the Gene Set Enrichment Analysis software (GSEA) to search for gene sets enriched in genes whose expression was highly correlated with *Dab2*. GSEA software was applied to a list of gene sets comprising adhesion, differentiation, proliferation and survival branches of CSF-1 receptor pathway as defined like in (*215*); the autophagy pathway as elaborated from (*216*); the gene sets of the immune system activation, angiogenesis regulation, Wnt signal transduction and the Yap conserved signature (*217*) from the Molecular Signatures Database (MSigDB) collection. Gene sets were considered significantly enriched at FDR ≤0.05 when weighted enrichment

statistic, Pearson's correlation as metric for gene ranking, and 1,000 permutations of gene sets.

Statistical analyses

Student's t-test was performed on parametric groups, while Wilcoxon-Mann-Whitney and One-way ANOVA tests were used on non-parametric groups. Values were considered significant at $p \leq 0.05$ and are indicated as $*p \leq 0.05$, $**p \leq 0.01$ and $***p \leq 0.001$. Values are reported as mean ± standard error (s.e.) or standard deviation (s.d.). All analyses were performed by using SigmaPlot (Systat Software Inc). Descriptive statistics was adopted. Follow-up was analyzed and reported according to Shuster (*218*). DAB2 expression data were obtained from the IHC staining on patient biopsies. The receiver operating characteristic (ROC) analysis was applied to the DAB2 continuous score to dichotomize the obtained values according to DFS for ILC patients. To correlate DAB2 expression with clinico-pathological data, Pearson's chi-squared test or Fisher's exact test were used, depending on sample size.

DFS, CSS and OS curves were elaborated by using the Kaplan-Meier method and significance was calculated with the Log-Rank test. p-values were considered significant when ≤ 0.05. The SPSS 18.0, R 2.6.1 and MedCalc 14.2.1 statistical programs were used for all analyses.

RESULTS

DAB2 is mainly expressed by tumor-associated macrophages localized along the tumor invasive frontline

Over the last few years, researchers focused their attention on the ability of TME cell components to generate a cancer-promoting environment. Cancer cells alter the normal hematopoiesis and promote the expansion of immature myeloid cells with pro-tumor and pro-metastatic functions (*15*). The comprehension of specific mechanisms of action used by myeloid cells in favoring malignant progression could support the development of new promising therapeutic strategies to block or eradicate cancer. For this reason, we decided to investigate the role of tumor-infiltrating myeloid cells in different tumor settings.

Previous studies of gene profiling analysis performed by our group on $CD11b^+$ tumor-infiltrating myeloid cells isolated from tumor-bearing mice showed a significant up-regulation of several genes in comparison to the same population purified from the spleen of healthy mice. Among these genes, we decided to concentrate our studied on *Dab2* (*193*). Despite numerous studies on tumor cells, the role of this protein in myeloid cells has not been investigated yet.

To confirm the data obtained by gene chip analysis, DAB2 expression on $CD11b^+$ cells isolated from primary tumors and spleens was assessed by western blot. The two isoforms of DAB2 (p96 and p67) were expressed in intratumoral myeloid cells, but not in splenic myeloid cells from both healthy and tumor-bearing mice (Figure 8A). These results highlighted that *Dab2* induction in myeloid cells was tumor-related and that DAB2 protein could have a role within the TME. This prompted us to explore the localization and the functions exerted by DAB2-expressing myeloid cells in a tumor-driven context.

We first analyzed the expression of DAB2 among different cells. Myeloid cells were FACS-sorted from primary tumors of mice challenged with highly metastatic MN-MCA1 fibrosarcoma cell line or MMTV-PyMT mice. These latter mice represent a model of autochthonous metastatic breast carcinoma (*219*). Protein expression was evaluated by western blot analysis, which revealed the two

isoforms of the DAB2 protein in TAMs isolated from MN-MCA1-bearing mice, to a much lower extent in monocytes (defined as $Ly6G^{-}$ $Ly6C^{high}$ cells) and completely absent in granulocytes (defined as $Ly6G^{+}$ $Ly6C^{low}$ cells) (Figure 8B). Moreover, DAB2 expression was detected in TAMs ($CD11b^{+}$ $MHCII^{+}$ cells) sorted from PyMT primary tumors but not in resident mammary tissue macrophages (MTMs: identified as $CD11b^{+}$ $MHCII^{high}$ cells) (Figure 8C) (*56*). We demonstrated that TAMs are DAB2-expressing cells (Figure 8D), and that DAB^{+} TAMs were mainly localized along the tumor border and not in the tumor core. In particular, DAB2 expression was detected in $F4/80^{+}$ TAMs localized around muscle fibers, partially or not-yet reached by invading tumor cells in the MN-MCA1 model (Figures 8E and 8F left). In PyMT tumors, DAB2-expressing $F4/80^{+}$ TAMs mainly resided along the border between tumor mass and surrounding healthy breast (Figures 8E and 8F right). Only few DAB2-expressing resident macrophages were found both in healthy muscle and in normal breast, suggesting that DAB2 upregulation in myeloid cells might occur only in a tumor-driven context.

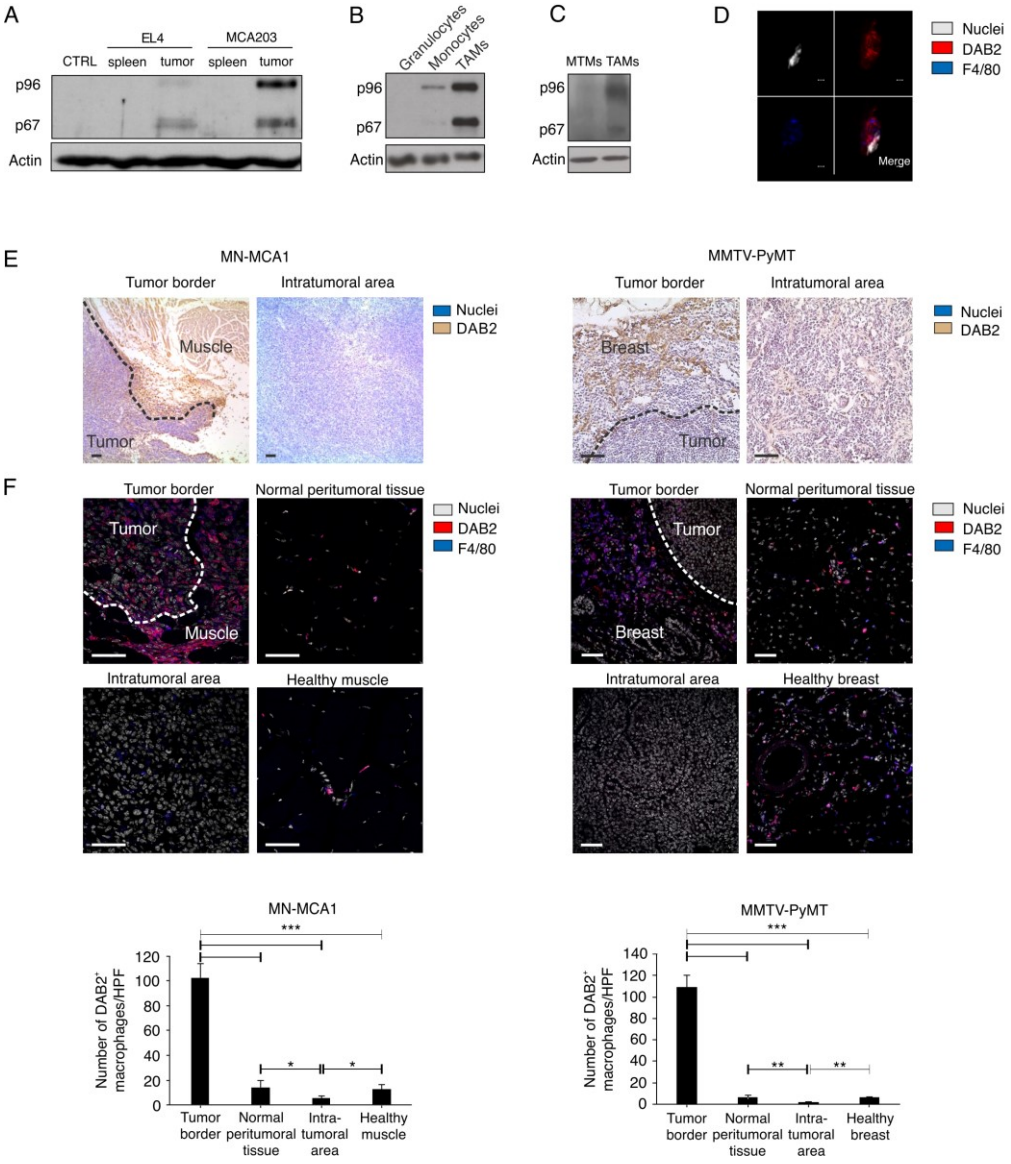

Figure 8. DAB2 protein is expressed in TAMs that localize along tumor borders.
(A) WB analysis for the expression of DAB2 isoforms (p96 and p67) in CD11b$^+$ cells isolated from spleens and tumors of mice injected with mouse lymphoblast (EL4) and fibrosarcoma (MCA203) cell lines. Splenic CD11b$^+$ cells from healthy mice were used as negative control (CTRL). Actin was used as loading control. (B,C) WB analysis for DAB2 expression on FACS-sorted myeloid cell subsets (granulocytes, monocytes, and TAMs) infiltrating primary tumors from either MN-MCA1-tumor bearing mice (B) or TAMs and MTMs from PyMT mice (C). Actin was used as loading control. (D) TAMs, FACS-sorted from MN-MCA1 tumors, were analyzed by IF for DAB2 and F4/80 expression. DAPI was used as nuclei marker. Scale bar: 50 µm. (E,F) Slices of primary tumors from MN-MCA1 tumor-bearing mice (left) or PyMT mice (right) were analyzed by IHC and IF. (E) Representative IHC images for DAB2 staining along the tumor borders (dashed lines) and within the tumor areas. (F) Representative IF images from different areas of the tumor and from healthy tissue. Scale bar: 50 µm. Below quantification of DAB2$^+$ TAMs on total TAMs evaluated on HPF images from different areas of either MN-MCA1 (left panel) or PyMT tumors (right panel).

DAB2-expressing TAMs support the metastatic process

In order to investigate the contribution of DAB2^{+} TAMs in tumor progression and metastatic spread, we generated a transgenic mouse model, the *Dab2*$^{flox/flox}$; Tie2-Cre (specifically *Dab2*$^{flox/flox}$; Tek-Cre, here referred as *Dab2* KO) strain, lacking the protein DAB2 in the entire myeloid cell lineage and in a portion of ECs (*54*). WT and *Dab2* KO mice were orthotopically injected in the quadriceps with syngeneic MN-MCA1 fibrosarcoma cells, which have high metastatic potential for the lungs. *Dab2* KO mice showed an impaired development of lung micrometastases compared to WT mice (Figures 9A and 9B), while there were no remarkable differences in the primary tumor growth (Figure 9C).

The effect of *Dab2* deficiency *in vivo* was further tested in two different breast cancer models, i.e. E0771 and MMTV-PyMT models. *Dab2* KO mice orthotopically injected with syngeneic E0771 cells showed a significant reduction in the number of lung metastases when compared to WT mice (Figures 9D and 9E), without any alteration in primary tumor growth (Figure 9F). Similarly, in PyMT-*Dab2*$^{flox/flox}$; Tie2-Cre^{+} (PyMT-*Dab2* KO) we depicted a decrease in metastasis number compared to their control littermates (PyMT-WT) (Figures 9G and 9H). Indeed, *Dab2* KO PyMT mice displayed a slightly slower growth of the primary tumor compared to control mice (Figure 9I), even though the tumor onset was unaltered (Figure 9L). To exclude the contribution of ECs in the metastatic process, we also generated *Dab2*$^{flox/flox}$; *LysMCre*$^{+}$ (*Dab2*$^{flox/flox}$; *Lyz2*-Cre) mouse strain, where Cre-mediated recombination results in deletion of the targeted gene only in monocytes/macrophages and neutrophils and not in the ECs (*53*). Also these mice, when challenged with MN-MCA1 cells, presented a reduction in the number of lung metastases (Figure 9M), reinforcing the role of DAB2^{+} myeloid cells in metastatic cascade.

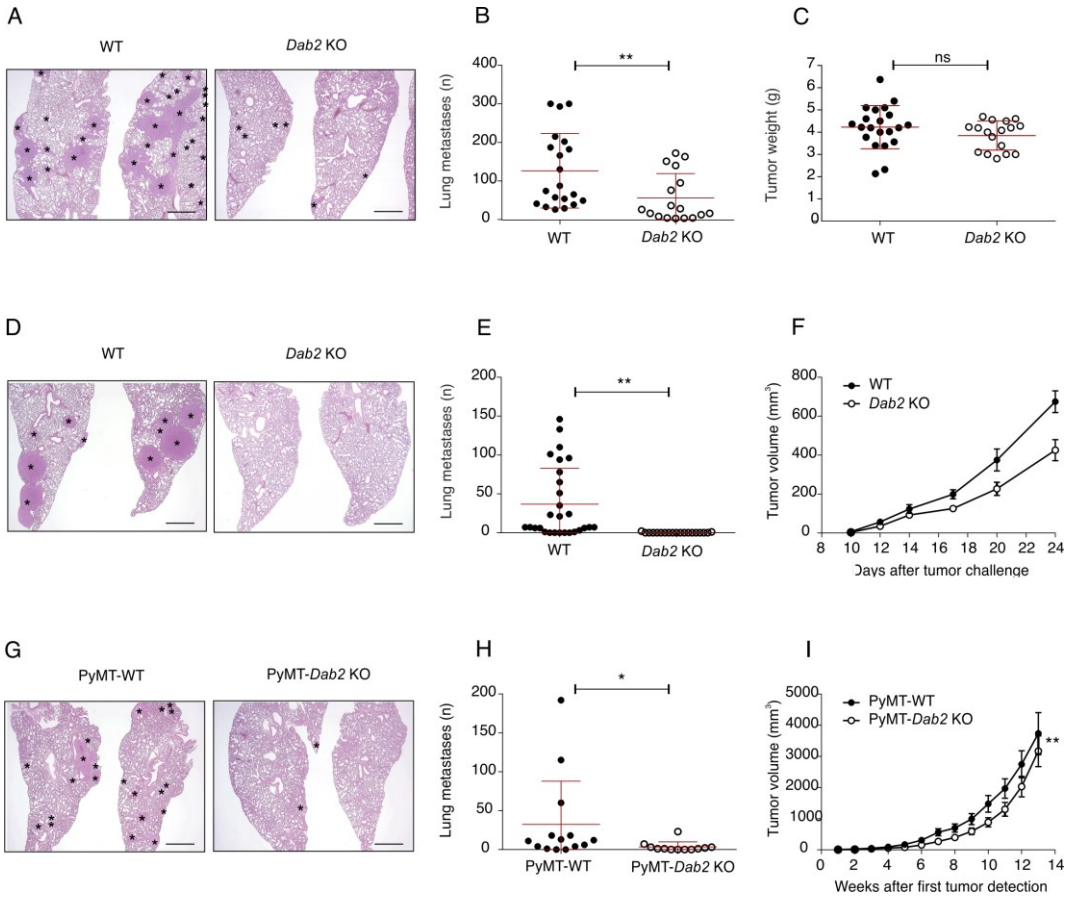

Figure 9. *Dab2* deficiency in myeloid cells affects the metastatic process.
(A) Representative H&E-stained microscopy images of the lung metastases in either WT or *Dab2* KO mice orthotopically injected with MN-MCA1 fibrosarcoma cells. Scale bar: 800 µm. (B) Quantification of lung metastases number by H&E staining on lung sections. (C) Primary tumor growth reported as tumor weight (g). WT (n=20) or *Dab2* KO (n=17), pooled from 3 independent experiments. (D) Representative H&E-stained microscopy images of the lung metastases in either WT or *Dab2* KO mice orthotopically injected with E0771 breast cancer cells. Scale bar: 800 µm. (E,F) Number of lung metastases (E) and primary tumor growth over time (F) are reported. WT (n=28) and *Dab2* KO mice (n=19), pooled from 3 independent experiments. (G) Representative H&E-stained microscopy images of the lung metastases in either WT or *Dab2* KO PyMT transgenic mice. Scale bar: 800 µm. (H) Quantification of lung metastasis numbers by H&E staining on lung sections of PyMT-WT (n=13) or PyMT-*Dab2* KO (n=12) mice. (I) Tumor growth reported as tumor volume (mm^3) evaluated over time. (L) PyMT-WT and PyMT-*Dab2* KO mice are compared for lung metastasis (log-rank p-value). (M) Lung metastasis numbers induced by MN-MCA1 tumor in $Dab2^{flox/flox}$-LysM-Cre mice and their littermates. Data are presented as mean ± s.e. *$p \leq 0.05$, **$p \leq 0.01$ and ***$p \leq 0.001$, Mann-Whitney test (B,C,E,H,M) and one-way analysis of variance (ANOVA) (F,I).

Absence of DAB2 *in vivo* does not affect the accumulation of tumor-infiltrating myeloid subpopulations or checkpoint therapy efficacy

Considering the participation of myeloid cells in regulating the anti-tumor immune response (*220*), we tested whether *Dab2* gene deficiency provoked any alteration in the immunosuppressive functions of tumor-infiltrating myeloid cells. As shown in Figure 10A, *Dab2* KO $CD11b^+$ cells were not impaired in their immunosuppressive activity as compared to WT $CD11b^+$ cells.

Moreover, analysis of different immune subpopulations infiltrating MN-MCA1, E0771 and PyMT tumors showed that the absence of DAB2 in mice did not affect the recruitment and the accumulation of any myeloid subsets. Indeed, the percentages of granulocytes, monocytes, DCs and TAMs were comparable between WT and *Dab2* KO mice (Figure 10B).

Moreover, *Dab2* deficiency in myeloid cells did not change the efficacy of immune checkpoint inhibitors. Anti PD-1 immunotherapy restrained primary tumor growth and increased mouse survival without significant differences between WT and *Dab2* KO mice injected with MCA205 fibrosarcoma cell line (Figures 10C and 10D). Taken together, these data denote that $DAB2^+$ TAMs are responsible for tumor cell spreading, but their mechanism of action is independent from the suppression of anti-tumor adaptive immune response.

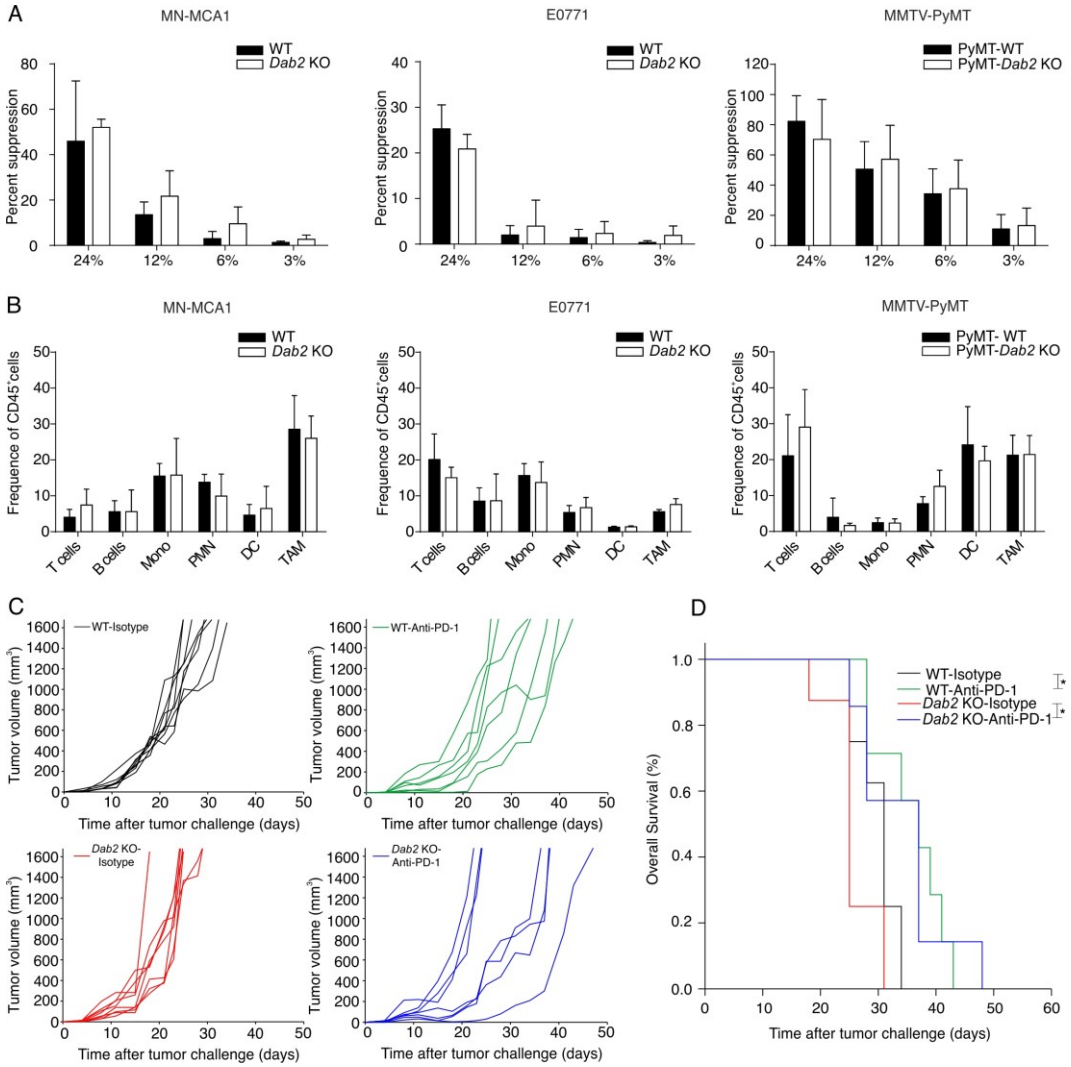

Figure 10. *Dab2* deficiency does not affect immune cell recruitment or myeloid cell inhibitory function.
(A) Different percentages of tumor-infiltrating CD11b$^+$ myeloid cells were tested for their ability to suppress the proliferation of OVA-specific, OT-I CD8$^+$ T cells stimulated by the SIINFEKL peptide in culture. Data reported as mean ± s.d., pooled from 3 independent experiments. (B) Accumulation of different immune populations among CD45$^+$-gated cells in MN-MCA1, E0771, and PyMT tumors from either WT or *Dab2* KO mice (MN-MCA1, n=6 mice/group; E0771, n=4 mice/group; PyMT, n=6 mice/group). (C-D) WT (n=16) or *Dab2* KO (n=16) mice were subcutaneously injected with MCA205 cells and treated with either anti-PD-1 antibody or with its isotype control. The tumor volume of each mouse per group was measured (C), whereas the survival is showed in the Kaplan-Meier curve ($p \leq 0.05$) (D).

DAB2$^+$ macrophages promote tumor cell invasiveness by ECM remodeling

Demonstrating that the mechanism by which DAB2$^+$ macrophages promote tumor cell invasiveness is not dependent on the activation of pro-tumor immune responses, we hypothesized that this process may be related to the remodeling of

the ECM, one of the main function of macrophages (*153*). Further proof that DAB2-expressing macrophages could be involved in the promotion of matrix reorganization is that these cells are localized at the tumor invasive front and thus they may be prone to favor tumor cell motility in the surrounding environment. In order to recapitulate these processes *in vitro*, we optimized an inverted invasion assay, where TAMs isolated from a WT or *Dab2* KO mice were tested for their ability to remodel the ECM and guide invasion of cancer cells (*221*). E0771 breast cancer cells and TAMs, isolated from tumor-bearing mice, were differently labeled and mixed in an EMC-mimicking matrix (matrigel). E0771 cells acquired an increased invasive ability through the tridimensional matrix when co-cultured with WT TAMs in comparison to E0771 cells alone or in co-culture with *Dab2*-deficient TAMs (Figures 11A and 11B), highlighting a DAB2-dependent matrix digestion followed by cancer cell dissemination.

To investigate the mechanism through which $DAB2^+$ macrophages move and drive tumor cell invasion, we took advantage of *in vitro*-differentiated BM-derived macrophages (BMDMs), obtained from WT or *Dab2* KO mice. BMDMs were seeded on transwell porous membrane and let migrate towards chemokines responsible of the recruitment of myeloid cells, including CXCL12 (stromal cell-derived factor 1 - SDF1), CCL2 (monocyte chemoattractant protein 1 - MCP1) and CCL3 (macrophage inflammatory protein 1-alpha or MIP-1-alpha) (Figure 11C) (*222*). Alternatively, cells were embedded in matrigel and let invade towards a serum gradient (Figure 11D). WT or *Dab2* KO BMDMs exhibited a similar directional movement towards chemokine gradients and a defective invasion through the substrate when lacking *Dab2*, indicating a defect in haptotaxis but not chemotaxis (*223*). Moreover, the ability of E0771 cells to invade the *Dab2* KO macrophage-remodeled matrigel was significantly impaired, confirming that tumor cells invasion requires DAB2-assisted matrix reorganization (Figure 11E). Furthermore, using a second harmonic generation analysis of primary explants of MN-MCA1 tumors, we demonstrated that, also *in vivo*, the ECM exhibited a less organized and loose structure in WT tumors compared to *Dab2* KO ones (Figure 11F-G).

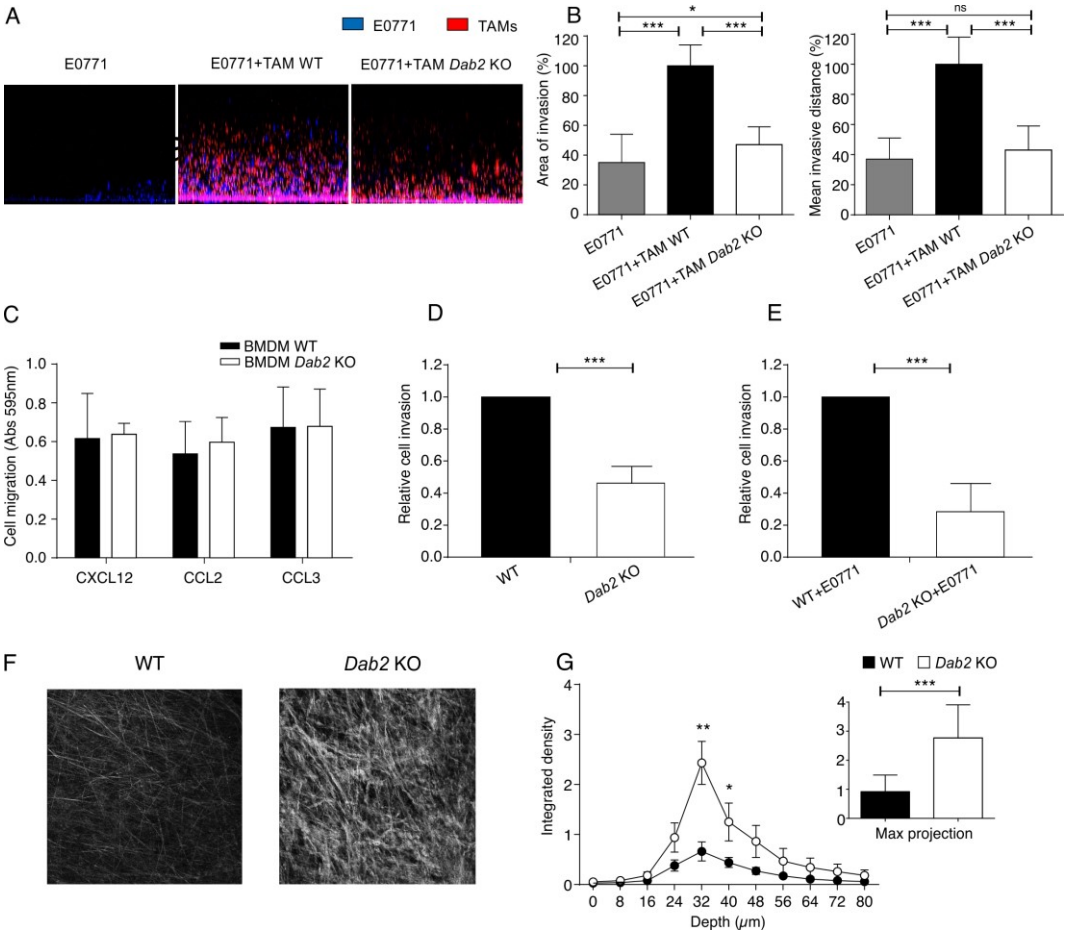

Figure 11. DAB2 regulates tissue invasion and ECM remodeling by macrophages.
(A) Representative image of inverted invasion assay of E0771 tumor cells, either alone or co-incubated with TAMs isolated from WT or *Dab2* KO tumor-bearing mice. (B) The area of invasion and the mean invasive distance of E0771 cells were evaluated by confocal microscopy. (A-B) Data are presented as mean ± s.d.; *p ≤ 0.05, **p ≤ 0.01 and ***p ≤ 0.001 by Student's *t*-test. (C) Chemotaxis assay of BMDM, either WT or *Dab2* KO, carried out in Boyden chambers. CXCL12 (100 μg/mL), CCL2 (100 μg/mL) and CCL3 (100 μg/mL) were added in the lower compartment. Cell migration was evaluated by measuring the absorbance at 595nm of invasive cells stained with crystal violet. (D) Transwell invasion assay of BMDM from WT or *Dab2* KO mice. The macrophages ability to remodel the matrix was evaluated measuring the absorbance at 595nm of invasive cells stained with crystal violet and reported as fold change over WT cells. (E) Transwell invasion assay with matrigel mixed with either WT or *Dab2* KO BMDMs. After 3 days of culture, macrophages were killed with puromycin and E0771 tumor cells were added on the top of the matrigel to monitor their movements through the pre-digested matrix. Cancer cells invasion was evaluated measuring the absorbance at 595nm of crystal violet-stained cells and reported as fold change over WT+E0771 cells. (F) Representative SHG images of COL fibrils organization in MN-MCA1 WT and *Dab2* KO tumors. (G) Quantification of the SHG signal (integrated density) of each single z-step or maximum projection intensity through 0–80 μm z-stack (insert) within MN-MCA1 (WT and *Dab2* KO) tumors. (B,C,D,E,G) Data are presented as mean ± s.e.; *p ≤ 0.05, **p ≤ 0.01 and ***p ≤0.001 by Student's t-test.

DAB2 regulates integrin traffic

DAB2 is an endocytic adaptor involved in the internalization and the recycling of membrane ITGs, a family of receptors that mediates the interactions between the cytoskeleton of a cell and the ECM (*182*). Active ITGs participate to FA assembling and are internalized by DAB2 for a subsequent re-collocation or degradation when unbound to their ligand (*192*). We demonstrated that DAB2 absence could compromise this turnover, leading to an accumulation of some ITGs on the cell surface. Indeed, *Dab2* deficiency in BMDMs is associated with significant lower ITG uptake and higher membrane expression of β1, α5 and α6 ITGs (Figure 12A). Notably, the ITGs surface level abundance in *Dab2* KO BMDMs was not associated with an increased protein expression (Figures 12B and 12C), indicating that DAB2 only regulates the ITG traffic between the cell surface and the cytoplasm.

We speculated that the ITG turnover defect observed in *Dab2*-depleted BMDMs was correlated with an impaired uptake of ECM proteins known to interact with specific ITGs. In particular, α1β1, α5β1 and α6β1 heterodimers, bind COL, FN and LN, respectively (Figure 12D) (*224*). During the matrix remodeling process, ECM proteins are degraded following the release of tissue proteases and, when ITGs are recycled by the endocytic machinery, they are transported inside the cell as fragments (*113*). In line with our expectations, the altered ITG surface distribution in *Dab2* KO BMDMs significantly reduced the ability to internalize FITC-labelled ECM fragments (Figure 12E). Our data indicate that DAB2-expressing macrophages regulate matrix remodeling through ITG recycling and ECM proteins internalization.

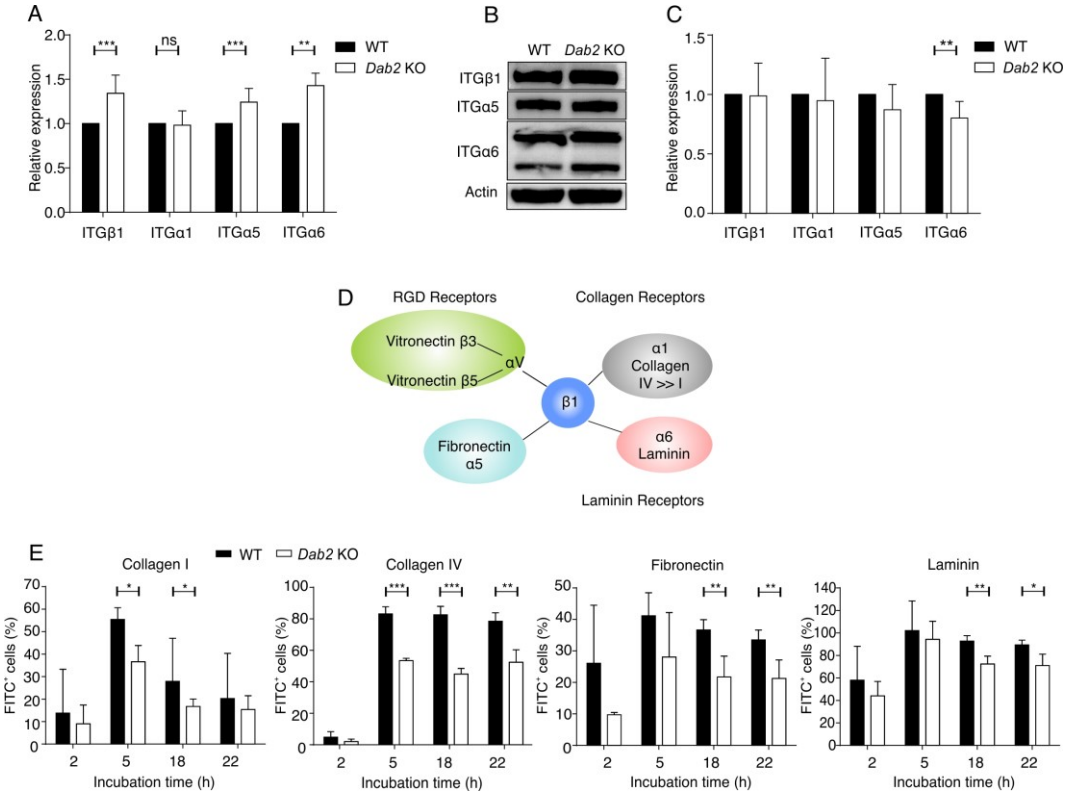

Figure 12. DAB2^{+} macrophages regulate ITG traffic.
(A) Surface expression of β1, α1, α5 and α6 ITGs evaluated by flow cytometry on either WT or *Dab2* KO BMDMs. The fold change of MFI relative to WT is reported for each ITG (n = 6 independent experiments). (B) Total expression of β1, α5 and α6 ITGs evaluated by WB. (C) Total expression of β1, α1, α5 and α6 ITGs evaluated by qRT-PCR analysis. (D) Schematic representation of some ITG receptors and their ligands. (E) Uptake of FITC-labeled ECM proteins by BMDMs is reported as percentage of FITC^{+} cells measured by flow cytometry at different time points (n=3 independent experiments).

DAB2 and integrins are required for cell-ECM interaction and tumor cell invasiveness

Cancer cells need continuous tissue remodeling for both local invasion and spreading to distant sites (*2*). To confirm the involvement of DAB2 in tumor and metastasis promotion through ECM reorganization, we exploited the genetic editing by CRISPR/Cas9 (Clustered Regularly Interspaced Short Palindromic Repeat/CRISPR-associated protein 9) technology and generated single clones with a mutation in the gene encoding DAB2.

As represented in Figure 13A, both DAB2 isoforms are detectable in cells transfected with a non-specific sgRNA CRISPR plasmid (control), while RAW264.7 *Dab2* KO CRISPR-engineered clones (referred as *Dab2*_1, *Dab2*_2 and *Dab2*_3 clones) show no protein expression.

Moreover, we explored whether DAB2 absence in RAW264.7 clones affected ITGs turnover, as already reported in *Dab2* KO BMDMs. We demonstrated that *Dab2* deletion did not impact on ITGα1 and ITGα6 recycling, but led to a highly significant increase of ITGβ1 and ITGα5 on the membrane (Figure 13B) (*225*). *Dab2*-depleted clones were also used to perform invasion and trailblazer assays. Similar to *Dab2* KO TAMs and BMDMs, *Dab2* absence in RAW264.7 clones affected ECM remodeling and impaired E0771 breast cancer cells invasion (Figure 13C).

To identify the ECM components critical for DAB2-mediated matrix remodeling, Boyden chambers were coated with a synthetic matrix supplemented with different ECM proteins. RAW264.7 WT controls displayed an increased invasive ability in comparison to *Dab2*-deleted clones, in the presence of the ECM proteins interacting with DAB2-regulated ITGs (i.e. FN, LN, COL I and IV) (Figure 13D). However, the motility of WT or *Dab2* KO clones was unaltered when exposed to VN, which binds αvβ3 ITG (*226*), a DAB2 independent dimer. Indeed, the surface levels of ITGαV in *Dab2* KO RAW264.7 clone were not significantly increased in comparison to the control clone (Figure 13E). These data suggest that ECM composition is a key factor for the invasion competence promoted by DAB2. Furthermore, we noticed that, after coating different amounts of ECM proteins, RAW264.7 control but not *Dab2* KO clone exhibited a dose-dependent invasiveness (Figure 13F). Nevertheless, where protein concentration was too high we could not observe differences, indicating that mechanotransduction and stiffness could have a role in the DAB2 expression modulation, as we will discuss later.

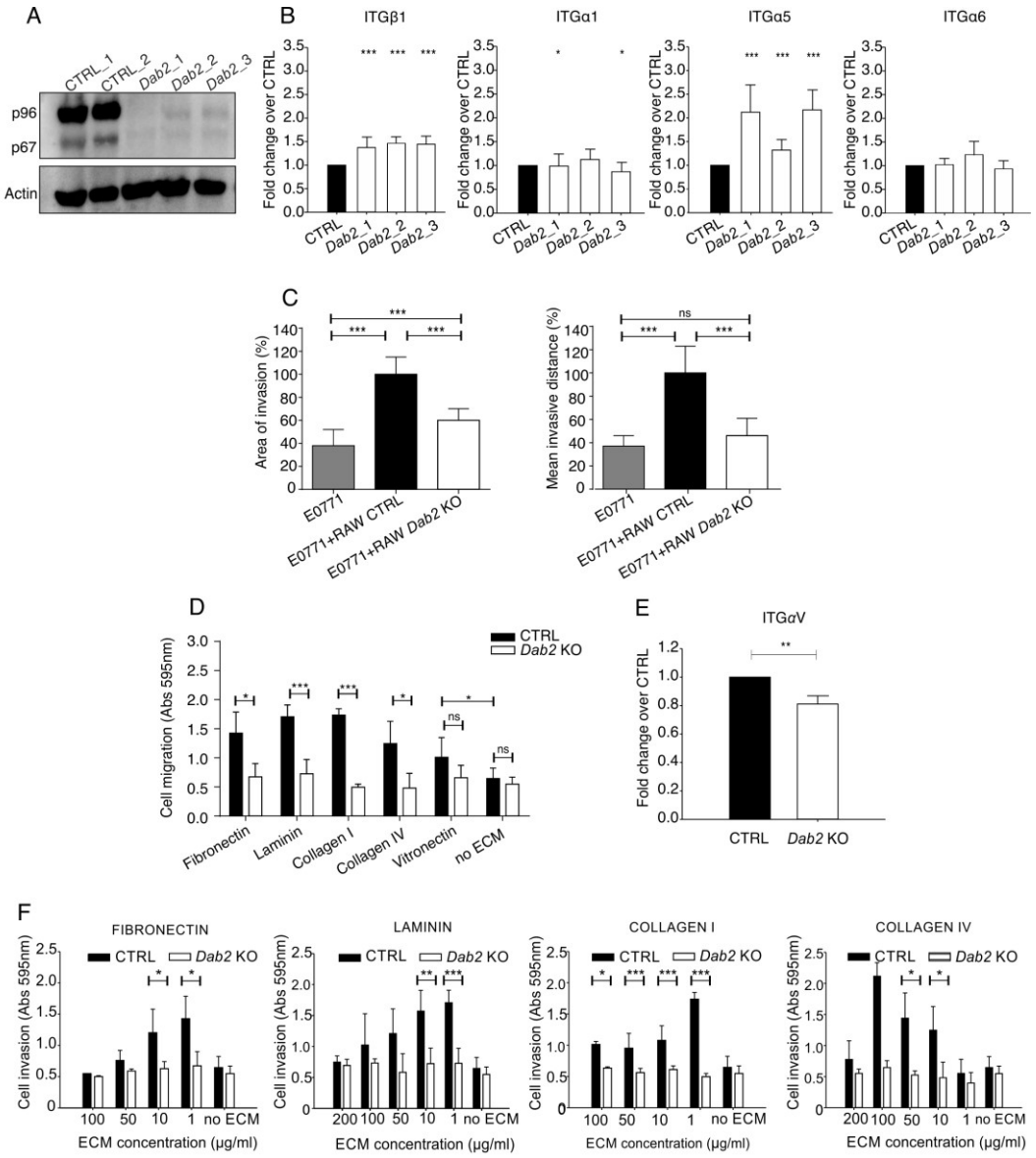

Figure 13. DAB2$^+$ macrophages favor tumor cell invasion by ITG and ECM interaction.
(A) Western blot analysis for the expression of DAB2 isoforms (p96 and p67) in RAW264.7, CTRL or *Dab2*-depleted clones. Actin was used as loading control. (B) Three different RAW264.7 CRISPR *Dab2* KO clones were analyzed by FC for the surface levels of β1, α1, α5 and α6 ITGs. The fold change of MFI relative to the controls is reported for each ITG. (C) Inverted *in vitro* invasion assays of RAW264.7 CTRL or *Dab2* KO single cell-derived clones co-cultured with E0771 tumor cells in a matrigel layer. The area of invasion and the mean invasive distance for either E0771 cells alone or in co-culture with RAW264.7 cells were quantified by confocal microscope (n=3 independent experiments). (D) Transwell invasion assay of RAW264.7 CTRL and *Dab2* KO single-cell-derived clones using a synthetic matrix (Puramatrix) supplemented with FN (1 µg/ml), LN (1 µg/ml), COL I (1 µg/ml), COL IV (10 µg/ml) or VN (1 µg/ml). Cell invasion was evaluated measuring the absorbance at 595nm of crystal violet stained cells. (E) RAW264.7 *Dab2* KO clone and CTRL were analyzed by FC for the surface levels of αV subunit. The fold change of MFI relative to the control is reported. (F) Transwell invasion assay of RAW264.7 CTRL and *Dab2* KO clones using a synthetic matrix (Puramatrix) supplemented with FN (100-1 µg/ml), LN (200-1 µg/ml), COL I (100-1 µg/ml) and COL IV (200-1 µg/ml). Cell invasion was evaluated measuring the absorbance at 595nm of crystal violet stained cells. Data are presented as mean ± s.d.; *p ≤ 0.05, **p ≤ 0.01 and ***p ≤ 0.001, by Student's *t*-test.

ECM-integrin interaction supports DAB2-mediated neoplastic spread

Considering that changes in structure and matrix composition enable ITGs to transmit biochemical and mechanical signals inside the cells and regulate cell migration and invasion (*177*), we chose to closely examine specific ITG functions.

Using the CRISPR/Cas9 genetic approach, we generated single cell-derived clones depleted for the expression of single ITGs. These *Itgβ1*, *Itgα5* and *Itgα6*-depleted RAW264.7 cells allowed us to investigate whether the loss of an ITG influences the surface expression of other ITGs and which is their contribution to macrophage motility and tumor cell invasiveness.

As we expected, *Itgβ*1-deficient clones did not show ITGβ1 expression. However, surprisingly, we observed that *Itg*β*1* deficiency leads to a highly significant ITGα5 cell surface reduction, while ITGα6 endocytosis was slightly affected (Figure 14A). In fact, it is widely known that ITGβ1 subunit is common to many heterodimers and its abrogation could impair the binding with other alpha subunits. In Figure 14B, *Itgα*5 abrogation did not involve the ITGβ1 and ITGα6 recycling, while *Itgα*6-deficient clones showed a slight but significant increase in ITGβ1 membrane levels in 2 out of 3 clones, and a robust increment of ITGα5 membrane expression, suggesting a compensatory mechanism (Figure 14C). As reported in Figure 14D, all *Itg*-deficient clones expressed similar levels of DAB2, implying that the outside-in ITG signaling was not a direct regulator of DAB2 expression.

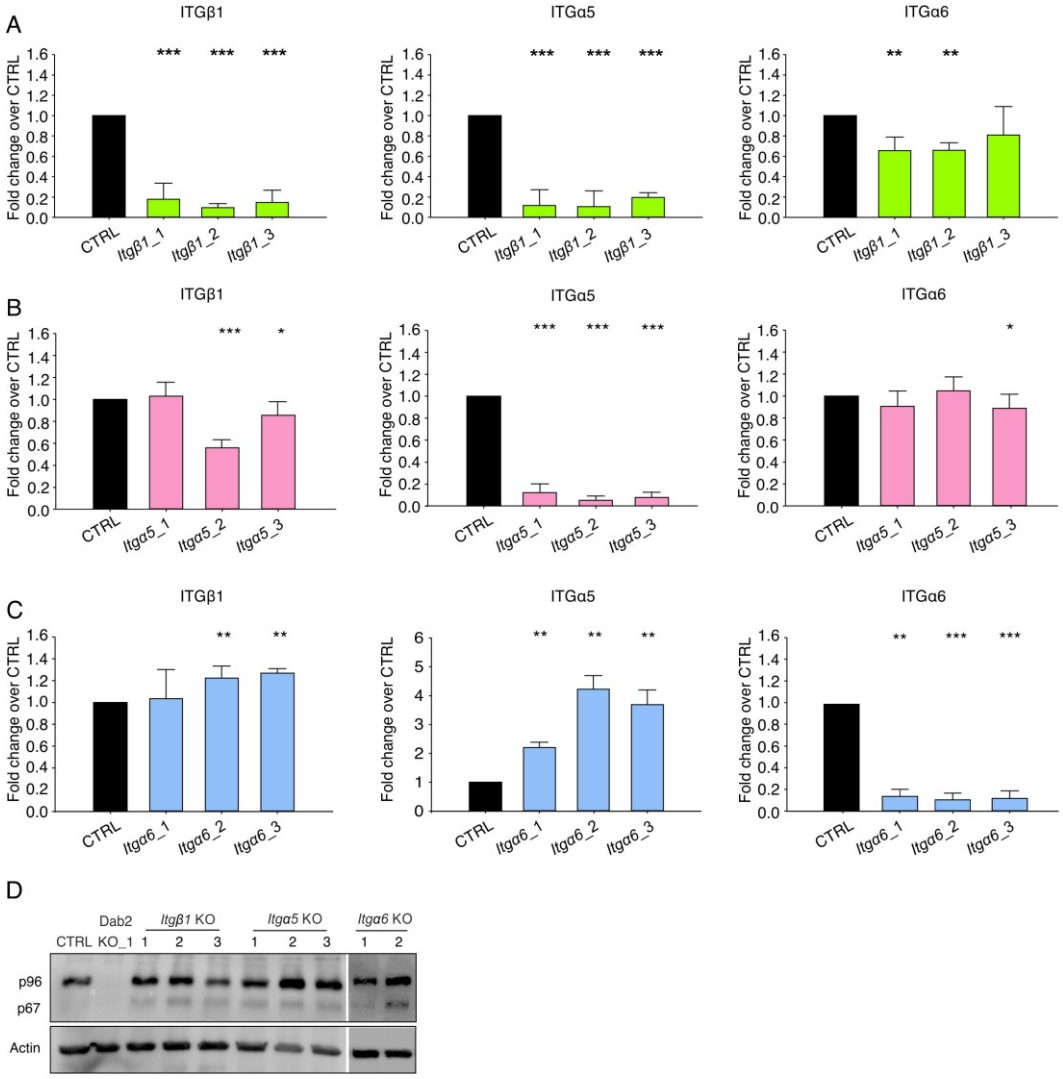

Figure 14. Characterization of *Itgs*-deleted clones.
(A, B, C) RAW264.7 *Itgβ*1 (A), *Itgα*5 (B) and *Itgα*6 (C) depleted clones (n=3 per group) and CTRL were analyzed by FC for the surface expression of β1, α5 and α6 ITGs respectively. The fold change of MFI relative to the control is reported for each ITG. (D) WB analysis for DAB2 expression isoforms (p96 and p67) in RAW264.7, CTRL or *Dab2*, *Itgβ1*, *Itgα5* and *Itgα6*-depleted clones. Actin was used as loading control.

Next, we analyzed the ability of *Itg*-deficient RAW 246.7 clones to remodel the ECM matrix and favor tumor cell spreading. Interestingly, only *Itgβ*1 and *Itgα*5 deleted clones showed a statistically significant impaired matrix remodeling and a consequent reduced invasion ability (Figures 15A), mirroring the same effect obtained by *Dab2* deletion and indicating that α5β1, but not α6β1 ITG heterodimers are required for macrophage-assisted ECM remodeling. In accordance with these data, E0771 tumor cell invasion was reduced only when β1

and α5 were deleted (Figures 15B and 15C), but was unaffected by the loss of α6 ITG (Figure 15D).

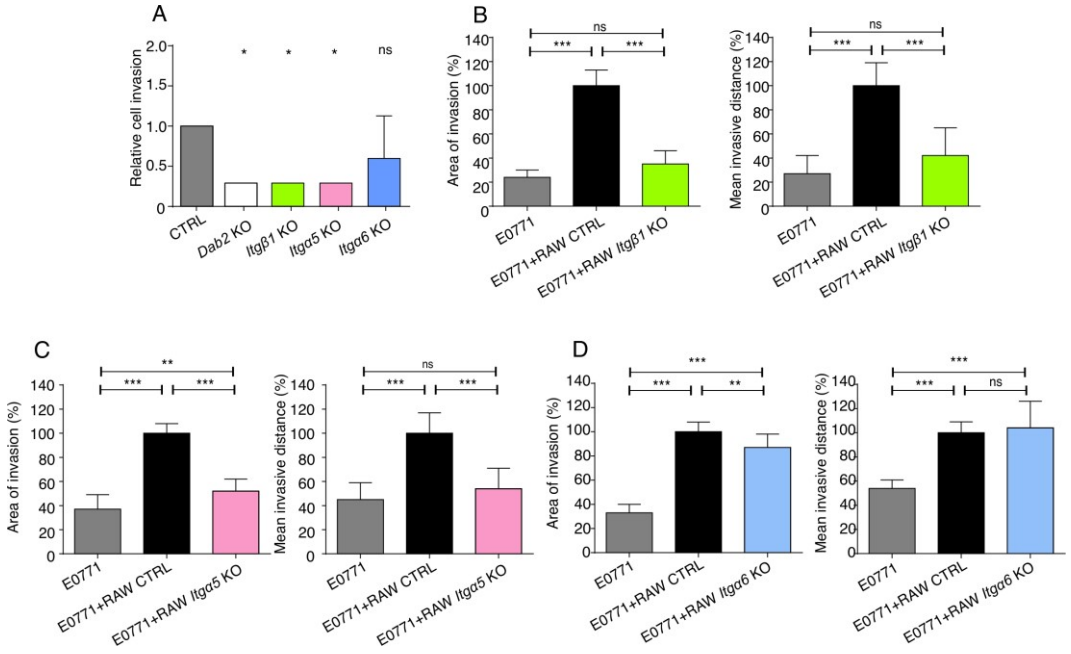

Figure 15. Effect of ITGs abrogation on ECM remodeling and macrophage-assisted tumor cell spreading.
(A) ITGs role in the matrix remodeling process mediated by RAW264.7 clones was evaluated on Boyden chambers coated with matrigel. The invasive ability of different clones was assessed measuring the absorbance at 595nm of invasive cells stained with crystal violet and reported as fold change over RAW264.7 CTRL cells. Data are representative of 3 independent experiments. (B, C, D) Inverted *in vitro* invasion assays of RAW264.7 CTRL or *Itgβ1* (B), *Itgα5* (C) and *Itgα6* KO (D) single-cell-derived clones co-cultured with E0771 tumor cells in a matrigel layer. The area of invasion and the mean invasive distance either for E0771 cells alone or in co-culture with RAW264.7 cells were quantified by confocal microscope (n=2 independent experiments). (A-D) Data are presented as mean ± s.d.; *p ≤ 0.05, **p ≤ 0.01 and ***p ≤ 0.001, by Student's *t*-test.

DAB2 expression is induced by chemical and mechanical stimuli

In order to define the factors responsible of DAB2 induction, we performed a gene set enrichment analysis (GSEA) to correlate *Dab2* expression in macrophages with known tumor-associated molecular pathways (Figure 16A). *Dab2* gene resulted enriched in WNT signaling, CSF1R pathways and YAP conserved signature. Among the resulting matches, the correlation between DAB2 and the signatures related to CSF1R and YAP appeared particularly interesting.

Considering that CSF-1 is a cytokine, abundantly secreted in the TME, we speculated that the same stimuli, which initiate the differentiation and proliferation of monocytes and macrophages, were also responsible for the expression of DAB2 (*227*). As predicted, both of DAB2 isoforms were upregulated during the CSF-1-driven *in vitro* BM-derived macrophage differentiation (Figure 16B).

To understand whether DAB2 expression was modulated only by the release of this cytokine or by additional mechanical stimuli, $CD11b^+$ cells isolated from tumor-free mice were cultured under adhesion or suspension, in presence of media supplemented with CSF-1 (100 ng/mL) or tumor cells supernatant containing CSF-1 (Figure 16C). *Dab2* expression resulted higher in response to CSF-1 and TDSFs when cells were cultured on a stiff surface, proposing an interplay between the chemical and mechanical stimuli in the *Dab2* induction during macrophage differentiation.

Mechanical cues and ECM stiffness are associated with the ability of cells to migrate and the activation of specific transcriptional programs. Among transcriptional factors regulated by ECM, we pointed our attention to YAP and TAZ, related to cancer progression and well-studied in tumor cells and cancer-associated fibroblasts (*196, 206*). However, YAP/TAZ role in macrophage mechanosensing has not been elucidated yet and the association between DAB2 and YAP has never been experimentally validated up to date. YAP protein was detectable in TAMs isolated from E0771, MN-MCA1 and PyMT tumors and in MTMs, which are negative for the expression of DAB2, suggesting that YAP modulation is independent from DAB2 (Figures 16D and 16E). IF analysis performed on PyMT tumor slices demonstrated that DAB2 is co-expressed with YAP and that $DAB2^+YAP^+$ cells are positive for the F4/80 staining (Figure 16F).

To confirm that DAB2 levels in macrophages can be influenced by mechanotrasduction, we tested conditional *Yap/Taz* KO mice in myeloid cell lineage. DAB2 expression was negligible in TAMs sorted from these mice, indicating that *Dab2* transcriptional regulation is under control of YAP/TAZ transcriptional complex *in vivo* (Figure 16G). The MN-MCA1 cells injection in *Yap/Taz* KO mice showed a reduction in lung metastases, comparable to *Dab2*

KO mice (Figure 16H), without any effect on leukocyte recruitment (Figure 16I). In conclusion, DAB2 expression was induced in TAMs by a synergism between both chemical and mechanical cues, disclosing the role of CSF-1 and YAP as regulators of DAB2.

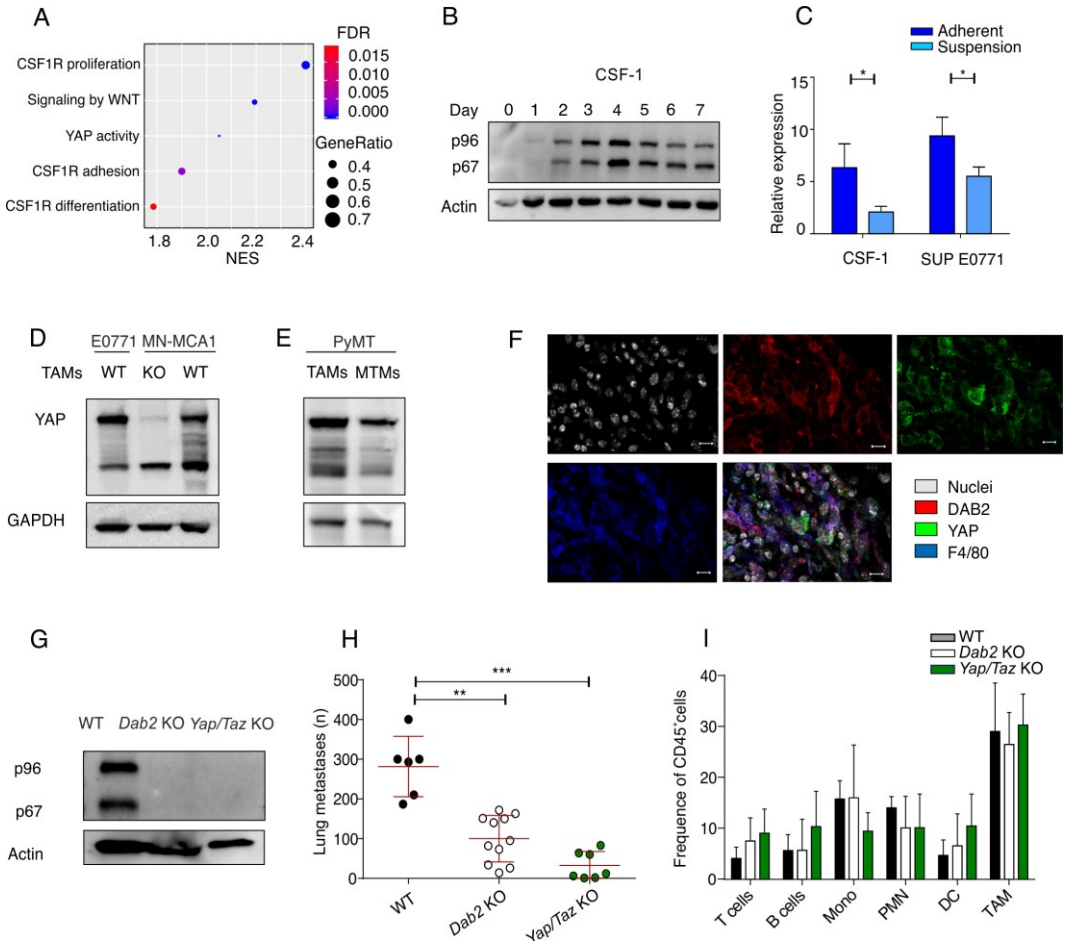

Figure 16. CSF-1 and YAP as regulators of DAB2 expression in TAMs.
(A) Gene set enrichment analysis (GSEA) for tumor-related pathways associated with *Dab2* expression in macrophages. (B) DAB2 expression evaluated by WB analysis on BM precursors from WT mice differentiated in the presence of CSF-1 for 7 days. Actin was used as loading control. (C) *Dab2* expression assessed by qRT-PCR on $CD11b^+$ cells isolated from BM of tumor-free mice and cultured for 6 hours either as adherent cells or in suspension, in presence of CSF-1 or supernatant of E0771 cells. Data are presented as mean ± s.d. *$p \leq 0.05$, **$p \leq 0.01$ and ***$p \leq 0.001$ by Student's *t*-test, pooled from 3 independent experiments. (D, E) WB analysis for YAP expression on FACS-sorted TAMs from E0771 and MN-MCA1 tumor–bearing WT or KO mice (D) or TAMs and MTMs isolated from PyMT mice (E). GAPDH was used as loading control. (F) IF performed to evaluate expression of YAP, DAB2 and F4/80 on PyMT tumor slices. Scale bar: 50 µm. (G) WB analysis for DAB2 expression on TAMs isolated from MN-MCA1 tumor bearing WT, *Dab2* KO and *Yap/Taz* KO mice. (H) Quantification of lung metastases in WT, *Dab2* KO, and *Yap/Taz* KO mice orthotopically injected with MN-MCA1 cells. (I) Accumulation of different immune populations among $CD45^+$-gated cells in MN-MCA1 tumors from WT (n=3), *Dab2* KO (n=3) or *Yap/Taz* KO (n=3) mice.

DAB2 is expressed in metastasis-associated macrophages (MAMs) and supports lung colonization

Our previous results indicate that DAB2^{+} macrophages are peculiar of TME and play a central role in matrix remodeling at primary tumor site, where they assist tumor cell spreading. However, DAB2 protein was also detected at the metastatic site and, in particular, its expression was specifically present in MAMs isolated from lungs of MN-MCA1 tumor-bearing mice and not in any other myeloid subsets (Figure 17A). Similar to the primary tumor, DAB2-expressing macrophages were localized near the metastatic borders, while only few DAB2^{+} cells were present in healthy areas of metastatic lungs (Figures 17B and 17C).

To investigate whether *Dab2* deletion in the hematopoietic compartment could affect the accumulation of myeloid cells in the metastatic site, we analyzed the myeloid infiltrate in the lungs of WT and *Dab2* KO mice injected with MN-MCA1 or E0771 cell lines (Figure 17D). We observed a similar accumulation of granulocytes (Ly6G^{+}Ly6C^{low} cells), monocytes (Ly6G^{-}Ly6C^{high} cells), tissue resident macrophages (TRMs, CD11c^{+}CD11b^{low} cells) and MAMs (Ly6G^{-} Ly6C$^{low/-}$F4/80^{+} cells) between WT and KO mice, suggesting that *Dab2* deficiency did not strongly impact the myeloid cell recruitment to distal metastatic tissue.

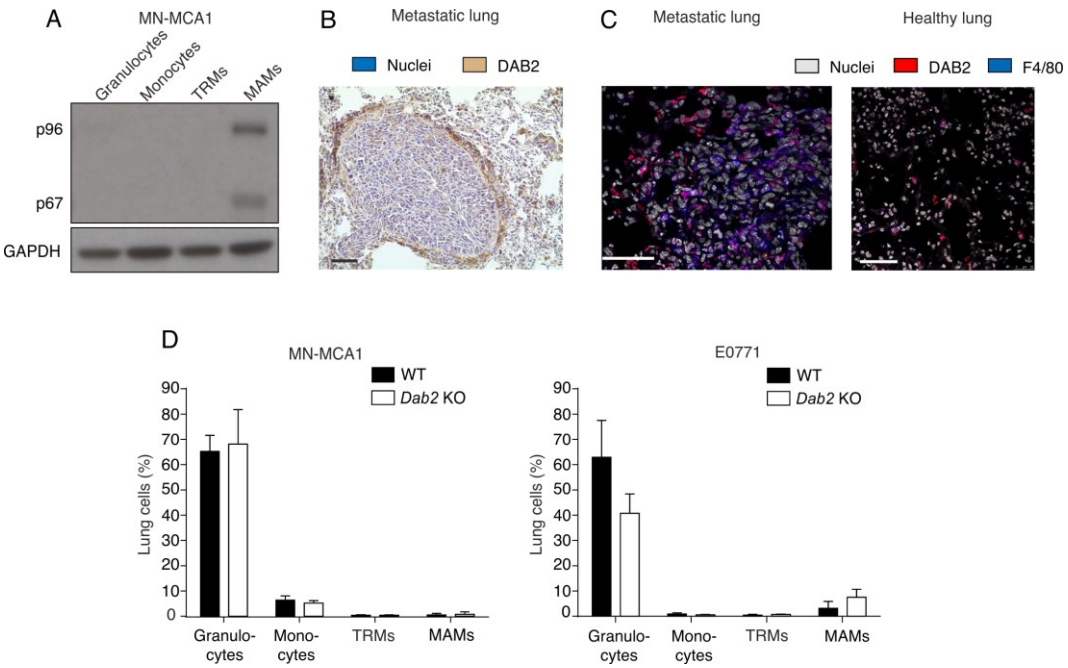

Figure 17. DAB2$^+$ macrophages are localized along metastasis border.
(A) WB analysis for DAB2 expression isoforms (p96 and p67) on FACS-sorted granulocytes, monocytes, TRMs and MAMs infiltrating lungs from MN-MCA1-bearing mice. GAPDH was used as loading control. (B) Lungs from MN-MCA1 tumor-bearing animals were stained for DAB2 by IHC; a representative image of metastasis is shown. (C) Exemplificative IF images of DAB2 and F4/80 double staining in the metastasis border (left) and in the healthy lung (right), are shown. Scale bars: 50 μm. (D) Percentage of different myeloid subpopulations within metastatic lungs on MN-MCA1 or E0771 tumor-bearing mice (n=3 mice/group). Error bars are mean ± s.e.

Moreover, the presence of DAB2$^+$ macrophages in distal areas suggests that these cells are not only involved in the first steps of metastatic cascade in the primary tumors (i.e. local invasion and intravasation) but they probably regulate additional phases, such as arrest and adhesion, extravasation, initial seeding and cell growth at the metastatic site (*14, 93*). Therefore, we experimentally dissociated the contribution of the primary tumor in distal steps of metastasis development by the intravenous injection of E0771 tumor cells in either WT or *Dab2* KO mice. This setting allowed us to confirm that DAB2-expressing cells are involved in the late phase of metastatic process since *Dab2* deficiency in myeloid cells negatively affected the number, burden and mean area of lung micrometastases (Figures 18A-C).

Inflammatory monocytes are able to support the extravasation of tumor cells from the blood to the lung (*93*). As previously reported in figure 1B, DAB2 was detectable at low levels also in tumor-infiltrating monocytes (Figure 18B); we thus decided to evaluate their possible assistance in endothelial trans-migration of cancer cells. E0771 tumor cells extravasation through an endothelial layer was comparable in presence of Ly6C$^+$ monocytes FACS-sorted from either WT or *Dab2* KO-tumor-bearing mice, dismissing the participation of DAB2 in this step (Figure 18D).

Moreover, generating mCherry/Luc-expressing E0771 tumor cells and combining bioluminescence imaging and flow cytometry analysis, we were able to study the process of tumor seeding and growth at the metastatic site. Pulmonary metastases started to be detectable in WT mice, intravenously injected with mCherry/Luc E0771 cells, 9 days after tumor cell challenge, whereas no significant luminescence was detectable in tumor-bearing, *Dab2* KO mice throughout the observation time (Figure 18E). The mCherry/Luc E0771 cells initially seeded the

lungs of WT and *Dab2* KO mice without remarkably differences. However, after 28 days, when WT mice had to be euthanized, we noticed that cancer cells proliferated from about 10^4 to 10^6 per lung, while they were barely detectable in *Dab2* KO mice (Figure 18F). These results suggest that DAB2 is required for the tumor cell expansion at the metastatic site, but not in the initial seeding.

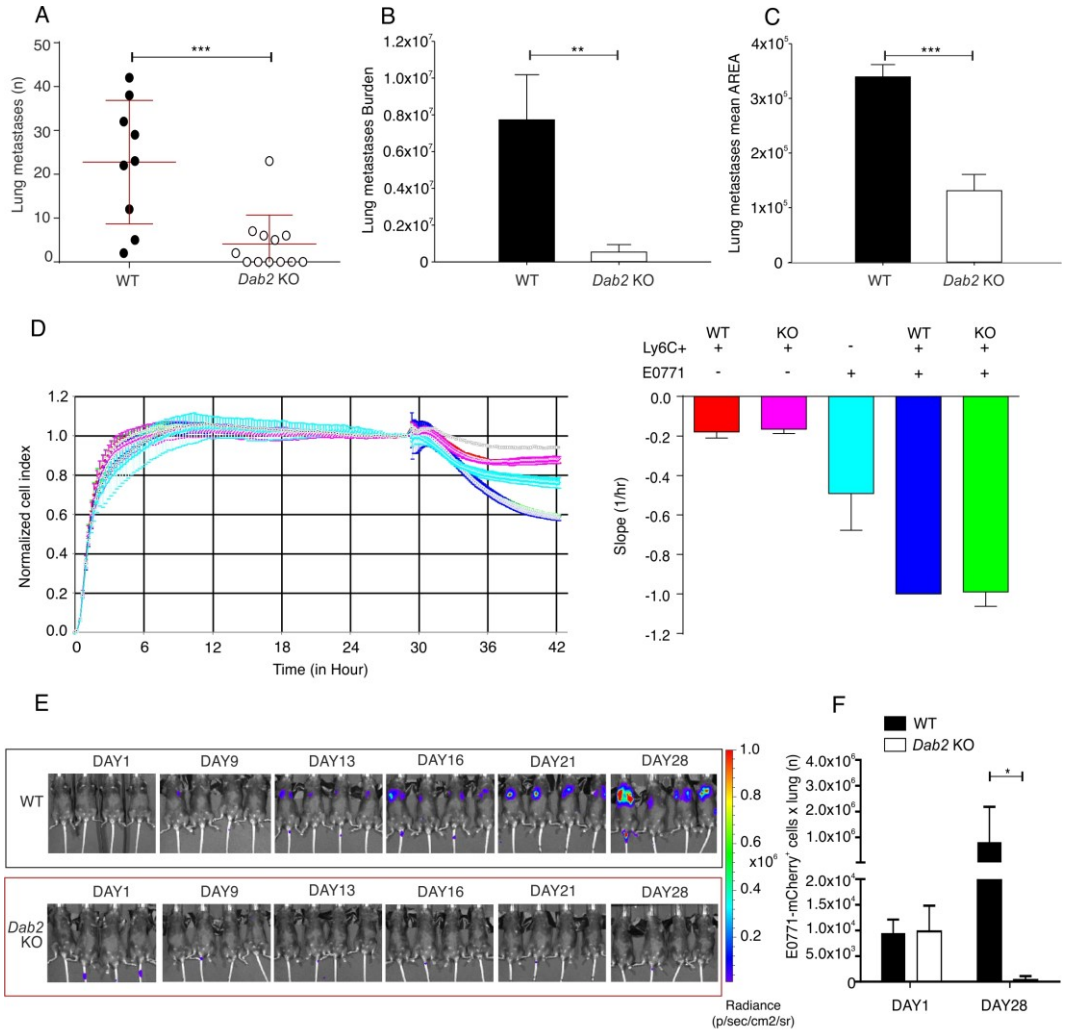

Figure 18. DAB2 expression in MAMs regulates lung colonization.
(A-C) Quantification of lung micrometastases number (A), burden (B) and mean area (C) at day 20 following E0771 i.v. injection in either WT (n=9) or *Dab2* KO (n=12) mice. (D) Trans-endothelial migration of Ly6C$^+$ monocytes, alone or in co-culture with E0771 tumor cells, evaluated using the xCELLiegence technology. Microelectrodes detect impedance changes proportional to the number of transmigrated cells. Cell invasion was assessed by slope analysis of the generated curves and reported as inverted histograms. Data represent mean ± s.d.; n=2 independent experiments. (E) Metastasis formation in WT and *Dab2* KO mice following mCherry/Luc E0771 cells i.v. injection, evaluated by bioluminescence imaging. (F) Absolute numbers of mCherry$^+$ E0771 cells per lung in WT and *Dab2* KO mice 1 or 28 days after tumor challenge (n= 3 mice/ group). Data are presented as mean ± s.d. *p ≤ 0.05, **p ≤ 0.01 and ***p ≤ 0.001 by Student's *t*-test.

The presence of DAB2$^+$ TAMs in cancer patients correlates with worse prognosis

To extend our findings in a clinical context, we examined the presence of DAB2 in human patients and investigated whether its levels could be correlated with prognosis. In particular, we focused our attention on breast cancer, which is a leading cause of cancer-related death, mainly for its metastatic potential. According to a histological point of view, breast cancer can be divided in invasive ductal and lobular carcinomas (IDCs and ILCs, respectively), while according to a molecular approach, three main subtypes have been identified (luminal, HER2 and triple negative) and correlated with tumor aggressiveness (*65, 104, 150*).

To confirm data obtained from MMTV-PyMT, a spontaneous breast cancer model of ILC, we assessed the possible prognostic role of DAB2$^+$ macrophages in a cohort of 32 patients with early-stage ILC tumors who underwent surgery. The presence of DAB2 positive, non-neoplastic and non-EC cells with macrophage morphology was evaluated in both peritumoral and intratumoral areas by IHC (Figure 19A). The number of DAB2$^+$ macrophages was significantly higher at invasive frontlines as compared to intratumoral areas, mirroring what already observed in our mouse models (Figure 19A). Moreover, high peritumoral and intratumoral DAB2 levels were associated with significantly worse 10-year DFS (Figure 19B). We can thus conclude that the presence of DAB2$^+$ macrophages at the tumor site, in both regions, could be considered as a prognostic marker for tumor progression and metastasis formation in patients with primary resected ILC.

Finally, we extended our analyses to a group of 59 early stage gastric cancer (GC) patients, who underwent complete resection. Among different cases, we observed heterogeneous levels of DAB2$^+$ macrophages (Figure 19C), which allowed us to stratify patients in low-expressing and high-expressing-DAB2. Patients with high DAB2 expression displayed a reduction in the 3-year CSS and OS (Figures 19D and 19E).

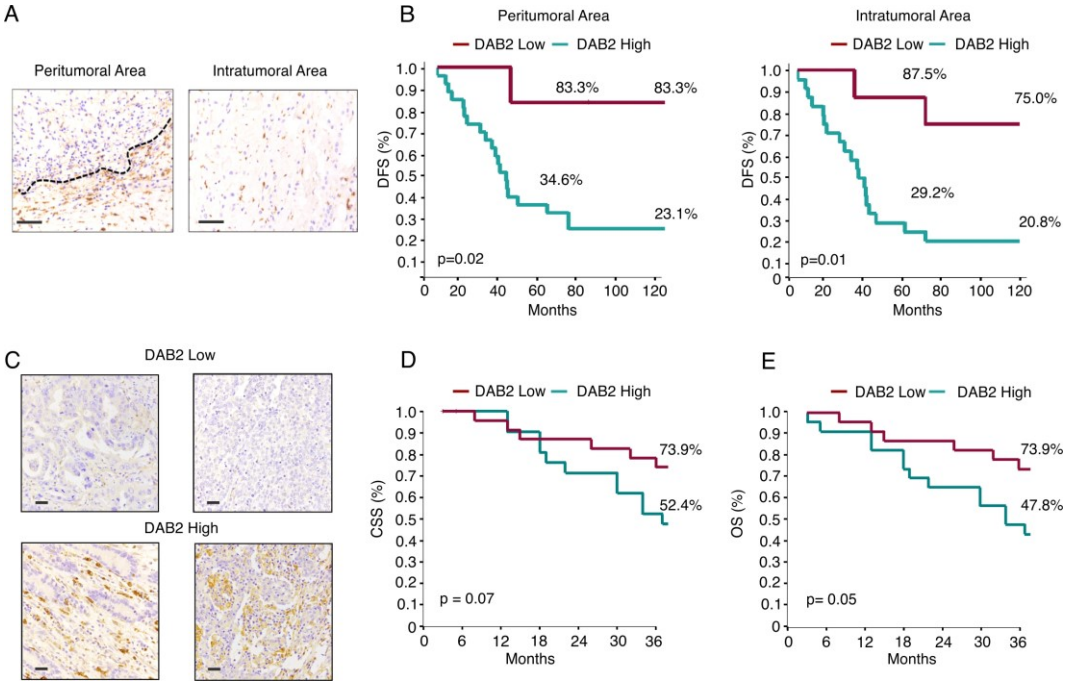

Figure 19. Prognostic value of DAB2 in different human cancers.
(A) Peritumoral and intratumoral DAB2 staining by IHC in pure, early-stage invasive lobular carcinoma (ILC). Scale bars: 100 μm. (B) Disease-Free Survival (DFS) according to peritumoral or intratumoral DAB2 staining (IHC, low versus high, ROC-derived optimal cut-offs) in 32 ILC patients undergone surgery (log-rank p-value). (C) Macrophages DAB2 scoring in gastric cancer patients (IHC). (D-E) Cancer-Specific- and Overall-Survival (CSS, OS) according to DAB2 expression in 59 samples from gastric cancer patients (log-rank p-value).

DISCUSSION AND FUTURE DEVELOPMENTS

Metastatic spread is a multi-step process responsible for as much as 90% of cancer-associated mortality (*5*). In this study, we focused our attention on the ability of tumor-associated stromal cells to generate a cancer-promoting environment and, in particular, on the role of tumor-infiltrating myeloid cells in malignant progression and metastatic spread. Among myeloid cells, TAMs are crucial for cancer cell invasion both for intravasation at the primary site as well as extravasation, tumor cell seeding and growth at the metastatic niche. Despite the increasing number of publications regarding the pro-tumor functions exerted by TAMs (*65, 67*), the molecular mechanisms through which these cells act are poorly known.

According to our data, DAB2, an adaptor protein involved in the CME (*195*), is highly expressed in TAMs at the primary site and MAMs at the metastatic niche and it can be considered as master regulator of the macrophage-assisted tumor cell invasion. Indeed, its deletion in the myeloid compartment significantly affects lung metastasis formation in different mouse tumor models (i.e. fibrosarcoma and breast cancer). Interestingly, in *Dab2* KO mice there are no remarkable differences in the primary tumor growth compared to WT littermates, indicating that $DAB2^+$ macrophages do not participate in the early phases of carcinogenesis. Moreover, the unaltered immunosuppressive function of tumor-infiltrating immune cells or their recruitment and accumulation at the tumor site suggests that DAB2-expressing macrophages support the invasion process independently from a negative effect on anti-tumor immune response.

The localization of $DAB2^+$ TAMs along tumor invasive frontline, and not in the tumor core or healthy tissues, induced us to speculate that they are predisposed to favor cancer cell expansion in the surrounding environment. Therefore, we evaluated whether $DAB2^+$ TAMs could promote tumor cell invasiveness through ECM remodeling, one of the main functions of macrophages. Distance covered by cancer cells through a 3D matrix was higher when they were co-cultured in presence of $DAB2^+$ TAMs, indicating a DAB2-mediated matrix remodeling necessary to guide cancer cell diffusion by a process called trailblazer effect (*135*). Moreover, a second harmonic generation analysis proved that COL fibers in *Dab2* KO mice were denser

and more organized than ones in WT mice, due to the macrophage inability to digest the matrix. Interestingly, we also showed that *Dab2* deficiency ablates haptotaxis, but does not impair macrophage migration towards a soluble chemokine gradient, i.e. chemotaxis. The mechanistic basis of this finding relies on the physical interaction between cells and ECM proteins as prerequisite for ECM remodeling and local migration.

DAB2 is an endocytic adaptor involved in the internalization and the recycling of transmembrane receptors such as ITGs, which play a crucial role in mediating the interactions between the cell and the nearby microenvironment (*192*). In particular, α1, α5 and α6 ITGs bind ITGβ1 on the surface of cells and the resulting dimers (α1β1, α5β1, α6β1) are able to interact with specific ECM proteins: COL, FN and LN, respectively (*224*). In this regard, *Dab2* ablation in BMDMs caused an altered ITG uptake with a consequent higher accumulation of α5, α6 and β1 ITGs on their surface compared to WT cells. These results are consistent with previous studies in which *Dab2* silencing in HeLa tumor cells led to an increase in α1, α2, α3 and β1 ITGs on the cell surface (*194, 195*). As expected, the defect in ITG turnover caused an impaired endocytosis of ECM fragments and a subsequent reduction in macrophage directional movement.

Confirming data previously obtained in BMDMs, *Dab2*-deficient RAW264.7 clones presented higher surface levels of β1 and α5 ITGs, a reduced capacity of matrix reorganization and a diminished invasive ability in crossing the 3D matrixes in comparison to DAB2-expressing clones. Considering that *Dab2* KO clones showed an impaired invasion only when exposed to ECM proteins interacting with DAB2-regulated ITGs, but not with VN (*226*), it can be concluded that the movement of these cells is dependent on ECM protein composition.

Furthermore, the genetic deletion of single ITG chains proved the prominent effect of α5β1 heterodimers in DAB2-assisted tumor cells invasion. Interestingly, this heterodimer preferentially binds FN, the major component of the p-mN (*14*), suggesting a role of $DAB2^{+}$ MAMs also at the metastatic site (*228, 229*). Moreover, α5β1-dependent adhesions are known to be involved in stabilizing the bond between ECs and tumor cells and favoring the intravascular arrest of CTCs,

allowing them to resist to the shear stress from the blood flow and extravasate (*230*).

The DAB2 continuous expression within TME is dependent on both chemical and mechanical stimuli. DAB2 is upregulated in naïve BM cells stimulated with soluble CSF-1, a cytokine responsible for monocyte and macrophage differentiation (*227*) and known to be related to tumor progression and metastases in PyMT mice (*231*). Noteworthy, data reported in literature prove that macrophages and tumor cells cooperate in the invasion process (*82*) due to the establishment of a paracrine loop. Indeed, macrophages release EGF, which supports cancer cell invasion and the formation of invadopodia, whereas CSF-1 produced by malignant cells promotes the secretion of EGF by macrophages. In turn, EGF assists the expression of CSF-1 by cancer cells. Disruption of this positive feedback loop by blockade of either EGF or CSF-1 receptor signaling can inhibit macrophage and tumor cell migration and invasion (*232*). Moreover, either elevated levels of CSF-1 in cancer cells or increased EGF signature in macrophages correlate with high-grade tumors and poor prognosis in breast cancer patients (*233*).

However, chemical stimuli are not the only factors involved in the DAB2 expression in differentiated macrophages; indeed, we showed that its induction is higher in presence of a mechanical stimulus. The composition and rigidity of ECM are considered pivotal factors for the cellular invasion and the activation of specific programs. Among factors modulated by the rigidity of the substrate, we focused our attention on YAP and TAZ transcriptional factors: soft matrices induce their cytoplasmic retention, while rigid matrices cause their nuclear transfer and activation (*196*). According to protein expression analysis, YAP was found in TAMs but also in MTMs, negative for the expression of DAB2, indicating that its expression is independent from DAB2 regulation. Moreover, DAB2 was not detected in TAMs isolated from *Yap/Taz* KO mice, allowing us to propose YAP as key regulator of DAB2. Moreover, an IF analysis showed that DAB2 is co-expressed with YAP and that $DAB2^{+}YAP^{+}$ cells are macrophages, as revealed by F4/80 staining. Similar to *Dab2* KO tumor-bearing mice, *Yap/Taz* KO mice

showed a reduced number in lung metastases, an unaltered primary tumor growth and no difference in the accumulation of infiltrating immune cells.

In order to confirm *in vitro* that DAB2 is under the control of YAP in TAMs, it would be interesting to explore whether the interaction with a COL-based substrate with different stiffness has an effect on *Dab2, Yap* and *Yap*-correlated genes (such as *Ctgf* and *Cyr61*) mRNA levels in TAMs. In addition, we plan to interfere with YAP expression *in vivo* using inhibitors, already in clinic, such us HA-1077 (*234*) and Visudyne (*235*).

In conclusion, for the first time, this project correlated DAB2 protein in macrophages with the transcriptional YAP/TAZ complex, demonstrating that DAB2 is regulated by mechanical cues and acts as connector between ITG endocytosis, ECM stiffness and macrophage-assisted tumor cell spreading.

Considering that $DAB2^+$ TAMs mainly localize along tumor borders, where the matrix is stiffer in comparison to the core, we hypothesize that macrophages movement could be guided not only by the ITG-ECM interaction but also by rigidity gradient (i.e. durotaxis) (*150, 236*). In order to mimic the TME and follow stromal changes recently reported for human breast cancer (*150*), COL I-fluorocrome conjugated with different concentrations could be stratified on chamber slides and WT or *Dab2* KO TAMs invasion across matrix layers could be evaluated by confocal microscopy.

DAB2-expressing TAMs are able to promote the ECM degradation favoring the invasion of cancer cells towards the endothelial vasculature; however, TAMs are known to participate also in other phases of the metastatic process, such as intravasation, extravasation, arrest and adhesion, seeding and tumor cell growth at the metastatic niche (*93*). DAB2 is mainly expressed in MAMs localized along tumor borders, reflecting the same gradient-like pattern already observed in the primary tumor mass. Moreover, $DAB2^+$ macrophages promote the malignant cell proliferation at the metastatic site, but not the initial seeding.

High levels of DAB2-expressing macrophages along tumor invasive frontline are indicative of a worse prognosis also in human hosts, and in particular in patients affected by early-stage ILC breast cancer and gastric cancer. Considering that sampling of tumor borders might not be always feasible in the clinical practice,

the possibility to detect DAB2$^+$ macrophages inside human tumors intensified its prognostic value.

These findings are in accordance with data reported in literature in which TAMs localization and density are associated with poor clinical outcome in several solid cancers, including bladder, breast, renal, prostate, and gastric cancer (*237*). To complete our studies, the analysis of DAB2 as prognostic marker has to be extended to a large cohort of patients as well as to IDC breast cancer patients, to the different molecular subtypes of breast cancer (luminal A/B *vs.* HER2 and triple negative) and to other metastatic diseases.

The results achieved with this work allow us to propose a role for DAB2 in the macrophage-assisted, mechanotransduction-driven metastatic process and consequently to advance DAB2 as target for anti-metastatic therapy. In the last few years, several macrophage-targeting drugs have been developed for depletion (e.g. CCR2 and CSF1R antagonists), reprogramming (e.g. PI3Kγ and HDAC inhibitors), or interference with their effector functions (e.g. ARG1 and Fc-receptors) and many clinical trials are ongoing (*104*). However, all these therapeutic strategies require further investigation due to their effects also on normal macrophages and to their considerable toxicity over time. Indeed, the knowledge of the TAM-specific targets, the immune reactions occurring during all the phases of carcinogenesis and the mechanism of immunosuppression are still limited.

In order to distinguish specific populations of tumor-infiltrating myeloid cells with pro-tumor activities, it would be interesting to exploit single-cell RNA sequencing and identify specific markers that license their targeting. Moreover, a restricted comprehension of molecular mechanisms underlying the metastatic cascade has led to the development of strategies based only on primary tumors (*8*), without considering the metastasis inhibition. A DAB2-directed treatment would interfere in the metastatic cascade, also operating after primary tumor resection to cure hidden or dormant metastases.

We foresee that use of nanoparticles loaded with nucleic acids interfering with DAB2 expression could represent a feasible strategy. Indeed, dendrimers functionalized to target CD124 and loaded with shRNA or miRNA are able to

target TAMs at the tumor site, where they can mediate the silencing of the genes of interest (*238*). Whether targeting DAB2 could also impact MAMs activity is a preliminary step to envision a combinatorial therapy with checkpoint inhibitors to specifically improve the anti-metastatic effect.

REFERENCES

1. D. Hanahan, R. A. Weinberg, Hallmarks of cancer: the next generation. *Cell* **144**, 646-674 (2011).
2. D. Hanahan, L. M. Coussens, Accessories to the crime: functions of cells recruited to the tumor microenvironment. *Cancer Cell* **21**, 309-322 (2012).
3. R. D. Schreiber, L. J. Old, M. J. Smyth, Cancer immunoediting: integrating immunity's roles in cancer suppression and promotion. *Science* **331**, 1565-1570 (2011).
4. F. Li, B. Tiede, J. Massague, Y. Kang, Beyond tumorigenesis: cancer stem cells in metastasis. *Cell Res* **17**, 3-14 (2007).
5. P. S. Steeg, Targeting metastasis. *Nat Rev Cancer* **16**, 201-218 (2016).
6. B. Z. Qian, J. W. Pollard, Macrophage diversity enhances tumor progression and metastasis. *Cell* **141**, 39-51 (2010).
7. G. S. Mack, A. Marshall, Lost in migration. *Nat Biotechnol* **28**, 214-229 (2010).
8. R. L. Anderson, T. Balasas, J. Callaghan, R. C. Coombes, J. Evans, J. A. Hall, S. Kinrade, D. Jones, P. S. Jones, R. Jones, J. F. Marshall, M. B. Panico, J. A. Shaw, P. S. Steeg, M. Sullivan, W. Tong, A. D. Westwell, J. W. A. Ritchie, U. K. Cancer Research, C. R. C. A. M. W. G. Cancer Therapeutics, A framework for the development of effective anti-metastatic agents. *Nat Rev Clin Oncol* **16**, 185-204 (2019).
9. B. Hotz, M. Arndt, S. Dullat, S. Bhargava, H. J. Buhr, H. G. Hotz, Epithelial to mesenchymal transition: expression of the regulators snail, slug, and twist in pancreatic cancer. *Clin Cancer Res* **13**, 4769-4776 (2007).
10. M. G. Kazanietz, M. J. Caloca, The Rac GTPase in Cancer: From Old Concepts to New Paradigms. *Cancer Res* **77**, 5445-5451 (2017).
11. S. Paget, The distribution of secondary growths in cancer of the breast. 1889. *Cancer Metastasis Rev* **8**, 98-101 (1989).
12. L. Weiss, P. M. Ward, Cell detachment and metastasis. *Cancer Metastasis Rev* **2**, 111-127 (1983).
13. D. X. Nguyen, P. D. Bos, J. Massague, Metastasis: from dissemination to organ-specific colonization. *Nat Rev Cancer* **9**, 274-284 (2009).
14. B. Psaila, D. Lyden, The metastatic niche: adapting the foreign soil. *Nat Rev Cancer* **9**, 285-293 (2009).
15. T. Kitamura, B. Z. Qian, J. W. Pollard, Immune cell promotion of metastasis. *Nat Rev Immunol* **15**, 73-86 (2015).
16. S. Hiratsuka, A. Watanabe, H. Aburatani, Y. Maru, Tumour-mediated upregulation of chemoattractants and recruitment of myeloid cells predetermines lung metastasis. *Nat Cell Biol* **8**, 1369-1375 (2006).
17. A. Hoshino, B. Costa-Silva, T. L. Shen, G. Rodrigues, A. Hashimoto, M. Tesic Mark, H. Molina, S. Kohsaka, A. Di Giannatale, S. Ceder, S. Singh, C. Williams, N. Soplop, K. Uryu, L. Pharmer, T. King, L. Bojmar, A. E. Davies, Y. Ararso, T. Zhang, H. Zhang, J. Hernandez, J. M. Weiss, V. D. Dumont-Cole, K. Kramer, L. H. Wexler, A. Narendran, G. K. Schwartz, J. H. Healey, P. Sandstrom, K. J. Labori, E. H. Kure, P. M. Grandgenett, M. A. Hollingsworth, M. de Sousa, S. Kaur, M. Jain, K. Mallya, S. K. Batra, W. R. Jarnagin, M. S. Brady, O. Fodstad, V. Muller, K. Pantel, A. J. Minn, M. J. Bissell, B. A. Garcia, Y. Kang, V. K. Rajasekhar, C. M. Ghajar, I. Matei, H. Peinado, J. Bromberg, D. Lyden, Tumour exosome integrins determine organotropic metastasis. *Nature* **527**, 329-335 (2015).
18. R. H. Adams, K. Alitalo, Molecular regulation of angiogenesis and lymphangiogenesis. *Nat Rev Mol Cell Biol* **8**, 464-478 (2007).
19. R. Kalluri, M. Zeisberg, Fibroblasts in cancer. *Nat Rev Cancer* **6**, 392-401 (2006).
20. S. Ugel, F. De Sanctis, S. Mandruzzato, V. Bronte, Tumor-induced myeloid deviation: when myeloid-derived suppressor cells meet tumor-associated macrophages. *J Clin Invest* **125**, 3365-3376 (2015).
21. W. B. Coley, II. Contribution to the Knowledge of Sarcoma. *Ann Surg* **14**, 199-220 (1891).

22. G. P. Dunn, A. T. Bruce, H. Ikeda, L. J. Old, R. D. Schreiber, Cancer immunoediting: from immunosurveillance to tumor escape. *Nat Immunol* **3**, 991-998 (2002).
23. J. Galon, A. Costes, F. Sanchez-Cabo, A. Kirilovsky, B. Mlecnik, C. Lagorce-Pages, M. Tosolini, M. Camus, A. Berger, P. Wind, F. Zinzindohoue, P. Bruneval, P. H. Cugnenc, Z. Trajanoski, W. H. Fridman, F. Pages, Type, density, and location of immune cells within human colorectal tumors predict clinical outcome. *Science* **313**, 1960-1964 (2006).
24. L. Zitvogel, L. Apetoh, F. Ghiringhelli, G. Kroemer, Immunological aspects of cancer chemotherapy. *Nat Rev Immunol* **8**, 59-73 (2008).
25. S. Ugel, E. Peranzoni, G. Desantis, M. Chioda, S. Walter, T. Weinschenk, J. C. Ochando, A. Cabrelle, S. Mandruzzato, V. Bronte, Immune tolerance to tumor antigens occurs in a specialized environment of the spleen. *Cell Rep* **2**, 628-639 (2012).
26. S. H. Naik, P. Sathe, H. Y. Park, D. Metcalf, A. I. Proietto, A. Dakic, S. Carotta, M. O'Keeffe, M. Bahlo, A. Papenfuss, J. Y. Kwak, L. Wu, K. Shortman, Development of plasmacytoid and conventional dendritic cell subtypes from single precursor cells derived in vitro and in vivo. *Nat Immunol* **8**, 1217-1226 (2007).
27. G. Rotta, E. W. Edwards, S. Sangaletti, C. Bennett, S. Ronzoni, M. P. Colombo, R. M. Steinman, G. J. Randolph, M. Rescigno, Lipopolysaccharide or whole bacteria block the conversion of inflammatory monocytes into dendritic cells in vivo. *J Exp Med* **198**, 1253-1263 (2003).
28. I. Truxova, L. Kasikova, M. Hensler, P. Skapa, J. Laco, L. Pecen, L. Belicova, I. Praznovec, M. J. Halaska, T. Brtnicky, E. Salkova, L. Rob, R. Kodet, J. Goc, C. Sautes-Fridman, W. H. Fridman, A. Ryska, L. Galluzzi, R. Spisek, J. Fucikova, Mature dendritic cells correlate with favorable immune infiltrate and improved prognosis in ovarian carcinoma patients. *J Immunother Cancer* **6**, 139 (2018).
29. D. Gabrilovich, Mechanisms and functional significance of tumour-induced dendritic-cell defects. *Nat Rev Immunol* **4**, 941-952 (2004).
30. L. A. Norian, P. C. Rodriguez, L. A. O'Mara, J. Zabaleta, A. C. Ochoa, M. Cella, P. M. Allen, Tumor-infiltrating regulatory dendritic cells inhibit CD8+ T cell function via L-arginine metabolism. *Cancer Res* **69**, 3086-3094 (2009).
31. D. H. Munn, A. L. Mellor, Indoleamine 2,3 dioxygenase and metabolic control of immune responses. *Trends Immunol* **34**, 137-143 (2013).
32. B. Baban, P. R. Chandler, M. D. Sharma, J. Pihkala, P. A. Koni, D. H. Munn, A. L. Mellor, IDO activates regulatory T cells and blocks their conversion into Th17-like T cells. *J Immunol* **183**, 2475-2483 (2009).
33. I. Marigo, S. Zilio, G. Desantis, B. Mlecnik, A. H. R. Agnellini, S. Ugel, M. S. Sasso, J. E. Qualls, F. Kratochvill, P. Zanovello, B. Molon, C. H. Ries, V. Runza, S. Hoves, A. M. Bilocq, G. Bindea, E. M. C. Mazza, S. Bicciato, J. Galon, P. J. Murray, V. Bronte, T Cell Cancer Therapy Requires CD40-CD40L Activation of Tumor Necrosis Factor and Inducible Nitric-Oxide-Synthase-Producing Dendritic Cells. *Cancer Cell* **30**, 377-390 (2016).
34. S. B. Coffelt, M. D. Wellenstein, K. E. de Visser, Neutrophils in cancer: neutral no more. *Nat Rev Cancer* **16**, 431-446 (2016).
35. Z. G. Fridlender, J. Sun, S. Kim, V. Kapoor, G. Cheng, L. Ling, G. S. Worthen, S. M. Albelda, Polarization of tumor-associated neutrophil phenotype by TGF-beta: "N1" versus "N2" TAN. *Cancer Cell* **16**, 183-194 (2009).
36. J. K. Sandhu, H. F. Privora, G. Wenckebach, H. C. Birnboim, Neutrophils, nitric oxide synthase, and mutations in the mutatect murine tumor model. *Am J Pathol* **156**, 509-518 (2000).
37. V. T. Phan, X. Wu, J. H. Cheng, R. X. Sheng, A. S. Chung, G. Zhuang, C. Tran, Q. Song, M. Kowanetz, A. Sambrone, M. Tan, Y. G. Meng, E. L. Jackson, F. V. Peale, M. R. Junttila, N. Ferrara, Oncogenic RAS pathway activation promotes resistance to anti-VEGF therapy through G-CSF-induced neutrophil recruitment. *Proc Natl Acad Sci U S A* **110**, 6079-6084 (2013).
38. S. B. Coffelt, K. Kersten, C. W. Doornebal, J. Weiden, K. Vrijland, C. S. Hau, N. J. M. Verstegen, M. Ciampricotti, L. Hawinkels, J. Jonkers, K. E. de Visser, IL-17-producing gammadelta T cells and neutrophils conspire to promote breast cancer metastasis. *Nature* **522**, 345-348 (2015).

39. A. J. Templeton, M. G. McNamara, B. Seruga, F. E. Vera-Badillo, P. Aneja, A. Ocana, R. Leibowitz-Amit, G. Sonpavde, J. J. Knox, B. Tran, I. F. Tannock, E. Amir, Prognostic role of neutrophil-to-lymphocyte ratio in solid tumors: a systematic review and meta-analysis. *J Natl Cancer Inst* **106**, dju124 (2014).
40. J. Albrengues, M. A. Shields, D. Ng, C. G. Park, A. Ambrico, M. E. Poindexter, P. Upadhyay, D. L. Uyeminami, A. Pommier, V. Kuttner, E. Bruzas, L. Maiorino, C. Bautista, E. M. Carmona, P. A. Gimotty, D. T. Fearon, K. Chang, S. K. Lyons, K. E. Pinkerton, L. C. Trotman, M. S. Goldberg, J. T. Yeh, M. Egeblad, Neutrophil extracellular traps produced during inflammation awaken dormant cancer cells in mice. *Science* **361**, (2018).
41. J. E. Talmadge, D. I. Gabrilovich, History of myeloid-derived suppressor cells. *Nat Rev Cancer* **13**, 739-752 (2013).
42. D. I. Gabrilovich, V. Bronte, S. H. Chen, M. P. Colombo, A. Ochoa, S. Ostrand-Rosenberg, H. Schreiber, The terminology issue for myeloid-derived suppressor cells. *Cancer Res* **67**, 425; author reply 426 (2007).
43. A. J. Montero, C. M. Diaz-Montero, C. E. Kyriakopoulos, V. Bronte, S. Mandruzzato, Myeloid-derived suppressor cells in cancer patients: a clinical perspective. *J Immunother* **35**, 107-115 (2012).
44. G. Gallina, L. Dolcetti, P. Serafini, C. De Santo, I. Marigo, M. P. Colombo, G. Basso, F. Brombacher, I. Borrello, P. Zanovello, S. Bicciato, V. Bronte, Tumors induce a subset of inflammatory monocytes with immunosuppressive activity on CD8+ T cells. *J Clin Invest* **116**, 2777-2790 (2006).
45. F. Arihara, E. Mizukoshi, M. Kitahara, Y. Takata, K. Arai, T. Yamashita, Y. Nakamoto, S. Kaneko, Increase in CD14+HLA-DR -/low myeloid-derived suppressor cells in hepatocellular carcinoma patients and its impact on prognosis. *Cancer Immunol Immunother* **62**, 1421-1430 (2013).
46. F. De Sanctis, S. Solito, S. Ugel, B. Molon, V. Bronte, I. Marigo, MDSCs in cancer: Conceiving new prognostic and therapeutic targets. *Biochim Biophys Acta* **1865**, 35-48 (2016).
47. V. Bronte, S. Brandau, S. H. Chen, M. P. Colombo, A. B. Frey, T. F. Greten, S. Mandruzzato, P. J. Murray, A. Ochoa, S. Ostrand-Rosenberg, P. C. Rodriguez, A. Sica, V. Umansky, R. H. Vonderheide, D. I. Gabrilovich, Recommendations for myeloid-derived suppressor cell nomenclature and characterization standards. *Nat Commun* **7**, 12150 (2016).
48. S. Mandruzzato, S. Brandau, C. M. Britten, V. Bronte, V. Damuzzo, C. Gouttefangeas, D. Maurer, C. Ottensmeier, S. H. van der Burg, M. J. Welters, S. Walter, Toward harmonized phenotyping of human myeloid-derived suppressor cells by flow cytometry: results from an interim study. *Cancer Immunol Immunother* **65**, 161-169 (2016).
49. R. Trovato, A. Fiore, S. Sartori, S. Cane, R. Giugno, L. Cascione, S. Paiella, R. Salvia, F. De Sanctis, O. Poffe, C. Anselmi, F. Hofer, S. Sartoris, G. Piro, C. Carbone, V. Corbo, R. Lawlor, S. Solito, L. Pinton, S. Mandruzzato, C. Bassi, A. Scarpa, V. Bronte, S. Ugel, Immunosuppression by monocytic myeloid-derived suppressor cells in patients with pancreatic ductal carcinoma is orchestrated by STAT3. *J Immunother Cancer* **7**, 255 (2019).
50. B. Molon, S. Ugel, F. Del Pozzo, C. Soldani, S. Zilio, D. Avella, A. De Palma, P. Mauri, A. Monegal, M. Rescigno, B. Savino, P. Colombo, N. Jonjic, S. Pecanic, L. Lazzarato, R. Fruttero, A. Gasco, V. Bronte, A. Viola, Chemokine nitration prevents intratumoral infiltration of antigen-specific T cells. *J Exp Med* **208**, 1949-1962 (2011).
51. B. Hoechst, J. Gamrekelashvili, M. P. Manns, T. F. Greten, F. Korangy, Plasticity of human Th17 cells and iTregs is orchestrated by different subsets of myeloid cells. *Blood* **117**, 6532-6541 (2011).
52. P. Sinha, V. K. Clements, S. K. Bunt, S. M. Albelda, S. Ostrand-Rosenberg, Cross-talk between myeloid-derived suppressor cells and macrophages subverts tumor immunity toward a type 2 response. *J Immunol* **179**, 977-983 (2007).
53. A. Fiore, S. Ugel, F. De Sanctis, S. Sandri, G. Fracasso, R. Trovato, S. Sartoris, S. Solito, S. Mandruzzato, F. Vascotto, K. L. Hippen, G. Mondanelli, U. Grohmann, G. Piro, C. Carbone, D. Melisi, R. T. Lawlor, A. Scarpa, A. Lamolinara, M. Iezzi, M. Fassan, S. Bicciato, B. R. Blazar, U. Sahin, P. J. Murray, V. Bronte, Induction of

immunosuppressive functions and NF-kappaB by FLIP in monocytes. *Nat Commun* **9**, 5193 (2018).

54. I. Marigo, E. Bosio, S. Solito, C. Mesa, A. Fernandez, L. Dolcetti, S. Ugel, N. Sonda, S. Bicciato, E. Falisi, F. Calabrese, G. Basso, P. Zanovello, E. Cozzi, S. Mandruzzato, V. Bronte, Tumor-induced tolerance and immune suppression depend on the C/EBPbeta transcription factor. *Immunity* **32**, 790-802 (2010).
55. B. Toh, X. Wang, J. Keeble, W. J. Sim, K. Khoo, W. C. Wong, M. Kato, A. Prevost-Blondel, J. P. Thiery, J. P. Abastado, Mesenchymal transition and dissemination of cancer cells is driven by myeloid-derived suppressor cells infiltrating the primary tumor. *PLoS Biol* **9**, e1001162 (2011).
56. R. A. Franklin, W. Liao, A. Sarkar, M. V. Kim, M. R. Bivona, K. Liu, E. G. Pamer, M. O. Li, The cellular and molecular origin of tumor-associated macrophages. *Science* **344**, 921-925 (2014).
57. C. Schulz, E. Gomez Perdiguero, L. Chorro, H. Szabo-Rogers, N. Cagnard, K. Kierdorf, M. Prinz, B. Wu, S. E. Jacobsen, J. W. Pollard, J. Frampton, K. J. Liu, F. Geissmann, A lineage of myeloid cells independent of Myb and hematopoietic stem cells. *Science* **336**, 86-90 (2012).
58. G. Hoeffel, J. Chen, Y. Lavin, D. Low, F. F. Almeida, P. See, A. E. Beaudin, J. Lum, I. Low, E. C. Forsberg, M. Poidinger, F. Zolezzi, A. Larbi, L. G. Ng, J. K. Chan, M. Greter, B. Becher, I. M. Samokhvalov, M. Merad, F. Ginhoux, C-Myb(+) erythro-myeloid progenitor-derived fetal monocytes give rise to adult tissue-resident macrophages. *Immunity* **42**, 665-678 (2015).
59. E. G. Perdiguero, F. Geissmann, The development and maintenance of resident macrophages. *Nat Immunol* **17**, 2-8 (2016).
60. A. Sica, A. Mantovani, Macrophage plasticity and polarization: in vivo veritas. *J Clin Invest* **122**, 787-795 (2012).
61. S. K. Biswas, A. Mantovani, Macrophage plasticity and interaction with lymphocyte subsets: cancer as a paradigm. *Nat Immunol* **11**, 889-896 (2010).
62. S. Gordon, P. R. Taylor, Monocyte and macrophage heterogeneity. *Nat Rev Immunol* **5**, 953-964 (2005).
63. A. Mantovani, S. Sozzani, M. Locati, P. Allavena, A. Sica, Macrophage polarization: tumor-associated macrophages as a paradigm for polarized M2 mononuclear phagocytes. *Trends Immunol* **23**, 549-555 (2002).
64. P. J. Murray, J. E. Allen, S. K. Biswas, E. A. Fisher, D. W. Gilroy, S. Goerdt, S. Gordon, J. A. Hamilton, L. B. Ivashkiv, T. Lawrence, M. Locati, A. Mantovani, F. O. Martinez, J. L. Mege, D. M. Mosser, G. Natoli, J. P. Saeij, J. L. Schultze, K. A. Shirey, A. Sica, J. Suttles, I. Udalova, J. A. van Ginderachter, S. N. Vogel, T. A. Wynn, Macrophage activation and polarization: nomenclature and experimental guidelines. *Immunity* **41**, 14-20 (2014).
65. L. Cassetta, S. Fragkogianni, A. H. Sims, A. Swierczak, L. M. Forrester, H. Zhang, D. Y. H. Soong, T. Cotechini, P. Anur, E. Y. Lin, A. Fidanza, M. Lopez-Yrigoyen, M. R. Millar, A. Urman, Z. Ai, P. T. Spellman, E. S. Hwang, J. M. Dixon, L. Wiechmann, L. M. Coussens, H. O. Smith, J. W. Pollard, Human Tumor-Associated Macrophage and Monocyte Transcriptional Landscapes Reveal Cancer-Specific Reprogramming, Biomarkers, and Therapeutic Targets. *Cancer Cell* **35**, 588-602 e510 (2019).
66. R. Zilionis, C. Engblom, C. Pfirschke, V. Savova, D. Zemmour, H. D. Saatcioglu, I. Krishnan, G. Maroni, C. V. Meyerovitz, C. M. Kerwin, S. Choi, W. G. Richards, A. De Rienzo, D. G. Tenen, R. Bueno, E. Levantini, M. J. Pittet, A. M. Klein, Single-Cell Transcriptomics of Human and Mouse Lung Cancers Reveals Conserved Myeloid Populations across Individuals and Species. *Immunity* **50**, 1317-1334 e1310 (2019).
67. C. Steidl, T. Lee, S. P. Shah, P. Farinha, G. Han, T. Nayar, A. Delaney, S. J. Jones, J. Iqbal, D. D. Weisenburger, M. A. Bast, A. Rosenwald, H. K. Muller-Hermelink, L. M. Rimsza, E. Campo, J. Delabie, R. M. Braziel, J. R. Cook, R. R. Tubbs, E. S. Jaffe, G. Lenz, J. M. Connors, L. M. Staudt, W. C. Chan, R. D. Gascoyne, Tumor-associated macrophages and survival in classic Hodgkin's lymphoma. *N Engl J Med* **362**, 875-885 (2010).

68. Y. Komohara, Y. Fujiwara, K. Ohnishi, M. Takeya, Tumor-associated macrophages: Potential therapeutic targets for anti-cancer therapy. *Adv Drug Deliv Rev* **99**, 180-185 (2016).
69. S. Wan, E. Zhao, I. Kryczek, L. Vatan, A. Sadovskaya, G. Ludema, D. M. Simeone, W. Zou, T. H. Welling, Tumor-associated macrophages produce interleukin 6 and signal via STAT3 to promote expansion of human hepatocellular carcinoma stem cells. *Gastroenterology* **147**, 1393-1404 (2014).
70. R. Hughes, B. Z. Qian, C. Rowan, M. Muthana, I. Keklikoglou, O. C. Olson, S. Tazzyman, S. Danson, C. Addison, M. Clemons, A. M. Gonzalez-Angulo, J. A. Joyce, M. De Palma, J. W. Pollard, C. E. Lewis, Perivascular M2 Macrophages Stimulate Tumor Relapse after Chemotherapy. *Cancer Res* **75**, 3479-3491 (2015).
71. A. Mancino, T. Lawrence, Nuclear factor-kappaB and tumor-associated macrophages. *Clin Cancer Res* **16**, 784-789 (2010).
72. H. Lu, K. R. Clauser, W. L. Tam, J. Frose, X. Ye, E. N. Eaton, F. Reinhardt, V. S. Donnenberg, R. Bhargava, S. A. Carr, R. A. Weinberg, A breast cancer stem cell niche supported by juxtacrine signalling from monocytes and macrophages. *Nat Cell Biol* **16**, 1105-1117 (2014).
73. E. Y. Lin, J. W. Pollard, Tumor-associated macrophages press the angiogenic switch in breast cancer. *Cancer Res* **67**, 5064-5066 (2007).
74. E. J. Yeo, L. Cassetta, B. Z. Qian, I. Lewkowich, J. F. Li, J. A. Stefater, 3rd, A. N. Smith, L. S. Wiechmann, Y. Wang, J. W. Pollard, R. A. Lang, Myeloid WNT7b mediates the angiogenic switch and metastasis in breast cancer. *Cancer Res* **74**, 2962-2973 (2014).
75. Q. Ebrahem, S. S. Chaurasia, A. Vasanji, J. H. Qi, P. A. Klenotic, A. Cutler, K. Asosingh, S. Erzurum, B. Anand-Apte, Cross-talk between vascular endothelial growth factor and matrix metalloproteinases in the induction of neovascularization in vivo. *Am J Pathol* **176**, 496-503 (2010).
76. R. Mazzieri, F. Pucci, D. Moi, E. Zonari, A. Ranghetti, A. Berti, L. S. Politi, B. Gentner, J. L. Brown, L. Naldini, M. De Palma, Targeting the ANG2/TIE2 axis inhibits tumor growth and metastasis by impairing angiogenesis and disabling rebounds of proangiogenic myeloid cells. *Cancer Cell* **19**, 512-526 (2011).
77. S. M. Zeisberger, B. Odermatt, C. Marty, A. H. Zehnder-Fjallman, K. Ballmer-Hofer, R. A. Schwendener, Clodronate-liposome-mediated depletion of tumour-associated macrophages: a new and highly effective antiangiogenic therapy approach. *Br J Cancer* **95**, 272-281 (2006).
78. V. Riabov, A. Gudima, N. Wang, A. Mickley, A. Orekhov, J. Kzhyshkowska, Role of tumor associated macrophages in tumor angiogenesis and lymphangiogenesis. *Front Physiol* **5**, 75 (2014).
79. D. Alishekevitz, S. Gingis-Velitski, O. Kaidar-Person, L. Gutter-Kapon, S. D. Scherer, Z. Raviv, E. Merquiol, Y. Ben-Nun, V. Miller, C. Rachman-Tzemah, M. Timaner, Y. Mumblat, N. Ilan, D. Loven, D. Hershkovitz, R. Satchi-Fainaro, G. Blum, J. P. Sleeman, I. Vlodavsky, Y. Shaked, Macrophage-Induced Lymphangiogenesis and Metastasis following Paclitaxel Chemotherapy Is Regulated by VEGFR3. *Cell Rep* **17**, 1344-1356 (2016).
80. S. Su, Q. Liu, J. Chen, J. Chen, F. Chen, C. He, D. Huang, W. Wu, L. Lin, W. Huang, J. Zhang, X. Cui, F. Zheng, H. Li, H. Yao, F. Su, E. Song, A positive feedback loop between mesenchymal-like cancer cells and macrophages is essential to breast cancer metastasis. *Cancer Cell* **25**, 605-620 (2014).
81. A. K. Bonde, V. Tischler, S. Kumar, A. Soltermann, R. A. Schwendener, Intratumoral macrophages contribute to epithelial-mesenchymal transition in solid tumors. *BMC Cancer* **12**, 35 (2012).
82. J. Wyckoff, W. Wang, E. Y. Lin, Y. Wang, F. Pixley, E. R. Stanley, T. Graf, J. W. Pollard, J. Segall, J. Condeelis, A paracrine loop between tumor cells and macrophages is required for tumor cell migration in mammary tumors. *Cancer Res* **64**, 7022-7029 (2004).
83. J. B. Wyckoff, Y. Wang, E. Y. Lin, J. F. Li, S. Goswami, E. R. Stanley, J. E. Segall, J. W. Pollard, J. Condeelis, Direct visualization of macrophage-assisted tumor cell intravasation in mammary tumors. *Cancer Res* **67**, 2649-2656 (2007).
84. J. Chen, Y. Yao, C. Gong, F. Yu, S. Su, J. Chen, B. Liu, H. Deng, F. Wang, L. Lin, H. Yao, F. Su, K. S. Anderson, Q. Liu, M. E. Ewen, X. Yao, E. Song, CCL18 from tumor-

associated macrophages promotes breast cancer metastasis via PITPNM3. *Cancer Cell* **19**, 541-555 (2011).
85. S. Sangaletti, E. Di Carlo, S. Gariboldi, S. Miotti, B. Cappetti, M. Parenza, C. Rumio, R. A. Brekken, C. Chiodoni, M. P. Colombo, Macrophage-derived SPARC bridges tumor cell-extracellular matrix interactions toward metastasis. *Cancer Res* **68**, 9050-9059 (2008).
86. K. Kessenbrock, V. Plaks, Z. Werb, Matrix metalloproteinases: regulators of the tumor microenvironment. *Cell* **141**, 52-67 (2010).
87. D. M. Kuang, Q. Zhao, C. Peng, J. Xu, J. P. Zhang, C. Wu, L. Zheng, Activated monocytes in peritumoral stroma of hepatocellular carcinoma foster immune privilege and disease progression through PD-L1. *J Exp Med* **206**, 1327-1337 (2009).
88. A. Sica, A. Saccani, B. Bottazzi, N. Polentarutti, A. Vecchi, J. van Damme, A. Mantovani, Autocrine production of IL-10 mediates defective IL-12 production and NF-kappa B activation in tumor-associated macrophages. *J Immunol* **164**, 762-767 (2000).
89. D. G. DeNardo, J. B. Barreto, P. Andreu, L. Vasquez, D. Tawfik, N. Kolhatkar, L. M. Coussens, CD4(+) T cells regulate pulmonary metastasis of mammary carcinomas by enhancing protumor properties of macrophages. *Cancer Cell* **16**, 91-102 (2009).
90. M. Murai, O. Turovskaya, G. Kim, R. Madan, C. L. Karp, H. Cheroutre, M. Kronenberg, Interleukin 10 acts on regulatory T cells to maintain expression of the transcription factor Foxp3 and suppressive function in mice with colitis. *Nat Immunol* **10**, 1178-1184 (2009).
91. M. M. Tiemessen, A. L. Jagger, H. G. Evans, M. J. van Herwijnen, S. John, L. S. Taams, CD4+CD25+Foxp3+ regulatory T cells induce alternative activation of human monocytes/macrophages. *Proc Natl Acad Sci U S A* **104**, 19446-19451 (2007).
92. M. Rath, I. Muller, P. Kropf, E. I. Closs, M. Munder, Metabolism via Arginase or Nitric Oxide Synthase: Two Competing Arginine Pathways in Macrophages. *Front Immunol* **5**, 532 (2014).
93. B. Z. Qian, J. Li, H. Zhang, T. Kitamura, J. Zhang, L. R. Campion, E. A. Kaiser, L. A. Snyder, J. W. Pollard, CCL2 recruits inflammatory monocytes to facilitate breast-tumour metastasis. *Nature* **475**, 222-225 (2011).
94. B. Qian, Y. Deng, J. H. Im, R. J. Muschel, Y. Zou, J. Li, R. A. Lang, J. W. Pollard, A distinct macrophage population mediates metastatic breast cancer cell extravasation, establishment and growth. *PLoS One* **4**, e6562 (2009).
95. S. Hiratsuka, K. Nakamura, S. Iwai, M. Murakami, T. Itoh, H. Kijima, J. M. Shipley, R. M. Senior, M. Shibuya, MMP9 induction by vascular endothelial growth factor receptor-1 is involved in lung-specific metastasis. *Cancer Cell* **2**, 289-300 (2002).
96. T. Kitamura, D. Doughty-Shenton, L. Cassetta, S. Fragkogianni, D. Brownlie, Y. Kato, N. Carragher, J. W. Pollard, Monocytes Differentiate to Immune Suppressive Precursors of Metastasis-Associated Macrophages in Mouse Models of Metastatic Breast Cancer. *Front Immunol* **8**, 2004 (2017).
97. Q. Chen, X. H. Zhang, J. Massague, Macrophage binding to receptor VCAM-1 transmits survival signals in breast cancer cells that invade the lungs. *Cancer Cell* **20**, 538-549 (2011).
98. D. Yan, J. Kowal, L. Akkari, A. J. Schuhmacher, J. T. Huse, B. L. West, J. A. Joyce, Inhibition of colony stimulating factor-1 receptor abrogates microenvironment-mediated therapeutic resistance in gliomas. *Oncogene* **36**, 6049-6058 (2017).
99. W. D. Tap, Z. A. Wainberg, S. P. Anthony, P. N. Ibrahim, C. Zhang, J. H. Healey, B. Chmielowski, A. P. Staddon, A. L. Cohn, G. I. Shapiro, V. L. Keedy, A. S. Singh, I. Puzanov, E. L. Kwak, A. J. Wagner, D. D. Von Hoff, G. J. Weiss, R. K. Ramanathan, J. Zhang, G. Habets, Y. Zhang, E. A. Burton, G. Visor, L. Sanftner, P. Severson, H. Nguyen, M. J. Kim, A. Marimuthu, G. Tsang, R. Shellooe, C. Gee, B. L. West, P. Hirth, K. Nolop, M. van de Rijn, H. H. Hsu, C. Peterfy, P. S. Lin, S. Tong-Starksen, G. Bollag, Structure-Guided Blockade of CSF1R Kinase in Tenosynovial Giant-Cell Tumor. *N Engl J Med* **373**, 428-437 (2015).
100. J. B. Mitchem, D. J. Brennan, B. L. Knolhoff, B. A. Belt, Y. Zhu, D. E. Sanford, L. Belaygorod, D. Carpenter, L. Collins, D. Piwnica-Worms, S. Hewitt, G. M. Udupi, W. M. Gallagher, C. Wegner, B. L. West, A. Wang-Gillam, P. Goedegebuure, D. C. Linehan, D. G. DeNardo, Targeting tumor-infiltrating macrophages decreases tumor-initiating cells,

relieves immunosuppression, and improves chemotherapeutic responses. *Cancer Res* **73**, 1128-1141 (2013).
101. M. A. Cannarile, M. Weisser, W. Jacob, A. M. Jegg, C. H. Ries, D. Ruttinger, Colony-stimulating factor 1 receptor (CSF1R) inhibitors in cancer therapy. *J Immunother Cancer* **5**, 53 (2017).
102. N. Koide, A. Nishio, T. Sato, A. Sugiyama, S. Miyagawa, Significance of macrophage chemoattractant protein-1 expression and macrophage infiltration in squamous cell carcinoma of the esophagus. *Am J Gastroenterol* **99**, 1667-1674 (2004).
103. K. J. Pienta, J. P. Machiels, D. Schrijvers, B. Alekseev, M. Shkolnik, S. J. Crabb, S. Li, S. Seetharam, T. A. Puchalski, C. Takimoto, Y. Elsayed, F. Dawkins, J. S. de Bono, Phase 2 study of carlumab (CNTO 888), a human monoclonal antibody against CC-chemokine ligand 2 (CCL2), in metastatic castration-resistant prostate cancer. *Invest New Drugs* **31**, 760-768 (2013).
104. L. Cassetta, J. W. Pollard, Targeting macrophages: therapeutic approaches in cancer. *Nat Rev Drug Discov* **17**, 887-904 (2018).
105. M. E. Maurer, J. A. Cooper, The adaptor protein Dab2 sorts LDL receptors into coated pits independently of AP-2 and ARH. *J Cell Sci* **119**, 4235-4246 (2006).
106. P. Liang, A. B. Pardee, Differential display of eukaryotic messenger RNA by means of the polymerase chain reaction. *Science* **257**, 967-971 (1992).
107. X. X. Xu, W. Yang, S. Jackowski, C. O. Rock, Cloning of a novel phosphoprotein regulated by colony-stimulating factor 1 shares a domain with the Drosophila disabled gene product. *J Biol Chem* **270**, 14184-14191 (1995).
108. F. B. Gertler, K. K. Hill, M. J. Clark, F. M. Hoffmann, Dosage-sensitive modifiers of Drosophila abl tyrosine kinase function: prospero, a regulator of axonal outgrowth, and disabled, a novel tyrosine kinase substrate. *Genes Dev* **7**, 441-453 (1993).
109. H. M. Albertsen, S. A. Smith, R. Melis, B. Williams, P. Holik, J. Stevens, R. White, Sequence, genomic structure, and chromosomal assignment of human DOC-2. *Genomics* **33**, 207-213 (1996).
110. X. X. Xu, T. Yi, B. Tang, J. D. Lambeth, Disabled-2 (Dab2) is an SH3 domain-binding partner of Grb2. *Oncogene* **16**, 1561-1569 (1998).
111. M. E. Maurer, J. A. Cooper, Endocytosis of megalin by visceral endoderm cells requires the Dab2 adaptor protein. *J Cell Sci* **118**, 5345-5355 (2005).
112. S. M. Morris, J. A. Cooper, Disabled-2 colocalizes with the LDLR in clathrin-coated pits and interacts with AP-2. *Traffic* **2**, 111-123 (2001).
113. P. T. Caswell, S. Vadrevu, J. C. Norman, Integrins: masters and slaves of endocytic transport. *Nat Rev Mol Cell Biol* **10**, 843-853 (2009).
114. S. M. Morris, M. D. Tallquist, C. O. Rock, J. A. Cooper, Dual roles for the Dab2 adaptor protein in embryonic development and kidney transport. *EMBO J* **21**, 1555-1564 (2002).
115. G. Spudich, M. V. Chibalina, J. S. Au, S. D. Arden, F. Buss, J. Kendrick-Jones, Myosin VI targeting to clathrin-coated structures and dimerization is mediated by binding to Disabled-2 and PtdIns(4,5)P2. *Nat Cell Biol* **9**, 176-183 (2007).
116. D. H. Yang, K. Q. Cai, I. H. Roland, E. R. Smith, X. X. Xu, Disabled-2 is an epithelial surface positioning gene. *J Biol Chem* **282**, 13114-13122 (2007).
117. H. T. McMahon, E. Boucrot, Molecular mechanism and physiological functions of clathrin-mediated endocytosis. *Nat Rev Mol Cell Biol* **12**, 517-533 (2011).
118. L. M. Traub, Tickets to ride: selecting cargo for clathrin-regulated internalization. *Nat Rev Mol Cell Biol* **10**, 583-596 (2009).
119. A. Sundborger, C. Soderblom, O. Vorontsova, E. Evergren, J. E. Hinshaw, O. Shupliakov, An endophilin-dynamin complex promotes budding of clathrin-coated vesicles during synaptic vesicle recycling. *J Cell Sci* **124**, 133-143 (2011).
120. S. Aghamohammadzadeh, K. R. Ayscough, Differential requirements for actin during yeast and mammalian endocytosis. *Nat Cell Biol* **11**, 1039-1042 (2009).
121. G. J. Doherty, H. T. McMahon, Mechanisms of endocytosis. *Annu Rev Biochem* **78**, 857-902 (2009).
122. A. Reider, B. Wendland, Endocytic adaptors--social networking at the plasma membrane. *J Cell Sci* **124**, 1613-1622 (2011).

123. Z. Sheng, W. Sun, E. Smith, C. Cohen, Z. Sheng, X. X. Xu, Restoration of positioning control following Disabled-2 expression in ovarian and breast tumor cells. *Oncogene* **19**, 4847-4854 (2000).
124. H. J. Tsai, C. L. Huang, Y. W. Chang, D. Y. Huang, C. C. Lin, J. A. Cooper, J. C. Cheng, C. P. Tseng, Disabled-2 is required for efficient hemostasis and platelet activation by thrombin in mice. *Arterioscler Thromb Vasc Biol* **34**, 2404-2412 (2014).
125. A. Hannigan, P. Smith, G. Kalna, C. Lo Nigro, C. Orange, D. I. O'Brien, R. Shah, N. Syed, L. C. Spender, B. Herrera, J. K. Thurlow, L. Lattanzio, M. Monteverde, M. E. Maurer, F. M. Buffa, J. Mann, D. C. Chu, C. M. West, M. Patridge, K. A. Oien, J. A. Cooper, M. C. Frame, A. L. Harris, L. Hiller, L. J. Nicholson, M. Gasco, T. Crook, G. J. Inman, Epigenetic downregulation of human disabled homolog 2 switches TGF-beta from a tumor suppressor to a tumor promoter. *J Clin Invest* **120**, 2842-2857 (2010).
126. J. H. Tong, D. C. Ng, S. L. Chau, K. K. So, P. P. Leung, T. L. Lee, R. W. Lung, M. W. Chan, A. W. Chan, K. W. Lo, K. F. To, Putative tumour-suppressor gene DAB2 is frequently down regulated by promoter hypermethylation in nasopharyngeal carcinoma. *BMC Cancer* **10**, 253 (2010).
127. A. Chao, C. Y. Lin, Y. S. Lee, C. L. Tsai, P. C. Wei, S. Hsueh, T. I. Wu, C. N. Tsai, C. J. Wang, A. S. Chao, T. H. Wang, C. H. Lai, Regulation of ovarian cancer progression by microRNA-187 through targeting Disabled homolog-2. *Oncogene* **31**, 764-775 (2012).
128. B. A. Hocevar, C. Prunier, P. H. Howe, Disabled-2 (Dab2) mediates transforming growth factor beta (TGFbeta)-stimulated fibronectin synthesis through TGFbeta-activated kinase 1 and activation of the JNK pathway. *J Biol Chem* **280**, 25920-25927 (2005).
129. B. A. Hocevar, F. Mou, J. L. Rennolds, S. M. Morris, J. A. Cooper, P. H. Howe, Regulation of the Wnt signaling pathway by disabled-2 (Dab2). *EMBO J* **22**, 3084-3094 (2003).
130. J. He, E. R. Smith, X. X. Xu, Disabled-2 exerts its tumor suppressor activity by uncoupling c-Fos expression and MAP kinase activation. *J Biol Chem* **276**, 26814-26818 (2001).
131. S. A. Mani, W. Guo, M. J. Liao, E. N. Eaton, A. Ayyanan, A. Y. Zhou, M. Brooks, F. Reinhard, C. C. Zhang, M. Shipitsin, L. L. Campbell, K. Polyak, C. Brisken, J. Yang, R. A. Weinberg, The epithelial-mesenchymal transition generates cells with properties of stem cells. *Cell* **133**, 704-715 (2008).
132. E. Janda, K. Lehmann, I. Killisch, M. Jechlinger, M. Herzig, J. Downward, H. Beug, S. Grunert, Ras and TGF[beta] cooperatively regulate epithelial cell plasticity and metastasis: dissection of Ras signaling pathways. *J Cell Biol* **156**, 299-313 (2002).
133. S. Xu, J. Zhu, Z. Wu, Loss of Dab2 expression in breast cancer cells impairs their ability to deplete TGF-beta and induce Tregs development via TGF-beta. *PLoS One* **9**, e91709 (2014).
134. Y. Jiang, X. He, P. H. Howe, Disabled-2 (Dab2) inhibits Wnt/beta-catenin signalling by binding LRP6 and promoting its internalization through clathrin. *EMBO J* **31**, 2336-2349 (2012).
135. J. M. Westcott, A. M. Prechtl, E. A. Maine, T. T. Dang, M. A. Esparza, H. Sun, Y. Zhou, Y. Xie, G. W. Pearson, An epigenetically distinct breast cancer cell subpopulation promotes collective invasion. *J Clin Invest* **125**, 1927-1943 (2015).
136. Y. Xie, Y. Zhang, L. Jiang, M. Zhang, Z. Chen, D. Liu, Q. Huang, Disabled homolog 2 is required for migration and invasion of prostate cancer cells. *Front Med* **9**, 312-321 (2015).
137. S. M. Cheong, H. Choi, B. S. Hong, Y. S. Gho, J. K. Han, Dab2 is pivotal for endothelial cell migration by mediating VEGF expression in cancer cells. *Exp Cell Res* **318**, 550-557 (2012).
138. F. Rosenbauer, A. Kallies, M. Scheller, K. P. Knobeloch, C. O. Rock, M. Schwieger, C. Stocking, I. Horak, Disabled-2 is transcriptionally regulated by ICSBP and augments macrophage spreading and adhesion. *EMBO J* **21**, 211-220 (2002).
139. S. E. Adamson, R. Griffiths, R. Moravec, S. Senthivinayagam, G. Montgomery, W. Chen, J. Han, P. R. Sharma, G. R. Mullins, S. A. Gorski, J. A. Cooper, A. Kadl, K. Enfield, T. J. Braciale, T. E. Harris, N. Leitinger, Disabled homolog 2 controls macrophage phenotypic polarization and adipose tissue inflammation. *J Clin Invest* **126**, 1311-1322 (2016).

140. M. S. Ahmed, S. E. Byeon, Y. Jeong, M. A. Miah, M. Salahuddin, Y. Lee, S. S. Park, Y. S. Bae, Dab2, a negative regulator of DC immunogenicity, is an attractive molecular target for DC-based immunotherapy. *Oncoimmunology* **4**, e984550 (2015).
141. T. Rozario, D. W. DeSimone, The extracellular matrix in development and morphogenesis: a dynamic view. *Dev Biol* **341**, 126-140 (2010).
142. C. J. Whatcott, C. H. Diep, P. Jiang, A. Watanabe, J. LoBello, C. Sima, G. Hostetter, H. M. Shepard, D. D. Von Hoff, H. Han, Desmoplasia in Primary Tumors and Metastatic Lesions of Pancreatic Cancer. *Clin Cancer Res* **21**, 3561-3568 (2015).
143. J. Molnar, K. S. Fong, Q. P. He, K. Hayashi, Y. Kim, S. F. Fong, B. Fogelgren, K. M. Szauter, M. Mink, K. Csiszar, Structural and functional diversity of lysyl oxidase and the LOX-like proteins. *Biochim Biophys Acta* **1647**, 220-224 (2003).
144. S. M. Kakkad, M. Solaiyappan, B. O'Rourke, I. Stasinopoulos, E. Ackerstaff, V. Raman, Z. M. Bhujwalla, K. Glunde, Hypoxic tumor microenvironments reduce collagen I fiber density. *Neoplasia* **12**, 608-617 (2010).
145. S. M. Wormann, L. Song, J. Ai, K. N. Diakopoulos, M. U. Kurkowski, K. Gorgulu, D. Ruess, A. Campbell, C. Doglioni, D. Jodrell, A. Neesse, I. E. Demir, A. P. Karpathaki, M. Barenboim, T. Hagemann, S. Rose-John, O. Sansom, R. M. Schmid, M. P. Protti, M. Lesina, H. Algul, Loss of P53 Function Activates JAK2-STAT3 Signaling to Promote Pancreatic Tumor Growth, Stroma Modification, and Gemcitabine Resistance in Mice and Is Associated With Patient Survival. *Gastroenterology* **151**, 180-193 e112 (2016).
146. V. Alvarez-Garcia, Y. Tawil, H. M. Wise, N. R. Leslie, Mechanisms of PTEN loss in cancer: It's all about diversity. *Semin Cancer Biol*, (2019).
147. N. S. Nagathihalli, J. A. Castellanos, C. Shi, Y. Beesetty, M. L. Reyzer, R. Caprioli, X. Chen, A. J. Walsh, M. C. Skala, H. L. Moses, N. B. Merchant, Signal Transducer and Activator of Transcription 3, Mediated Remodeling of the Tumor Microenvironment Results in Enhanced Tumor Drug Delivery in a Mouse Model of Pancreatic Cancer. *Gastroenterology* **149**, 1932-1943 e1939 (2015).
148. M. H. Jenkins, W. Croteau, D. W. Mullins, C. E. Brinckerhoff, The BRAF(V600E) inhibitor, PLX4032, increases type I collagen synthesis in melanoma cells. *Matrix Biol* **48**, 66-77 (2015).
149. D. E. Kuczek, A. M. H. Larsen, M. L. Thorseth, M. Carretta, A. Kalvisa, M. S. Siersbaek, A. M. C. Simoes, A. Roslind, L. H. Engelholm, E. Noessner, M. Donia, I. M. Svane, P. T. Straten, L. Grontved, D. H. Madsen, Collagen density regulates the activity of tumor-infiltrating T cells. *J Immunother Cancer* **7**, 68 (2019).
150. I. Acerbi, L. Cassereau, I. Dean, Q. Shi, A. Au, C. Park, Y. Y. Chen, J. Liphardt, E. S. Hwang, V. M. Weaver, Human breast cancer invasion and aggression correlates with ECM stiffening and immune cell infiltration. *Integr Biol (Camb)* **7**, 1120-1134 (2015).
151. K. Zhang, C. A. Corsa, S. M. Ponik, J. L. Prior, D. Piwnica-Worms, K. W. Eliceiri, P. J. Keely, G. D. Longmore, The collagen receptor discoidin domain receptor 2 stabilizes SNAIL1 to facilitate breast cancer metastasis. *Nat Cell Biol* **15**, 677-687 (2013).
152. J. O'Brien, T. Lyons, J. Monks, M. S. Lucia, R. S. Wilson, L. Hines, Y. G. Man, V. Borges, P. Schedin, Alternatively activated macrophages and collagen remodeling characterize the postpartum involuting mammary gland across species. *Am J Pathol* **176**, 1241-1255 (2010).
153. D. H. Madsen, H. J. Jurgensen, M. S. Siersbaek, D. E. Kuczek, L. Grey Cloud, S. Liu, N. Behrendt, L. Grontved, R. Weigert, T. H. Bugge, Tumor-Associated Macrophages Derived from Circulating Inflammatory Monocytes Degrade Collagen through Cellular Uptake. *Cell Rep* **21**, 3662-3671 (2017).
154. T. Mammoto, A. Jiang, E. Jiang, D. Panigrahy, M. W. Kieran, A. Mammoto, Role of collagen matrix in tumor angiogenesis and glioblastoma multiforme progression. *Am J Pathol* **183**, 1293-1305 (2013).
155. B. F. Matte, A. Kumar, J. K. Placone, V. G. Zanella, M. D. Martins, A. J. Engler, M. L. Lamers, Matrix stiffness mechanically conditions EMT and migratory behavior of oral squamous cell carcinoma. *J Cell Sci* **132**, (2019).
156. D. A. Senthebane, T. Jonker, A. Rowe, N. E. Thomford, D. Munro, C. Dandara, A. Wonkam, D. Govender, B. Calder, N. C. Soares, J. M. Blackburn, M. I. Parker, K. Dzobo, The Role of Tumor Microenvironment in Chemoresistance: 3D Extracellular Matrices as Accomplices. *Int J Mol Sci* **19**, (2018).

157. L. Liu, S. X. Zhang, W. Liao, H. P. Farhoodi, C. W. Wong, C. C. Chen, A. I. Segaliny, J. V. Chacko, L. P. Nguyen, M. Lu, G. Polovin, E. J. Pone, T. L. Downing, D. A. Lawson, M. A. Digman, W. Zhao, Mechanoresponsive stem cells to target cancer metastases through biophysical cues. *Sci Transl Med* **9**, (2017).
158. R. Pankov, K. M. Yamada, Fibronectin at a glance. *J Cell Sci* **115**, 3861-3863 (2002).
159. N. Balanis, M. K. Wendt, B. J. Schiemann, Z. Wang, W. P. Schiemann, C. R. Carlin, Epithelial to mesenchymal transition promotes breast cancer progression via a fibronectin-dependent STAT3 signaling pathway. *J Biol Chem* **288**, 17954-17967 (2013).
160. I. Eke, K. Storch, M. Krause, N. Cordes, Cetuximab attenuates its cytotoxic and radiosensitizing potential by inducing fibronectin biosynthesis. *Cancer Res* **73**, 5869-5879 (2013).
161. B. Erdogan, M. Ao, L. M. White, A. L. Means, B. M. Brewer, L. Yang, M. K. Washington, C. Shi, O. E. Franco, A. M. Weaver, S. W. Hayward, D. Li, D. J. Webb, Cancer-associated fibroblasts promote directional cancer cell migration by aligning fibronectin. *J Cell Biol* **216**, 3799-3816 (2017).
162. X. N. Meng, Y. Jin, Y. Yu, J. Bai, G. Y. Liu, J. Zhu, Y. Z. Zhao, Z. Wang, F. Chen, K. Y. Lee, S. B. Fu, Characterisation of fibronectin-mediated FAK signalling pathways in lung cancer cell migration and invasion. *Br J Cancer* **101**, 327-334 (2009).
163. T. K. Eigentler, B. Weide, F. de Braud, G. Spitaleri, A. Romanini, A. Pflugfelder, R. Gonzalez-Iglesias, A. Tasciotti, L. Giovannoni, K. Schwager, V. Lovato, M. Kaspar, E. Trachsel, H. D. Menssen, D. Neri, C. Garbe, A dose-escalation and signal-generating study of the immunocytokine L19-IL2 in combination with dacarbazine for the therapy of patients with metastatic melanoma. *Clin Cancer Res* **17**, 7732-7742 (2011).
164. F. Schaffner, A. M. Ray, M. Dontenwill, Integrin alpha5beta1, the Fibronectin Receptor, as a Pertinent Therapeutic Target in Solid Tumors. *Cancers (Basel)* **5**, 27-47 (2013).
165. R. Nishiuchi, J. Takagi, M. Hayashi, H. Ido, Y. Yagi, N. Sanzen, T. Tsuji, M. Yamada, K. Sekiguchi, Ligand-binding specificities of laminin-binding integrins: a comprehensive survey of laminin-integrin interactions using recombinant alpha3beta1, alpha6beta1, alpha7beta1 and alpha6beta4 integrins. *Matrix Biol* **25**, 189-197 (2006).
166. M. P. Marinkovich, Tumour microenvironment: laminin 332 in squamous-cell carcinoma. *Nat Rev Cancer* **7**, 370-380 (2007).
167. S. Subbaram, C. M. Dipersio, Integrin alpha3beta1 as a breast cancer target. *Expert Opin Ther Targets* **15**, 1197-1210 (2011).
168. I. C. Sroka, T. A. Anderson, K. M. McDaniel, R. B. Nagle, M. B. Gretzer, A. E. Cress, The laminin binding integrin alpha6beta1 in prostate cancer perineural invasion. *J Cell Physiol* **224**, 283-288 (2010).
169. Y. Qin, S. Rodin, O. E. Simonson, F. Hollande, Laminins and cancer stem cells: Partners in crime? *Semin Cancer Biol* **45**, 3-12 (2017).
170. P. Bornstein, Diversity of function is inherent in matricellular proteins: an appraisal of thrombospondin 1. *J Cell Biol* **130**, 503-506 (1995).
171. B. Felding-Habermann, D. A. Cheresh, Vitronectin and its receptors. *Curr Opin Cell Biol* **5**, 864-868 (1993).
172. M. Aaboe, B. V. Offersen, A. Christensen, P. A. Andreasen, Vitronectin in human breast carcinomas. *Biochim Biophys Acta* **1638**, 72-82 (2003).
173. J. E. Bartsch, E. D. Staren, H. E. Appert, Adhesion and migration of extracellular matrix-stimulated breast cancer. *J Surg Res* **110**, 287-294 (2003).
174. G. Schneider, E. Bryndza, A. Poniewierska-Baran, K. Serwin, M. Suszynska, Z. P. Sellers, M. L. Merchant, A. Kaliappan, J. Ratajczak, M. Kucia, N. C. Garbett, M. Z. Ratajczak, Evidence that vitronectin is a potent migration-enhancing factor for cancer cells chaperoned by fibrinogen: a novel view of the metastasis of cancer cells to low-fibrinogen lymphatics and body cavities. *Oncotarget* **7**, 69829-69843 (2016).
175. D. Seiffert, Constitutive and regulated expression of vitronectin. *Histol Histopathol* **12**, 787-797 (1997).
176. J. A. Joyce, J. W. Pollard, Microenvironmental regulation of metastasis. *Nat Rev Cancer* **9**, 239-252 (2009).
177. M. J. Paszek, N. Zahir, K. R. Johnson, J. N. Lakins, G. I. Rozenberg, A. Gefen, C. A. Reinhart-King, S. S. Margulies, M. Dembo, D. Boettiger, D. A. Hammer, V. M. Weaver, Tensional homeostasis and the malignant phenotype. *Cancer Cell* **8**, 241-254 (2005).

178. O. Chaudhuri, S. T. Koshy, C. Branco da Cunha, J. W. Shin, C. S. Verbeke, K. H. Allison, D. J. Mooney, Extracellular matrix stiffness and composition jointly regulate the induction of malignant phenotypes in mammary epithelium. *Nat Mater* **13**, 970-978 (2014).
179. C. Colpaert, P. Vermeulen, E. Van Marck, L. Dirix, The presence of a fibrotic focus is an independent predictor of early metastasis in lymph node-negative breast cancer patients. *Am J Surg Pathol* **25**, 1557-1558 (2001).
180. V. Sosa, T. Moline, R. Somoza, R. Paciucci, H. Kondoh, L. L. ME, Oxidative stress and cancer: an overview. *Ageing Res Rev* **12**, 376-390 (2013).
181. A. Katsumi, A. W. Orr, E. Tzima, M. A. Schwartz, Integrins in mechanotransduction. *J Biol Chem* **279**, 12001-12004 (2004).
182. J. Z. Kechagia, J. Ivaska, P. Roca-Cusachs, Integrins as biomechanical sensors of the microenvironment. *Nat Rev Mol Cell Biol* **20**, 457-473 (2019).
183. P. P. Provenzano, P. J. Keely, Mechanical signaling through the cytoskeleton regulates cell proliferation by coordinated focal adhesion and Rho GTPase signaling. *J Cell Sci* **124**, 1195-1205 (2011).
184. C. Lawson, S. T. Lim, S. Uryu, X. L. Chen, D. A. Calderwood, D. D. Schlaepfer, FAK promotes recruitment of talin to nascent adhesions to control cell motility. *J Cell Biol* **196**, 223-232 (2012).
185. M. Guarino, Src signaling in cancer invasion. *J Cell Physiol* **223**, 14-26 (2010).
186. S. K. Mitra, D. D. Schlaepfer, Integrin-regulated FAK-Src signaling in normal and cancer cells. *Curr Opin Cell Biol* **18**, 516-523 (2006).
187. G. W. McLean, V. J. Fincham, M. C. Frame, v-Src induces tyrosine phosphorylation of focal adhesion kinase independently of tyrosine 397 and formation of a complex with Src. *J Biol Chem* **275**, 23333-23339 (2000).
188. P. Schedin, P. J. Keely, Mammary gland ECM remodeling, stiffness, and mechanosignaling in normal development and tumor progression. *Cold Spring Harb Perspect Biol* **3**, a003228 (2011).
189. M. T. Herrera Abreu, W. E. Hughes, K. Mele, R. J. Lyons, D. Rickwood, B. C. Browne, H. L. Bennett, P. Vallotton, T. Brummer, R. J. Daly, Gab2 regulates cytoskeletal organization and migration of mammary epithelial cells by modulating RhoA activation. *Mol Biol Cell* **22**, 105-116 (2011).
190. S. Kumar, V. M. Weaver, Mechanics, malignancy, and metastasis: the force journey of a tumor cell. *Cancer Metastasis Rev* **28**, 113-127 (2009).
191. J. Debnath, K. R. Mills, N. L. Collins, M. J. Reginato, S. K. Muthuswamy, J. S. Brugge, The role of apoptosis in creating and maintaining luminal space within normal and oncogene-expressing mammary acini. *Cell* **111**, 29-40 (2002).
192. N. R. Paul, G. Jacquemet, P. T. Caswell, Endocytic Trafficking of Integrins in Cell Migration. *Curr Biol* **25**, R1092-1105 (2015).
193. W. T. Chao, J. Kunz, Focal adhesion disassembly requires clathrin-dependent endocytosis of integrins. *FEBS Lett* **583**, 1337-1343 (2009).
194. A. Teckchandani, N. Toida, J. Goodchild, C. Henderson, J. Watts, B. Wollscheid, J. A. Cooper, Quantitative proteomics identifies a Dab2/integrin module regulating cell migration. *J Cell Biol* **186**, 99-111 (2009).
195. A. Teckchandani, E. E. Mulkearns, T. W. Randolph, N. Toida, J. A. Cooper, The clathrin adaptor Dab2 recruits EH domain scaffold proteins to regulate integrin beta1 endocytosis. *Mol Biol Cell* **23**, 2905-2916 (2012).
196. S. Dupont, L. Morsut, M. Aragona, E. Enzo, S. Giulitti, M. Cordenonsi, F. Zanconato, J. Le Digabel, M. Forcato, S. Bicciato, N. Elvassore, S. Piccolo, Role of YAP/TAZ in mechanotransduction. *Nature* **474**, 179-183 (2011).
197. S. Piccolo, S. Dupont, M. Cordenonsi, The biology of YAP/TAZ: hippo signaling and beyond. *Physiol Rev* **94**, 1287-1312 (2014).
198. F. Zanconato, M. Cordenonsi, S. Piccolo, YAP/TAZ at the Roots of Cancer. *Cancer Cell* **29**, 783-803 (2016).
199. A. Totaro, T. Panciera, S. Piccolo, YAP/TAZ upstream signals and downstream responses. *Nat Cell Biol* **20**, 888-899 (2018).
200. F. Zanconato, M. Cordenonsi, S. Piccolo, YAP and TAZ: a signalling hub of the tumour microenvironment. *Nat Rev Cancer* **19**, 454-464 (2019).

201. O. Croci, S. De Fazio, F. Biagioni, E. Donato, M. Caganova, L. Curti, M. Doni, S. Sberna, D. Aldeghi, C. Biancotto, A. Verrecchia, D. Olivero, B. Amati, S. Campaner, Transcriptional integration of mitogenic and mechanical signals by Myc and YAP. *Genes Dev* **31**, 2017-2022 (2017).
202. F. Zanconato, M. Forcato, G. Battilana, L. Azzolin, E. Quaranta, B. Bodega, A. Rosato, S. Bicciato, M. Cordenonsi, S. Piccolo, Genome-wide association between YAP/TAZ/TEAD and AP-1 at enhancers drives oncogenic growth. *Nat Cell Biol* **17**, 1218-1227 (2015).
203. B. Zhao, L. Li, L. Wang, C. Y. Wang, J. Yu, K. L. Guan, Cell detachment activates the Hippo pathway via cytoskeleton reorganization to induce anoikis. *Genes Dev* **26**, 54-68 (2012).
204. L. Garcia-Prat, M. Martinez-Vicente, E. Perdiguero, L. Ortet, J. Rodriguez-Ubreva, E. Rebollo, V. Ruiz-Bonilla, S. Gutarra, E. Ballestar, A. L. Serrano, M. Sandri, P. Munoz-Canoves, Autophagy maintains stemness by preventing senescence. *Nature* **529**, 37-42 (2016).
205. H. Hayashi, T. Higashi, N. Yokoyama, T. Kaida, K. Sakamoto, Y. Fukushima, T. Ishimoto, H. Kuroki, H. Nitta, D. Hashimoto, A. Chikamoto, E. Oki, T. Beppu, H. Baba, An Imbalance in TAZ and YAP Expression in Hepatocellular Carcinoma Confers Cancer Stem Cell-like Behaviors Contributing to Disease Progression. *Cancer Res* **75**, 4985-4997 (2015).
206. F. Calvo, N. Ege, A. Grande-Garcia, S. Hooper, R. P. Jenkins, S. I. Chaudhry, K. Harrington, P. Williamson, E. Moeendarbary, G. Charras, E. Sahai, Mechanotransduction and YAP-dependent matrix remodelling is required for the generation and maintenance of cancer-associated fibroblasts. *Nat Cell Biol* **15**, 637-646 (2013).
207. G. Wang, X. Lu, P. Dey, P. Deng, C. C. Wu, S. Jiang, Z. Fang, K. Zhao, R. Konaparthi, S. Hua, J. Zhang, E. M. Li-Ning-Tapia, A. Kapoor, C. J. Wu, N. B. Patel, Z. Guo, V. Ramamoorthy, T. N. Tieu, T. Heffernan, D. Zhao, X. Shang, S. Khadka, P. Hou, B. Hu, E. J. Jin, W. Yao, X. Pan, Z. Ding, Y. Shi, L. Li, Q. Chang, P. Troncoso, C. J. Logothetis, M. J. McArthur, L. Chin, Y. A. Wang, R. A. DePinho, Targeting YAP-Dependent MDSC Infiltration Impairs Tumor Progression. *Cancer Discov* **6**, 80-95 (2016).
208. L. Morsut, K. P. Yan, E. Enzo, M. Aragona, S. M. Soligo, O. Wendling, M. Mark, K. Khetchoumian, G. Bressan, P. Chambon, S. Dupont, R. Losson, S. Piccolo, Negative control of Smad activity by ectodermin/Tif1gamma patterns the mammalian embryo. *Development* **137**, 2571-2578 (2010).
209. A. Filippi, E. Dal Sasso, L. Iop, A. Armani, M. Gintoli, M. Sandri, G. Gerosa, F. Romanato, G. Borile, Multimodal label-free ex vivo imaging using a dual-wavelength microscope with axial chromatic aberration compensation. *J Biomed Opt* **23**, 1-9 (2018).
210. M. S. Sasso, G. Lollo, M. Pitorre, S. Solito, L. Pinton, S. Valpione, G. Bastiat, S. Mandruzzato, V. Bronte, I. Marigo, J. P. Benoit, Low dose gemcitabine-loaded lipid nanocapsules target monocytic myeloid-derived suppressor cells and potentiate cancer immunotherapy. *Biomaterials* **96**, 47-62 (2016).
211. S. Solito, L. Pinton, F. De Sanctis, S. Ugel, V. Bronte, S. Mandruzzato, I. Marigo, Methods to Measure MDSC Immune Suppressive Activity In Vitro and In Vivo. *Curr Protoc Immunol* **124**, e61 (2019).
212. L. Chang, L. Azzolin, D. Di Biagio, F. Zanconato, G. Battilana, R. Lucon Xiccato, M. Aragona, S. Giulitti, T. Panciera, A. Gandin, G. Sigismondo, J. Krijgsveld, M. Fassan, G. Brusatin, M. Cordenonsi, S. Piccolo, The SWI/SNF complex is a mechanoregulated inhibitor of YAP and TAZ. *Nature* **563**, 265-269 (2018).
213. L. S. Ojalvo, C. A. Whittaker, J. S. Condeelis, J. W. Pollard, Gene expression analysis of macrophages that facilitate tumor invasion supports a role for Wnt-signaling in mediating their activity in primary mammary tumors. *J Immunol* **184**, 702-712 (2010).
214. L. S. Ojalvo, W. King, D. Cox, J. W. Pollard, High-density gene expression analysis of tumor-associated macrophages from mouse mammary tumors. *Am J Pathol* **174**, 1048-1064 (2009).
215. F. J. Pixley, E. R. Stanley, CSF-1 regulation of the wandering macrophage: complexity in action. *Trends Cell Biol* **14**, 628-638 (2004).
216. P. A. Jaeger, T. Wyss-Coray, All-you-can-eat: autophagy in neurodegeneration and neuroprotection. *Mol Neurodegener* **4**, 16 (2009).

217. M. Cordenonsi, F. Zanconato, L. Azzolin, M. Forcato, A. Rosato, C. Frasson, M. Inui, M. Montagner, A. R. Parenti, A. Poletti, M. G. Daidone, S. Dupont, G. Basso, S. Bicciato, S. Piccolo, The Hippo transducer TAZ confers cancer stem cell-related traits on breast cancer cells. *Cell* **147**, 759-772 (2011).
218. J. J. Shuster, Median follow-up in clinical trials. *J Clin Oncol* **9**, 191-192 (1991).
219. L. Strauss, S. Sangaletti, F. M. Consonni, G. Szebeni, S. Morlacchi, M. G. Totaro, C. Porta, A. Anselmo, S. Tartari, A. Doni, F. Zitelli, C. Tripodo, M. P. Colombo, A. Sica, RORC1 Regulates Tumor-Promoting "Emergency" Granulo-Monocytopoiesis. *Cancer Cell* **28**, 253-269 (2015).
220. D. I. Gabrilovich, S. Ostrand-Rosenberg, V. Bronte, Coordinated regulation of myeloid cells by tumours. *Nat Rev Immunol* **12**, 253-268 (2012).
221. T. J. McArdle, B. M. Ogle, F. K. Noubissi, An In Vitro Inverted Vertical Invasion Assay to Avoid Manipulation of Rare or Sensitive Cell Types. *J Cancer* **7**, 2333-2340 (2016).
222. N. Nagarsheth, M. S. Wicha, W. Zou, Chemokines in the cancer microenvironment and their relevance in cancer immunotherapy. *Nat Rev Immunol* **17**, 559-572 (2017).
223. L. Lara Rodriguez, I. C. Schneider, Directed cell migration in multi-cue environments. *Integr Biol (Camb)* **5**, 1306-1323 (2013).
224. J. Cooper, F. G. Giancotti, Integrin Signaling in Cancer: Mechanotransduction, Stemness, Epithelial Plasticity, and Therapeutic Resistance. *Cancer Cell* **35**, 347-367 (2019).
225. M. Y. Abshire, K. S. Thomas, K. A. Owen, A. H. Bouton, Macrophage motility requires distinct alpha5beta1/FAK and alpha4beta1/paxillin signaling events. *J Leukoc Biol* **89**, 251-257 (2011).
226. M. A. Horton, The alpha v beta 3 integrin "vitronectin receptor". *Int J Biochem Cell Biol* **29**, 721-725 (1997).
227. D. Laoui, E. Van Overmeire, P. De Baetselier, J. A. Van Ginderachter, G. Raes, Functional Relationship between Tumor-Associated Macrophages and Macrophage Colony-Stimulating Factor as Contributors to Cancer Progression. *Front Immunol* **5**, 489 (2014).
228. B. Costa-Silva, N. M. Aiello, A. J. Ocean, S. Singh, H. Zhang, B. K. Thakur, A. Becker, A. Hoshino, M. T. Mark, H. Molina, J. Xiang, T. Zhang, T. M. Theilen, G. Garcia-Santos, C. Williams, Y. Ararso, Y. Huang, G. Rodrigues, T. L. Shen, K. J. Labori, I. M. Lothe, E. H. Kure, J. Hernandez, A. Doussot, S. H. Ebbesen, P. M. Grandgenett, M. A. Hollingsworth, M. Jain, K. Mallya, S. K. Batra, W. R. Jarnagin, R. E. Schwartz, I. Matei, H. Peinado, B. Z. Stanger, J. Bromberg, D. Lyden, Pancreatic cancer exosomes initiate pre-metastatic niche formation in the liver. *Nat Cell Biol* **17**, 816-826 (2015).
229. R. N. Kaplan, R. D. Riba, S. Zacharoulis, A. H. Bramley, L. Vincent, C. Costa, D. D. MacDonald, D. K. Jin, K. Shido, S. A. Kerns, Z. Zhu, D. Hicklin, Y. Wu, J. L. Port, N. Altorki, E. R. Port, D. Ruggero, S. V. Shmelkov, K. K. Jensen, S. Rafii, D. Lyden, VEGFR1-positive haematopoietic bone marrow progenitors initiate the pre-metastatic niche. *Nature* **438**, 820-827 (2005).
230. N. Osmani, G. Follain, M. J. Garcia Leon, O. Lefebvre, I. Busnelli, A. Larnicol, S. Harlepp, J. G. Goetz, Metastatic Tumor Cells Exploit Their Adhesion Repertoire to Counteract Shear Forces during Intravascular Arrest. *Cell Rep* **28**, 2491-2500 e2495 (2019).
231. E. Y. Lin, A. V. Nguyen, R. G. Russell, J. W. Pollard, Colony-stimulating factor 1 promotes progression of mammary tumors to malignancy. *J Exp Med* **193**, 727-740 (2001).
232. S. Goswami, E. Sahai, J. B. Wyckoff, M. Cammer, D. Cox, F. J. Pixley, E. R. Stanley, J. E. Segall, J. S. Condeelis, Macrophages promote the invasion of breast carcinoma cells via a colony-stimulating factor-1/epidermal growth factor paracrine loop. *Cancer Res* **65**, 5278-5283 (2005).
233. R. S. McDermott, L. Deneux, V. Mosseri, J. Vedrenne, K. Clough, A. Fourquet, J. Rodriguez, J. M. Cosset, X. Sastre, P. Beuzeboc, P. Pouillart, S. M. Scholl, Circulating macrophage colony stimulating factor as a marker of tumour progression. *Eur Cytokine Netw* **13**, 121-127 (2002).
234. A. Pocaterra, G. Santinon, P. Romani, I. Brian, A. Dimitracopoulos, A. Ghisleni, A. Carnicer-Lombarte, M. Forcato, P. Braghetta, M. Montagner, F. Galuppini, M. Aragona,

G. Pennelli, S. Bicciato, N. Gauthier, K. Franze, S. Dupont, F-actin dynamics regulates mammalian organ growth and cell fate maintenance. *J Hepatol* **71**, 130-142 (2019).

235. J. Feng, J. Gou, J. Jia, T. Yi, T. Cui, Z. Li, Verteporfin, a suppressor of YAP-TEAD complex, presents promising antitumor properties on ovarian cancer. *Onco Targets Ther* **9**, 5371-5381 (2016).
236. C. M. Lo, H. B. Wang, M. Dembo, Y. L. Wang, Cell movement is guided by the rigidity of the substrate. *Biophys J* **79**, 144-152 (2000).
237. J. Guo, Y. Yan, Y. Yan, Q. Guo, M. Zhang, J. Zhang, D. Goltzman, Tumor-associated macrophages induce the expression of FOXQ1 to promote epithelial-mesenchymal transition and metastasis in gastric cancer cells. *Oncol Rep* **38**, 2003-2010 (2017).
238. S. Zilio, J. L. Vella, A. C. De la Fuente, P. M. Daftarian, D. T. Weed, A. Kaifer, I. Marigo, K. Leone, V. Bronte, P. Serafini, 4PD Functionalized Dendrimers: A Flexible Tool for In Vivo Gene Silencing of Tumor-Educated Myeloid Cells. *J Immunol* **198**, 4166-4177 (2017).